

Electrokinetic Management of Biosolids for the Inactivation of Helminth Ova

André Habel

A Thesis in
the Department
of Building, Civil,
and Environmental Engineering

Presented in Partial Fulfillment of the Requirements
for the Degree of Master of Applied Science in
Civil Engineering at
Concordia University
Montreal, Quebec, Canada

September 2010
© André Habel, 2010

CONCORDIA UNIVERSITY

School of Graduate Studies

This is to certify that the thesis prepared

By: André Habel

Entitled: **Electrokinetic Management of Biosolids for the Inactivation of Helminth Ova**

and submitted in partial fulfillment of the requirements for the degree of

Master of Applied Sciences (Civil Engineering)

Complies with the regulations of the University and meets the accepted standards with respect to originality and quality.

Signed by the final examining committee:

Dr. R. Zmeureanu Chair

Dr. M. Elektorowicz Supervisor

Dr. D. Jovanovic Examiner External (to program)

Dr. C. Mulligan Examiner

Dr. R. Zmeureanu Examiner

Approved by Dr. T. Zayed, GPD
Department of Building, Civil and Environmental Engineering

Dr. R. Drew
Dean of Faculty of Engineering and Computer Science

Date Septembre 23, 2010

Abstract

Electrokinetic Management of Biosolids for the Inactivation of Helminth Ova

André Habel

The presumed risk to public health has led to a growing interest in the production of exceptional quality biosolids intended to contain undetectable levels of three classes of pathogens: bacteria, enteric viruses, and helminth eggs (parasitic intestinal worms). This study assessed the performance of an enhanced electrokinetic technology which permits the simultaneous dewatering, heavy metal removal and inactivation of the swine helminth, *Ascaris suum*, from wastewater sludge in one operational unit for the production of exceptional quality biosolids. The process is based on the electrokinetic (EK) phenomena, initiated by the introduction of direct electric current through the biosolids, preceded by a brief period of ohmic heating. A series of bench-scale tests were performed on combined primary and secondary sewage sludges obtained from the wastewater treatment plant in Auteuil, QC. Two additional tests were repeated at a pilot scale with success. The results demonstrated that the enhanced EK treatment is capable of delivering a product virtually free of viable *Ascaris suum* ova introduced to the conditioned sludge with a brief exposure at a temperature of 55°C. In addition, dewatering levels up to 23 % total solids (TS) and mean removal levels of over 54 %, 30 %, and 24 % for heavy metals such as Zn, Cd, and Pb, respectively, within a period of 3 days were reported. Consequently, the sanitized biosolids generated during the enhanced EK treatment process can be transformed into a high quality soil amendment that could be safely applied to agricultural lands.

Acknowledgement

I am forever grateful to Dr. Maria Elektorowicz for the chance to pursue a graduate program under her supervision and for providing me with the opportunity to travel to Cornell University to become skilled at performing *Ascaris suum* assay. Her invaluable insight into electrokinetics enabled me to gain a better grasp of the phenomenon and her guidance and patience throughout the course of my thesis.

I would like to acknowledge Dr. Dwight D. Bowman and Janice L. Liotta from Cornell University for their generosity with respect to their time and lab facility, and imparting the skills to tame *Ascaris suum*.

My thanks to Mario Gagné, Superintendant - Division Assainissement, Service de l'environnement, Ville de Laval (WWTP in Auteuil, QC), for his collaboration and consent to procure biosolids for this project.

I would like also to acknowledge the financial support of this research by the National Science and Engineering Research Council (NSERC) Strategic Grant (STPGP 306885) awarded to Dr. M. Elektorowicz from Concordia University and Dr. J. Oleszkiewicz from the University of Manitoba.

I am deeply indebted to my spouse, Laila, for her patience and desultory dedication throughout my ceaseless academic life, and also to my daughter and son, Lia and Aden, for the motivation to surpass my limitations.

Table of Contents

List of Figures.....	ix
List of Tables.....	xiv
Nomenclature.....	xv
1. Introduction.....	1
1.1. Problem Statement.....	1
1.2. Objectives.....	3
2. Literature Review.....	4
2.1. Biosolids Generation and Characteristics.....	4
2.1.1. Wastewater Treatment Process and Biosolids Production from the WWTP in Auteuil, QC.....	7
2.1.1.1. Plant Units Description.....	8
2.1.3. Methods for Biosolids Dewatering.....	15
2.1.4. Methods of Heavy Metal Removal from Biosolids.....	16
2.1.5. Methods of Pathogens Reduction in Biosolids.....	18
2.1.5.1. Chemical methods.....	19
2.1.5.2. Physical methods.....	19
2.1.5.3. Inactivation Methods for the Pathogen Surrogate, <i>Ascaris suum</i> , from Biosolids.....	21
2.2. Electrokinetic Technologies.....	25
2.2.1. Theoretical Aspects of the Electrokinetic Phenomena.....	26
2.2.1.1. Principal of Electrophoresis.....	28
2.2.1.2. Electrolysis.....	31

2.2.1.3. Principal of Electroosmosis	33
2.2.2. Previous Studies on EK Treatment of Biosolids.....	36
2.2.3. Thermal Treatment by Ohmic Heating.....	39
2.2.4. Ion Exchange Textiles.....	45
2.3. Innovative EK Technology	47
3. Experimental Methodology.....	48
3.1. Set-up of Bench and Pilot Units.....	50
3.1.1. Bench-Scale Units.....	50
3.1.2. Pilot-Scale Units	53
3.2. Equipment and Materials	55
3.3. Chemical and Physical Characteristics of Biosolids.....	58
3.4. <i>Ascaris suum</i> egg Chamber Design and Placement.....	59
3.4.1. Preparation of <i>Ascaris suum</i> eggs	61
3.4.2. Procedure for Collecting and Processing <i>Ascaris suum</i> eggs from Chambers ..	62
3.5. Experimental Parameters and Variables Studied.....	65
3.5.1. Conditioners.....	65
3.5.1.1. Temperature Impact on Conductivity	66
3.5.1.2. Voltage Gradient Impact on Temperature	66
3.6. <i>Ascaris suum</i> Ova Inactivation Experiments.....	67
3.6.1. Bench-Scale Treatment of <i>Ascaris suum</i> Eggs	67
3.6.2. Pilot Scale <i>Ascaris suum</i> ova Inactivation Experiments.....	70
3.7. Measurements and Analyses.....	73
3.7.1. Electrical Parameters and Temperature Measurements	73

3.7.2. pH Analysis.....	74
3.7.3. Heavy Metal Analysis.....	74
3.7.4. Ion Analysis	75
3.7.5. Percent Total Solids (%TS) and Volatile Solids (%VS) Analyses.....	76
4. Results.....	78
4.1. Results of Bench-Scale Experiments.....	78
4.1.1. Inactivation experiments of <i>Ascaris suum</i> Eggs	78
4.1.2. Effect of Conditioner Type on Dewatering, Conductivity and Heating Rate.....	84
4.1.3. Effect of Conditioner Concentration on Dewatering, Conductivity and Heating Rate	86
4.1.4. Effect of Temperature on the Conductivity of Various Conditioner Concentrations	89
4.1.5. Effect of Applied Voltage Gradients on Heating Rates.....	91
4.1.6. Energy Consumption	95
4.1.7. Results of the Bench-Scale EK Experiments.....	96
4.1.7.1. Sludge Dewatering.....	97
4.1.7.2. pH and Ion Distribution	102
4.1.7.3. Heavy Metal Distribution	107
4.2. Results of Pilot Scale EK Experiments.....	110
4.2.1. Sludge Dewatering.....	113
4.2.2. pH and Ion Distribution	118
4.2.3. Heavy Metal Distribution	123
5. Discussion and Conclusion	131

5.1. Assessment of <i>Ascaris suum</i> Ova Inactivation by Joule Heating	132
5.2. Selection of Treatment Parameters	135
5.3. Contaminant Removal Efficiencies	138
6. Recommendations for Further Studies.....	141
7. References	142

List of Figures

Figure 2.1 Schematic representation of a sludge floc	6
Figure 2.2 Treatment units of the Wastewater Treatment Plant in Auteuil, Qc	8
Figure 2.3 Hatching <i>Ascaris suum</i> larva (x400 magnification).....	22
Figure 2.4 <i>Ascaris suum</i> ova with the outer uterine layer partially intact (x400 magnification).....	22
Figure 2.5 Structure of the <i>Ascaris</i> Genus egg-shell	22
Figure 2.6 Overview of the electrokinetic phenomena in a sludge matrix	27
Figure 2.7 Schematic representation of the distribution of ions around a charged particle in solution.....	34
Figure 2.8 Conceptual model of ohmic heating.....	40
Figure 3.1 Flow chart of experimental methodology.....	50
Figure 3.2 Bench-scale EK unit.....	52
Figure 3.3 Diagram of bench-scale EK unit	52
Figure 3.4 Steel plate electrodes (left: inactivation trials, right: dewatering trials).....	53
Figure 3.5 Diagram of the pilot-scale EK unit.....	54
Figure 3.6 <i>Ascaris suum</i> egg chambers (open and closed) with nylon mesh	60
Figure 3.7 Example of viable (embryonated) <i>Ascaris suum</i> ova (x200 magnification)....	63
Figure 3.8 Example of inactivated (unembryonated) <i>Ascaris suum</i> ova (x200 magnification).....	63
Figure 3.9 General layout of the pilot-scale EK unit.....	71
Figure 3.10 Multifunctional electrode	72

Figure 4.1 Percentage of viable <i>Ascaris suum</i> eggs as a function of temperature during bench-scale experiments comparing the inactivation of egg between ohmic and convective heating trials.....	79
Figure 4.2 Example of <i>Ascaris suum</i> ova subjected to 50°C for 10 minutes during bench-scale experiments (x200 magnification).....	80
Figure 4.3 Example of inactivated <i>Ascaris suum</i> ova subjected to 55°C for 10 minutes during bench-scale experiments (x200 magnification).....	80
Figure 4.4 Sludge temperature and final % TS vs. conditioner type with 3 V/cm for 45 min and 0.5 V/cm for 67 hrs	85
Figure 4.5 Sludge conductivities at room temperature as a function of the type and concentration of conditioners.....	86
Figure 4.6 Sludge temperature and % TS vs. AN concentration with the application of 3 V/cm for 63 min and 0.5 V/cm for 67 hrs.....	87
Figure 4.7 Heating rates for the various AN concentrations, each subjected to an electric field strength of 3 V/cm	87
Figure 4.8 Changes in sludge conductivity with time.....	88
Figure 4.9 Conductivity of sludge as a function of temperature with respect to the AN concentration	90
Figure 4.10 Comparison of conductivity and temperature relationship with respect to the water content of the sludge.....	90
Figure 4.11 1D bench-scale tests: visualization of current lines	91
Figure 4.12 Heating rate in sludge as a function of the applied DC volage gradient (average $\kappa = 16.61 \pm 1.16$ mS/cm)	93

Figure 4.13	Evolution of amperage rates in function of applied DC voltage gradient (average $\kappa = 16.61 \pm 16$ mS/cm)	93
Figure 4.14	Evolution of heating rates as a function of the applied AC voltage gradient (average $\kappa = 16.50 \pm 17$ mS/cm)	94
Figure 4.15	Evolution of amperage rates in function of applied AC voltage gradient (average $\kappa = 16.50 \pm 17$ mS/cm)	94
Figure 4.16	Heating rates in function of applied DC and AC fields.....	95
Figure 4.17	Comparison of energy consumption between DC and AC power to reach 60°C (average $\kappa = 16.57 \pm 16$ mS/cm)	96
Figure 4.18	Volume of sludge liquor collected during bench-scale EK experiments	98
Figure 4.19	Distribution of TS between electrodes in bench-scale EK experiments	99
Figure 4.20	Final average of TS content of the bench-scale EK experiments.....	100
Figure 4.21	Distribution of volatile solids between electrodes in bench-scale EK experiments	100
Figure 4.22	Volatile solids reduction in bench-scale EK experiments.....	100
Figure 4.23	pH profiles of the bench-scale EK experiments.....	102
Figure 4.24	Nitrate distributions for the unconditioned sludge in the bench-scale EK experiments.....	104
Figure 4.25	Nitrate distributions for the AN conditioned sludge in the bench-scale EK experiments.....	104
Figure 4.26	Ammonium distributions for the unconditioned sludge in the bench-scale EK experiments	105

Figure 4.27 Ammonium distributions for the AN conditioned sludge in the bench-scale EK experiments	105
Figure 4.28 Phosphate distributions for the unconditioned sludge in the bench-scale EK experiments	106
Figure 4.29 Phosphate distributions for the AN conditioned sludge in the bench-scale EK experiments	106
Figure 4.30 Cadmium distribution between electrodes in the bench-scale EK experiments	107
Figure 4.31 Chromium distribution between electrodes in the bench-scale EK experiments	108
Figure 4.32 Copper distribution between electrodes in the bench-scale EK experiments	108
Figure 4.33 Iron distribution between electrodes in the bench-scale EK experiments..	109
Figure 4.34 Lead distribution between electrodes in the bench-scale EK experiments	109
Figure 4.35 Zinc distribution between electrodes in the bench-scale EK experiments.	110
Figure 4.36 Simulation of the distribution of current lines during the pilot-scale EK experiments	112
Figure 4.37 Volume of sludge liquors collected during pilot test 1.....	113
Figure 4.38 Volume of sludge liquors collected during pilot test 2.....	114
Figure 4.39 Percent total solids distribution in pilot tests (1) and (2).....	116
Figure 4.40 Final average total solids of the pilot-scale experiments.....	117
Figure 4.41 Percent volatile solids distribution in pilot tests (1) and (2).....	118
Figure 4.42 Illustration of dewatered biosolids (after 70 h)	118

Figure 4.43	pH distribution in pilot tests (1) and (2)	119
Figure 4.44	Ammonium distribution in pilot tests (1) and (2).....	120
Figure 4.45	Ammonium concentration in the sludge liquor of pilot tests 1 and 2	120
Figure 4.46	Nitrate distribution in pilot tests (1) and (2).....	121
Figure 4.47	Nitrate concentration in the sludge liquor of pilot tests 1 and 2.....	122
Figure 4.48	Phosphate distribution in pilot tests (1) and (2).....	122
Figure 4.49	Phosphate concentration in the sludge liquor of pilot tests 1 and 2	123
Figure 4.50	Cadmium distribution in pilot tests (1) and (2)	124
Figure 4.51	Collection of cadmium in sludge liquors of pilot tests (1) and (2) and onto the ionic exchange textiles of pilot test 2	124
Figure 4.52	Lead distribution in pilot tests (1) and (2).....	127
Figure 4.53	Collection of lead in sludge liquors of pilot tests (1) and (2) and onto the ionic exchange textiles of pilot test 2	128
Figure 4.54	Zinc distribution in pilot tests (1) and (2).....	129
Figure 4.55	Collection of zinc in sludge liquors of pilot tests (1) and (2) and onto the ionic exchange textiles of pilot test 2	130
Figure 4.56	Chromium distribution in pilot tests (1) and (2).....	125
Figure 4.57	Collection of chromium in sludge liquors of pilot tests (1) and (2) and onto the ionic exchange textiles of pilot test 2.....	128
Figure 4.58	Iron distribution in pilot tests (1) and (2)	128
Figure 4.59	Collection of iron in sludge liquors of pilot tests (1) and (2) and onto the ionic exchange textiles of pilot test 2	129
Figure 4.60	Copper distribution in pilot tests (1) and (2)	126

Figure 4.61 Collection of copper in sludge liquors of pilot tests (1) and (2) and onto the ionic exchange textiles of pilot test 2	127
Figure 5.1 Heating rates in function of initial power input per unit volume (all AC ohmic heating trials).....	137

List of Tables

Table 2.1 Norms on biosolids in Quebec and the US	14
Table 2.2 Mobility of some inorganic ions	30
Table 3.1 Biosolids characteristics	59
Table 3.2 Typical composition and solubility of conditioners used	66
Table 3.3 Designed treatment conditions for bench-scale EK experiments	69
Table 3.4 Designed treatment conditions for pilot-scale EK experiments	70
Table 4.1 Results of bench-scale EK experiments on <i>Ascaris suum</i> viability	82
Table 4.2 Treatment conditions obtained during bench-scale EK experiments	97
Table 4.3 Total volume of liquor types collected in bench-scale EK experiments	98
Table 4.4 Total volume of liquor collected in the pilot-scale EK experiments	115
Table 5.1 Energy cost estimate for the enhanced EK experiments	138

Nomenclature

ϵ_0	Permittivity of vacuum, $\epsilon_0 = 8.85 \times 10^{-12} \text{ C} \cdot \text{V}^{-1} \cdot \text{m}^{-1}$
ϵ_r	Relative permittivity of the solution ($\text{C} \cdot \text{V}^{-1} \cdot \text{m}^{-1}$)
η	Viscosity ($\text{kg} \cdot \text{m}^{-1} \cdot \text{s}^{-1}$)
κ	Conductivity of the sludge ($\Omega^{-1} \cdot \text{m}^{-1}$) or ($\text{S} \cdot \text{m}^{-1}$)
μ_a	Apparent mobility ($\text{m}^2 \cdot \text{V}^{-1} \cdot \text{s}^{-1}$)
μ_{eo}	Electroosmotic mobility ($\text{m}^2 \cdot \text{V}^{-1} \cdot \text{s}^{-1}$)
μ_{ep}	Electrophoretic mobility ($\text{m}^2 \cdot \text{V}^{-1} \cdot \text{s}^{-1}$)
μ_i	Ionic mobility ($\text{m}^2 \cdot \text{V}^{-1} \cdot \text{s}^{-1}$)
ζ	Zeta potential (V)
a	Relative increase in conductivity per degree increase in temperature (K^{-1})
A	Cross-sectional area of the cell (m^2)
c	Concentration ($\text{mol} \cdot \text{m}^{-3}$)
E	Applied electric field strength ($\text{V} \cdot \text{m}^{-1}$)
F	electrostatic force (N)
I	Current (A)
P_{Joule}	Power dissipated as a result of Joule heating (W)
P_{heat}	Amount of heat liberation (W)
r	Effective radius of particle (m)
R	Electric resistance (Ω)
T	Absolute temperature (K)
U	Applied potential (V)
V	Voltage (V)
W	Dissipated power per volume of sludge ($\text{W} \cdot \text{m}^{-3}$)
q	Effective charge of ion (C)
AC	Alternating current (VAC)
DC	Direct current (VDC)
AN	Ammonium nitrate
DAP	Diammonium phosphate
EK	Electrokinetic

EDTA Ethylenediamine tetraacetate
FC Fecal coliform
NTA Nitritotriacetic acid
TS Total solids
TSS Total suspended solids
VS Volatile solids
WWTP Wastewater treatment plant

Electrokinetic Management of Biosolids for the Inactivation of Helminth Ova

1. Introduction

1.1. Problem Statement

Wastewater treatment plants essentially work by relying on microorganisms to consume sewage waste, but in the process produce vast amounts of sludge (biosolids). The development of a sustainable management method of sewage sludge is a major concern for most countries. The amount of biosolids generated in Canada is about 0.4 million dry tons per year; 47 % of which is incinerated and 4 % is landfilled (Apedaile, 2001). Currently, only about 43 % of biosolids are applied to land, mainly in rural areas. Moreover, the production of biosolids in the US is approximately 7.6 million dry tones per year, with about two thirds applied to land (Acquisto, et al., 2006). This still leaves over 2.5 million dry tones of potential biosolids incinerated and landfilled.

Biosolids reuse in the form of land application should be promoted as future production is likely to increase throughout North America and the world. However, the potential risk associated with the dispersal of such sludge must be addressed in order for this to be a viable means of disposal. Technologies to manage biosolids have focused primarily on dewatering as a method of reducing sludge masses. However, the major concerns with the biosolids constituents are the inclusion of significant quantities of human pathogens, heavy metals, and more recently, endocrine disrupting chemicals (Spinosa, 2007) which when applied to arable land may pose a risk to the environment and human health. To minimize these risks, various government agencies require that agriculturally applied

biosolids be treated to reduce the threat of disease causing pathogens. The presumed risk to public health has led to a growing interest in the production of exceptional quality biosolids intended to contain minimal levels of three classes of pathogen: bacteria, enteric viruses, and helminth eggs (parasitic intestinal worms) (MDDEP, 2008; US EPA, 1999). Of the classes of pathogens present in biosolids, helminth ova are the most resistant to many types of sanitation methods. Ova of the genus *Ascaris* have the highest inactivation resistance and survive under numerous treatment conditions (Reimers, et al. 1986b; Feachem, et al., 1983).

The handling and dewatering of sewer sludge is one of the most energy demanding processes in a WWTP (Malcolm Pirnie Inc., 1995). The costs of biosolid treatment represent about 30 % to 50 % of the total operating costs of wastewater treatment (Dewil, et al., 2005); great attention is, therefore, being directed on treatment processes to reduce the amount of sludge generated and improve the dewaterability of the sludge. Because of the increasing costs of sludge disposal through landfilling and of the increasing emission controls on incineration, the development of technologies capable of the simultaneous removal of water and pollutants, including the inactivation various pathogenic agents introduced in wastewater will enable a broader beneficial utilization of biosolids as either agricultural fertilizer or soil conditioner.

1.2. Objectives

The primary objective of this study is to evaluate the feasibility of applying an enhanced electrokinetic (EK) process in the disinfection of biosolids, using *Ascaris suum* ova as the surrogate pathogen, and defining the temperature at which 99.9 % inactivation (3 log reduction) is attained. The secondary objectives consist of further assessments of the impact of the EK process in terms of its dewatering and heavy metal removal ability for the purpose of producing high quality biosolids that can safely be used as a soil amendment. This thesis incorporates some elements of the pending patent for the electrokinetic sludge management (EKDIM) (US Patent 12/571,482).

To achieve these objectives, the thesis is subdivided into the following sections:

- Section 1 describes the statement of the problems and the goals of this research
- Section 2 contains a comprehensive literature review explaining some theoretical aspects of the EK processes, wastewater sludge characteristics and treatment methods, and details concerning the helminth pathogen.
- Section 3 details the methodology of the study and analytical techniques used.
- Section 4 features the results of both bench and pilot scale experiments.
- In section 5, a discussion of the results and the conclusions derived are presented.
- Finally, section 6 includes the recommendations generated by this study

2. Literature Review

2.1. Biosolids Generation and Characteristics

The US Environmental Protection Act (US EPA) and the Ministère du Développement Durable, de l'Environnement et des Parcs (MDDEP), which regulates the production and use of biosolids in the Province of Quebec, define the term “Biosolids” as that portion of sewage sludge that have undergone adequate treatment in reducing pathogens and attraction to vectors (e.g. insects and rodents) in order to permit their application to land.

The reclamation and use of fertilizing materials is regulated by the Quebec Environmental Quality Act. The Criteria for Reclamation of Fertilizer Materials cover a wide range of organic material, including sewage biosolids, for a wide range of potential uses. The Criteria specifically addresses the use of fertilizing residuals both for horticultural applications as well as for the manufacture of soil mixes. These fertilizing residuals are classified according to contaminants and pathogen content, as well as by odour.

Unlike Canada, the United States has national biosolids standards that are the responsibility of the US EPA. The standards are contained in Part 503 of Chapter 40 of the Code of Federal Regulations. The regulation includes standards for pollution limits, management practices, monitoring requirements, operational standards record keeping and reporting. The US regulations have three general criteria for biosolids quality. The quality of the biosolids determines the level of restrictions placed on the use of the biosolids. These categories are:

- Ceiling pollutant concentration,
- Pathogen content (Class A and B), and
- Process control criteria to control vector attraction.

Biosolids that meet the strictest level of all three categories are labeled ‘exceptional quality’ and have no restrictions placed on their use and distribution under the regulation. Biosolids that are not ‘exceptional quality’ have restriction placed on use and distribution, depending upon where they rank in each category.

The physical and chemical properties of sludge are contingent on the origins of the wastewater. Wastewaters can be generated from domestic, commercial, and industrial sources. Sludges collected in wastewater treatment plants (WWTP) are generally divided into categories, depending on their treatment processes. Primary sludges are the main product of WWTP. This sludge is generated by the primary treatment process which generally consists of the gravity settling units. This sludge contains suspended organic and inorganic particles in the influent wastewater. Secondary sludges are the products of biological processes used to degrade the organic waste contained in the wastewater. This sludge is generated by various suspended solids or filter type bioreactors. A third category referred to as chemical sludge is produced by the addition of various chemical coagulants to primary and/or secondary sludge to improve the settleability and dewaterability of the suspended particulates (Tchobanoglous, 2003).

The following illustration (Figure 2.1) is a schematic representation of a sludge floc showing the water associated with the sludge particles (Kiely, 1997).

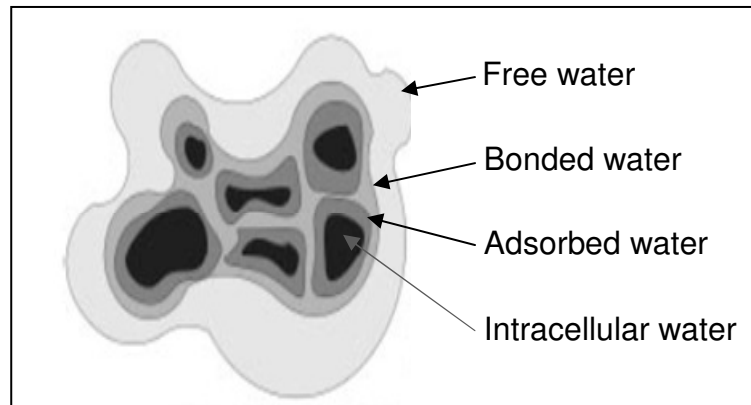


Figure 2.1. Schematic representation of a sludge floc

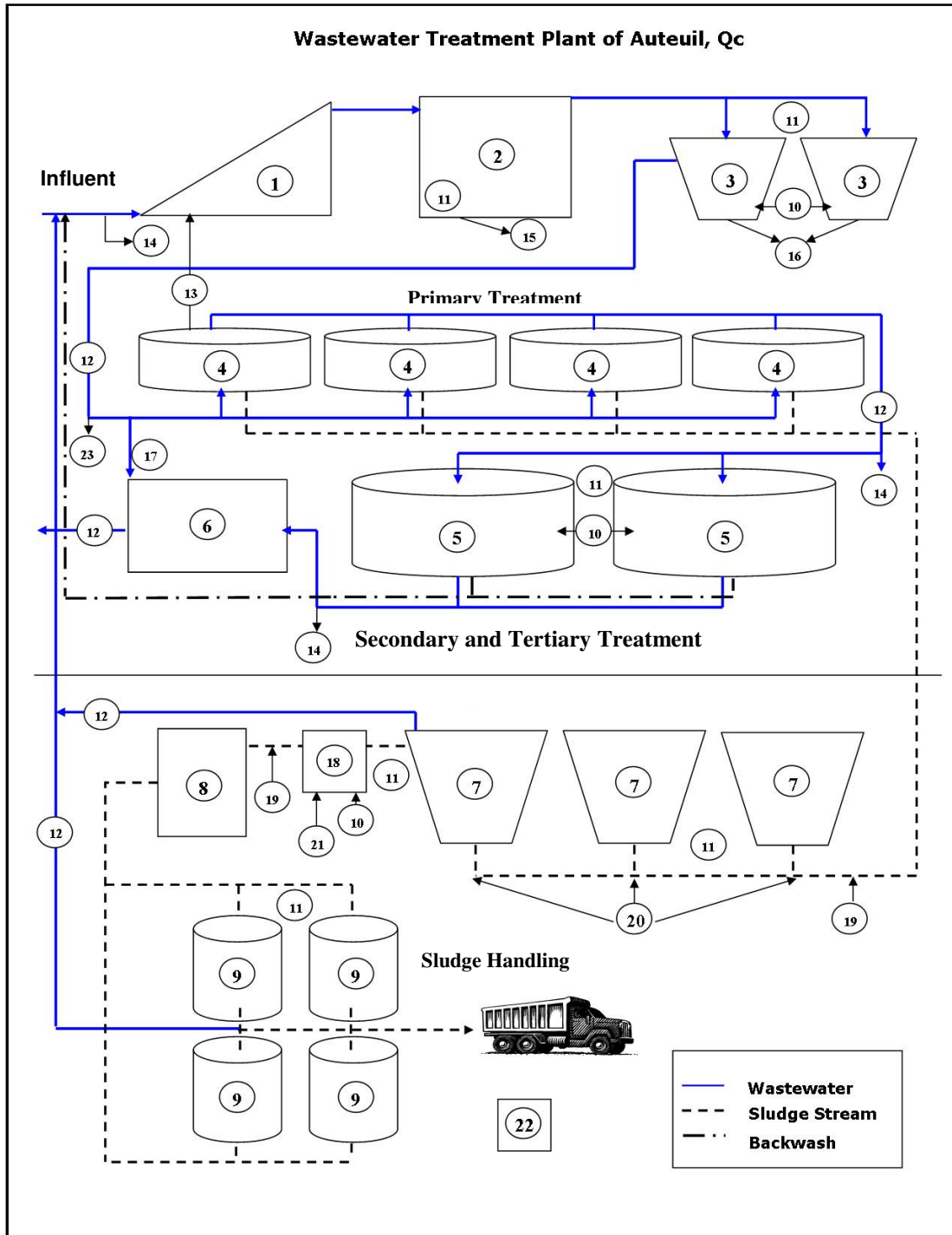
The various forms of water found are (Oleszkiewicz & Mavinic, 2002):

- Free water not associated with the surface chemistry of the solids. This water can be easily be removed by simple thickening, increasing the total solid (TS) content from 1 to 4–8 %.
- Bonded water can be removed by applying mechanical pressure of centrifugal force, removing about 95 % of all water, and resulting in a sludge cake with up to 20 % TS.
- Adsorbed water can be removed by mechanical dewatering, but only after being chemically treated with either cationic or anionic polymer; thus increasing the sludge cake from 20 to 22–35 % TS.
- Intracellular water can only be removed through energy intensive methods, such as thermal drying. The final product is a solid with an approximate TS content of 92 % to 98 %.

2.1.1. Wastewater Treatment Process and Biosolids Production from the WWTP in Auteuil, QC.

The sludge collected for use in this thesis originated from a WWTP in Auteuil, QC. This plant belongs to the fixed film wastewater treatment systems; specifically, it belongs to the family of biological aerated filter (BAF). Unlike other fixed film processes BAF's are able to carry out solids separation as well as aerobic biological treatment. Thus carbonaceous removal, filtration of particulates, and nitrification can be carried out in a single unit. Wastewater percolates down a granular support medium called Biocarbone[®], which consists of vitrified clay or schist particles having an average diameter of 5 mm, and is purified by the microbial activity and by the physical action of this support medium through the partial filtration of suspended solids. The Biocarbone[®] method is a flooded, aerated granular bed through which wastewater flows counter-current to the diffused air introduced at the base of the bed. The oxygen introduced and the biodegradable constituents of the wastewater lead to the growth of heterotrophic microorganisms which colonize the surface of the packing elements forming the biofilm. Eventually, the biofilter clogs due to the production of biomass and the retention of suspended particles; consequently, some of the growing biomass and entrapped particles must be removed periodically. This is done with an air and backwashed water mixture driven through the bottom of the granular bed (Information provided is based on a site visit).

2.1.1.1. Plant Units Description



(Adapted from an informational pamphlet: Station d'Épuration Auteuil)

Figure 2.2. Treatment units of the Wastewater Treatment Plant in Auteuil, Qc

Unit description for figure 2.2

Wastewater Treatment

- 1 – Wastewater Pump
- 2 – Screening unit
- 3 – Sedimentation unit
- 4 – Primary Settling unit
- 5 – Biofiltration unit
- 6 – UV treatment unit

Sludge Handling

- 7 – Flotation unit
- 8 – Flocculation unit
- 9 – Centrifugation unit
- 18 – Sludge containment unit

Other units

- 10 – Air supply injection (4 pumps)
- 11 – Air extraction unit for purification (22)
- 12 – Flow meter
- 13 – Foam condenser
- 14 – Storm pump
- 15 – Waste compactor
- 16 – Sand screw
- 17 – Diverted flow to the UV treatment unit
- 19 – Polymer injection
- 20 – Pressurized water injection
- 21 – Iron sulphate injection
- 22 – Air purification unit
- 23 – Diverted flow to the entrance of the

The wastewater is pumped into the plant by two Archimedes' screws (1). If the influent wastewater discharge exceeds the maximum flow capacity of the plant, limited to 115 000 m³/day, the excess flow is diverted directly to the receiving water body (14). The flow entering the station is directed to a primary screening unit (2) containing two large screens, then to two grit chambers (vortex configuration) (3). The former removes solids larger than 13 mm in diameter and are then placed into a waste compactor (15); the latter removes particles with diameters greater than 0.2 mm, which are disposed of with a sand screw (16). Air is bubbled through the grit chamber to promote sedimentation (10) and foul air from both units is removed (11) and can be treated by means of activated carbon filters (22).

The wastewater is then directed to four primary settlers (4). As the water flows to the settling unit, the flow is measured by a Parshall flume (12) which ensures that flows above 100 000 m³/day are prevented from entering the settlers and overwhelming them.

The floating debris is skimmed off the top and pumped back to the entrance of the plant (23). The settlers have a removal efficiency of 80 % for total suspended solids (TSS) and 65 % for biological oxygen demand (BOD). The sludge depositing to the bottom is pumped out and directed to the sludge handling units, whereas the floating residues are skimmed, condensed and sent back to the entrance of the plant (13). The effluent leaving the settlers flows through another Parshall flume, again to monitor that the excess flow does not overwhelm the biofilters. This portion of the effluent can also be diverted to the tertiary UV treatment unit directly (17), if necessary.

The secondary treatment is accomplished by two biofilter units (5) that remove most of the remaining TSS and BOD. Each biofilter unit contains ten cells filled with the biocarbon[®] medium. Both units are monitored electronically and the number of cells in use at one time is automatically adjusted according to the incoming flow in order to keep the hydraulic loading rate relatively constant. On average, twelve cells out of twenty are in operation for a mean flow of 38 000 m³/day, which results in a mean flow of 3580 m³/d per cell at all time. The hydraulic residence time can vary between 1 and 3 hours per cell. Each cell is supplied with oxygen by two air pumps (10) at a rate of 1100 m³/h during filtration, and a rate of 400 m³/h during idle periods in order to maintain aerobic conditions throughout the biofilm. The foul air can be exhausted (11) and sent to an activated carbon treatment unit as needed.

An important maintenance operation is backwashing. Backwashing is performed in each cell on average every 15 hours, or when a hydraulic head of 70 cm above the granular medium develops, indicating that the porosity has reached a critical value. Part of the filtered water is used to flush out the biomass and solids accumulated on the medium.

This backwashed water is returned to the entrance of the plant to be reprocessed by the primary treatment units. A final tertiary phase of the wastewater treatment process is disinfection. The unit includes two medium pressure UV lamps. Disinfection is achieved by UV treatment units (8) that can inactivate up to 99.9 % of pathogenic microorganisms, like *E. coli* and *Salmonella*. The final effluent is discharged into the Rivière des Milles-Iles via a 60 inch sewer pipe draining in the middle of the river.

The accumulated sludge blanket removed from the base of the primary settling units is directed to the sludge handling units. This sludge ranges between 1 % and 2 % total solids (TS). The sludge stream enters three dissolved air flotation (DAF) units (7). The sludge is introduced at the bottom of the unit and is recirculated in the unit where pressurized air at 60 psi (20) and a cationic polymer (19) at a dose of 2.5 kg/ton dried total solids (TS) are injected. Once the sludge/polymers mixture enters the tank at atmospheric pressure microscopic air bubbles are formed entrapping the sludge flocs which rises to the surface where this supernatant is skimmed from the top and pumped to the centrifugation units. This dissolved air flotation treatment increases the sludge content to 4 % TS. Each flotation unit has a volume of 125 m³ with a flow capacity of 120 to 240 m³/day. The supernatant is sent back to the entrance of the plant. Again, the foul air can be collected and sent to the air treatment unit (11).

The thickened sludge is accumulated in a storage tank (18) and is kept aerated (10). Iron sulphate is added to the sludge and the foul air is circulated out of the unit (11). The stocking capacity is 400 m³ and is only used for short-term stocking. The thickened sludge is finally mixed with 8 kg/tonne of dried TS dose of polymers inside the flocculator (8), essentially consisting of a swelling in the pipe to create turbulent

conditions, directly before it enters the mechanical dewatering units (9) made up of four centrifuges. These units have a production rate of 100 kg dewatered solids/hr and can capture 95 % of total suspended solids (TSS). By centrifugal force, the dewatered sludge (or cake) can be thickened up to 28 % TS. The average cake production is about 19 500 kg/day. The captured water (or centrate) is recycled to the head of the plant. The sludge cake is stored in large containers before being disposed of in trucks and sent to solid waste landfills (information provided bases on site visit and pamphlet: Station d'Épuration Auteuil at www.info.ville.laval.qc.ca/wlav2/docs/folders/documents/environnement/auteuil.pdf).

The sludge used during this study was collected between the floatation units and flocculation units; thus, the samples consisted mostly of thickened primarily sludge with some secondary sludge derived from the backwash water used to remove excess biofilm from the biofilter units.

2.1.2. Regulations Regarding Biosolids

The US regulations have three general criteria for biosolids quality. The quality of the biosolids determines the level of restrictions placed on their application. These categories include ceiling pollutant concentration, pathogen content, and vector attraction control. Biosolids that meet the strictest level of all three categories are called exceptional quality (EQ) and have no restrictions placed on their use and distribution under the regulation. Biosolids that are not 'exceptional quality' have restriction placed on use and distribution, depending upon where they rank in each category (US EPA, 1999).

Guidelines for the beneficial use of fertilizing residuals in Quebec are strongly inspired by American USEPA regulations; these are outlined in Table 2.1 for different classes of biosolids being applied to land or offered for sale as fertilizers. The *Ministère du Développement Durable, de l'Environnement et des Parcs* (MDDEP) considers that a fertilizing residual is of category P1 (analogous to the USEPA Class A category) when the following pathogens are below the analytical detection limit: Enteric viruses, Viable Helminth eggs, and Salmonella. These organisms have been selected by virtue of their pathogenicity, their relative abundance in human waste, and their greater resistance to disinfection techniques. These are, in effect, representative pathogens and their absence implies that all other pathogens were destroyed or are found at concentrations below the limits of detection. Another requirement of the P1 category is to reduce the potential of the biosolids to attract vectors, that is to say, rodents, birds, insects, and other organisms that can spread pathogens. This is to a large part achieved by the reduction of volatile organic compounds which cause strong odors or by placing a barrier between the sewage sludge and vectors. The resulting P1 category of biosolid has no restriction on their application as agricultural fertilizers.

Those biosolids that do not meet the P1 criteria, but that have subjected to partial disinfection can nevertheless be used as fertilizer. However, since there remain pathogens, preventive measures must be set in place to mitigate their exposure to humans and animals to protect public health and the environment. These partially disinfected biosolids are classified as P2 and P3 by the MDDEP (analogous to the USEPA Classes B and C) according to their levels of disinfection: 1 log or 2 log reduction in bacteria and viruses, respectively. Preventive measures include restrictive use of these biosolids for

fertilizing crops destined to human consumption and include certain guidelines respecting the proximities to groundwater wells and surface waters. Other provisions also include protective clothing worn by laborers and hygienic protocols for workers manipulating these later classes of biosolids and public land access immediately after the application (US EPA, 1999).

Table 2.1 Norms on biosolids in Quebec and the US

Parameter	MDDEP Category C1P1 ^a (mg/kg dry weight)	MDDEP Category C2P2 ^a (mg/kg dry weight)	USEPA Exceptional Quality (EQ) ^b (mg/kg dry weight)	USEPA Pollutant Concentration(PC) ^b (mg/kg dry weight)
Arsenic	13	75	41	41
Cadmium	3	10	39	39
Chromium	210	1060	—	—
Cobalt	34	150	—	—
Copper	100	757	1500	1500
Lead	150	500	300	300
Mercury	0.8	5	17	17
Molybdenum	5	20	—	—
Nickel	62	180	420	420
Selenium	2	14	100	100
Zinc	500	1850	2800	2800
Dioxin (ng/kg)	17	50	—	—
Furan (ng/kg)	17	50	—	—
Pathogens	<1000 MPN E.coli/g TS and <3 MPN salmonella/4g TS	<2 000 000 MPN fecal coliform /g TS with some end-use restriction	<1000 MPN fecal coliform/g TS or <3 MPN salmonella/4g TS, <1 enteric virus (PFU)/4g TS, <1 viable helminth egg/4g TS	<2 000 000 MPN fecal coliform/g TS with some end use restriction

Note: MPN = Most Probable Number; PFU = Plaque Forming Units.

a) MENV, Interim Criteria for the Reclamation of Fertilizing Residuals, Quebec 2002, Table 3.4

b) USEPA, Plain English guide to the EPA part 503 boissolids rule, EPA/832/R-93/003.

Apart from the pathogenic criteria, biosolids are classified according to their pollutant content. The Quebec norms apply a C1 to C3 classification system to identify the heavy metal concentration limits for each category. The Quebec equivalent of “Exceptional quality” biosolids would thus be classified as “C1P1” according to this system. Another requirement of exceptional quality biosolids is the reduction in the attraction of disease vectors. Insects, birds, rodents, and domestic animals may transport sewage sludge and pathogens from sewage sludge to humans. These vectors are attracted to sewage sludge as a food source, and the reduction of the attraction of vectors to sewage sludge to prevent the spread of pathogens. Vector attraction reduction can be accomplished in two ways: by treating the sewage sludge to the point at which vectors will no longer be attracted to the biosolids (i.e. by reducing its volatile organic content) or by placing a barrier between the sewage sludge and vectors. Usually, the disinfection treatments of the biosolids will also solve the vector attraction issues.

2.1.3. Methods for Biosolids Dewatering

Sludge water removal usually occurs in a two step process. Sludge thickening is employed prior to the dewatering process in order to increase the efficiency of the dewatering equipment. The suspended solids are generally concentrated by gravity settling and compaction in primary clarifiers, and can be pumped to a variety of mechanical alternatives: dissolved-air flotation (DAF) thickening, gravity belt thickening, or centrifuge thickening (Metcalf and Eddy, 2003). The thickening process can only increase to TS content up to about 4 %. The sludge is still in liquid form and further dewatering is required to reduce its final volume in order to reduce disposal costs. The dewatering stage employed is often a mechanical process to decrease the moisture

content of the sludge. The main dewatering techniques include: centrifugation, belt filter press, drying beds, and lagoons. The sludge cake produced can reach a TS content as high as 28 % with the use of polymers to increase flocculation levels (Metcalf and Eddy, 2003).

2.1.4. Methods of Heavy Metal Removal from Biosolids

Relatively few methods exist to extract heavy metals from contaminated sludge. The most tested and applied method is the chemical extraction process. The chemicals used in this process may be inorganic acids (e.g., H_2SO_4 , HCl and HNO_3), organic acids (e.g., citric and oxalic acids), chelating agents (EDTA and NTA), and some inorganic chemicals (e.g., ferric chloride); each attaining different extraction efficiencies for the metals depending on the nature of the sludge. The final removal of the solubilized heavy metals from the extracting solution can be accomplished by precipitation process followed by settling or by an ion exchange system. Common precipitating reagents include alkalis such as lime ($\text{Ca}(\text{OH})_2$), CaO , NaOH , NaHCO_3 , and sulfides such as NaS , H_2S , or FeS (Brooks, 1991).

Using sludge dosed with 1 M acid (H_2SO_4) to decrease the pH to about 2 and a contact time of 24 h, Jenkins and Scheybeler (1981) were able to obtain maximum removal efficiencies for Cd, Cr, Fe, Ni and Zn of about 70 % or greater. Removal efficiency for Pb was lower with only 13 %. Preliminary estimates indicated that about 0.5 metric ton of sulfuric acid would be required for each dry metric ton of sludge solids for metal removal of more than 50 %. The solubilized metals were subsequently recovered by precipitation with lime, after the pH was adjusted to 7.0.

Despite the relatively high extraction efficiencies achieved with the chemical extraction method, the high acid requirements (0.5–0.8 g acid per g of dry sludge) and operational difficulties such as the requirement of corrosion resistant apparatus and need to neutralize the acidic sludge to an acceptable pH put constraints on the utilization of the chemical method. Furthermore, inorganic acids are not biodegradable, which makes the process environmentally unattractive. Organic acids, however, are more promising since higher metal extraction efficiency can be achieved at milder acidic conditions (pH 3 to 4) compared to inorganic acids at the same pH. Moreover, organic acids are readily degradable under aerobic and anaerobic conditions making the decontaminated sludge suitable for composting after dewatering. Nevertheless, chemical extraction is an expensive and complex process requiring large quantities of acids, neutralizing alkali, and rinse water (Babel and del Mundo Dacera, 2006).

Another common approach to deal with metal contaminants is their stabilization using lime amendment with an aim at reducing the availability of heavy metals in sludge compost (Wong, 1999) or sludge-amended soil (Brallier, et al., 1996) through the precipitation of soluble ions; however, lime treatment is not a permanent solution as the metals can potentially resolubilize if the pH decreases significantly.

More recently, a promising approach to metal removal is the application of the electrokinetic phenomena to a sludge medium (Elektorowicz and Oleszkiewicz, 2009; Elektorowicz, et al., 2007) and will be examined with greater detail in Chapter 2.2.

2.1.5. Methods of Pathogens Reduction in Biosolids

Biosolids used as agricultural fertilizer must meet minimum microbiological requirements at the time when it is ready to be used. The inactivation of pathogens in biosolids can be achieved by various physical and/or chemical methods. The physical stressors include temperature, desiccation and radioactive irradiation (gamma and beta). The chemical stressors are generally associated with alkaline agents (raising the pH and causing exothermic reactions), acidic agents (lowering the pH and causing exothermic reactions), oxidation and reduction agents (attacking organic compounds leading to the stabilization of biosolids) and non-charged disinfectants (used to disinfect helminth ova and bacterial spores) (Reimers, et al., 2005).

The mechanisms for pathogen inactivation include the following (Metcalf and Eddy, 2003):

- Modification of the cell permeability
- Modification of the protoplasm
- Alteration of the DNA
- Disruption of proteins or protein synthesis
- Inhibition of enzyme activity
- Induction of abnormal redox processes

A variety of factors influence the disinfection efficiency, including the contact time and temperature, the chemical nature and concentration of the disinfecting agent, the nature and intensity of the physical agent, the concentration and age of the microorganisms, and the nature of the liquid medium in which they bathe.

2.1.5.1. Chemical methods

A variety of chemical agents can be used to inactivate microorganisms. These include halogens and their derivatives: Cl_2 , Br_2 , I_2 , HOCl , ClO_2 , etc.; oxygenated and strongly oxidizing compounds: hydrogen peroxide, ozone, phenols, alcohols potassium permanganate, etc.; metal ions: Ag^+ , Cu^+ , Fe^{2+} , etc.; quaternary ammonium compounds: NR_4^+ , with R being alkyl groups; strong acids and bases, and enzymes (Metcalf and Eddy, 2003).

More recently, the use of ferrate for the stabilization and disinfection of biosolids has been advanced by Reimers et al. (2005). Ferrate (VI) (FeO_4^{2-}) when added to sewage sludge reacts with water and creates not only high pH conditions, but also acts as a powerful oxidizing agent. However, unlike chlorine or ozone disinfection, it has the advantage of not creating toxic by-products like trihalomethanes and haloacetic acids.

Ferrate (VI) have been successfully used, in concentrations of 30 to 35 g/l, as an agent for alkaline treatment and as an alternative to lime stabilization. Inactivation of bacteria (e.g., *Clostridium perfringens*), viruses, and helminth ova using ferrate as a disinfectant have been reported (Reimers, et al., 2005).

2.1.5.2. Physical methods

The physical treatment methods proven to meet Class A objectives and approved by the EPA commonly consist of excessive thermal treatments which uses specific time-temperature regimes to inactivate pathogens depending on the percent TS content of the biosolids. Inactivation rates of pathogens vary widely over the temperature range used for sludge treatment (20°C to 80°C); therefore, the maximum temperature attained and the temperature profile during treatment are critically important factors (Feachem, et al.,

1983). For instance, the required minimum time to achieve Class A pathogen inactivation criteria when a sludge with over 7 % TS is heated at 60°C is 12.6 hours; the time needed to meet the same objective drops to 30 minutes with a temperature of 70°C. The mechanism of inactivation is consistent with protein denaturation (Aitken, et al., 2005).

Other physical treatments combine a high pH environment with an exothermic process through the use of lime (alkaline stabilization). To meet the Class A requirement, the alkaline treatment method prescribes raising the pH of the sludge above 12 for a minimum of 12 hours while maintaining the heat generation above 52°C. The pH must remain above 12 for an additional 60 hours, and followed by air drying the biosolids to no less than 50 % dry weight (USEPA, 1999). For treatment methods not currently recognized by the regulatory bodies, all the three types pathogen limit requirements (*salmonella*, enteric viruses, and helminth eggs) must be tested for and met, together with vector attraction reduction. In addition, the biosolids must meet fecal coliform density limit of less than 1000 MPN per gram of total solids (dry weight basis), at the time the sewage is used. Testing for enteric viruses and viable helminth ova can be complicated by the fact that they are not always present in the untreated biosolids. In this case, the treated biosolids are analyzed to see if these organisms survived treatment by spiking the biosolids with known quantities of these pathogens. If the results of the treatment process are below the critical limits, the biosolid meets Class A requirements and will continue to do so as long as the treatment process is operated under the same conditions.

Other hybrid methods, for instance, using electrochemical (EC) disinfection were investigated with some success using *Escherichia coli* (*E. coli*) as the studied pathogen (Li, et al., 2004). Although the killing mechanism of EC disinfection is not fully

understood, it was postulated that the production of short-lived energy rich free radicals, such as O_2^- , OH^- , and ClO_2^- , formed during electrolysis may play a significant role in the germicidal action (Patermarakis and Fountoukidid, 1990). The research conducted by Li et al. (2004) observed a killing efficiency for *E. coli* of 99.9 % in their plug-flow disinfectant column with a current density and contact time as low as 3.5 mA/cm^2 and 3 seconds, respectively. In another study aimed at identifying the mechanism of bactericidal activity of low amperage DC current, Lui et al. (1997) correlated the production of hydrogen peroxide (H_2O_2) in the cathode area with antibacterial activity carried out on *Staphylococcus epidermis* and *aureus*. The production of H_2O_2 at the cathode requires oxygen as expressed in the half-cell reaction describing the electrolysis of hydrogen ions: $O_2 + 2H^+ + 2e^- \rightarrow H_2O_2$. The role of H_2O_2 as the primary bactericidal agent was confirmed in tests carried out under anaerobic conditions, where no zones of inhibition were observed. Using a continuous flow two electrode cell optimized for the synthesis of hydrogen peroxide by the cathodic reduction of oxygen, Drogui et al. (2001) was able to generate a maximum concentration of hydrogen peroxide of 12 mg/l; producing a 3 log reduction in Fecal coliforms from a WWTP effluent after 250 minutes of contact time and an applied current of 1.5 A.

2.1.5.3. Inactivation Methods for the Pathogen Surrogate, *Ascaris suum*, from Biosolids

The parasitic worm or helminth, *Ascaris suum*, is a nematode that infects the intestinal tracts of pigs. Female worms may produce as many as 2 million eggs daily during her lifetime. Figure 2.3 shows the motile larval stage hatching from an ovum whose outer uterine layer has been dissolved with bleach to reveal the interior; while Figure 2.4

illustrates a viable ovum with its outer uterine layer left partially intact after bleaching.



Figure 2.3 Hatching *Ascaris suum* larva (x400 magnification)

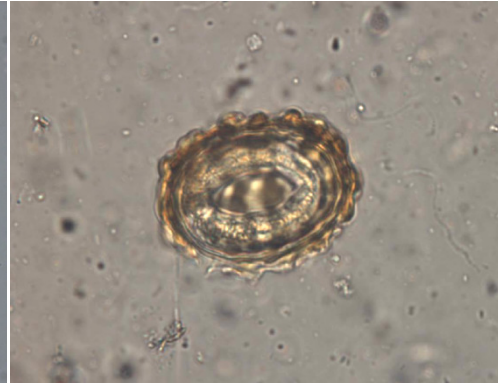
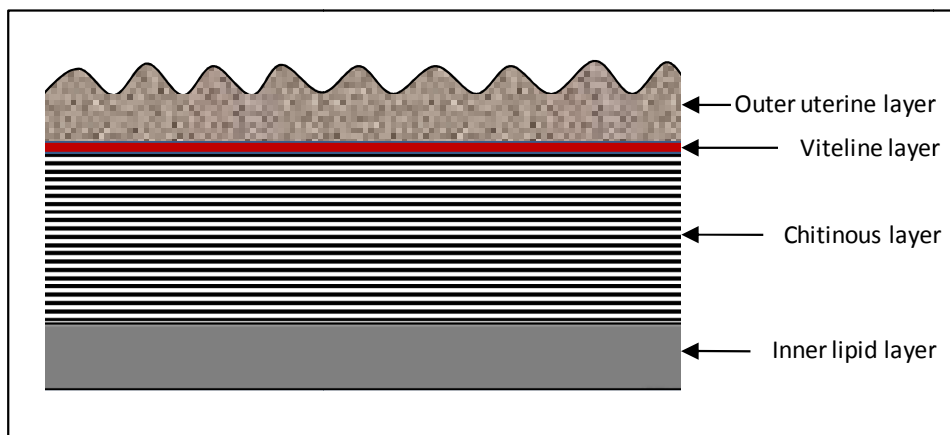


Figure 2.4 *Ascaris suum* ova with the outer uterine layer partially intact (x400 magnification)

These helminth eggs are generally used to assess pathogen inactivation in biosolids since these are generally regarded as the most difficult to inactivate compared to other indicator pathogens (Brewster, et al., 2003). These thick-shelled eggs are resistant to freezing and drying and have the highest survival rate, measured in years, as compared to other indicator organisms like bacteria and viruses which are measured in months (Larsen & Roestroff, 1999). *Ascaris suum*, a swine helminthes, is used as a surrogate for the homologous human parasite, *Ascaris lumbricoides*, because it is considered to be physiologically and morphologically identical (Anderson & Jaenike, 1997).



(Adapted from Wharton (1980))

Figure 2.5 Structure of the *Ascaris* Genus egg-shell

The ova of the *Ascaris* family are extremely resistant to external conditions. The egg shell of the *Ascaris* Genus is composed of four layers (see Figure 2.5): two external lipoprotein coats (the uterine and vitaline layers), a central chitin shell providing structural strength and a thin inner lipid membrane. It is this latter layer which is responsible for the extreme impermeability of the nematode egg-shell to environmental conditions and known to be permeable only to organic solvents and lipid soluble gases such as ammonia (Barrett, 1976). The inner membrane consists of 75 % lipids in association with 25 % proteins. The lipid fraction in *Ascarids* consists of a unique mixture of α -glycosides called ascarosides that are important in the control of the shell's permeability and hatching processes (Wharton, 1983). In an exhaustive investigation of the permeability in *Ascaris* eggs by Barret (1976), decoated and deshelled *Ascaris* eggs were exposed to a wide range of organic and inorganic reagents for 24 hours at 25°C to see if any of them had any effect on the inner lipid layer's permeability. The compounds tested included acids, bases, protein disrupting agents, detergents, oxidizing and reducing agents, organic and inorganic ions, and a variety of proteolytic, amolytic, and lipolytic enzymes. The final results showed that none of the 50 or so compounds tested had any effect on the permeability of eggs, ascertained by the incorporation of the staining fluid: acid fuchsin, suggesting a total lack of reactive groups in the ascaroside membrane. His research did, however, reveal a temperature dependence on the permeability of the *Ascaris* egg. A sudden increase in permeability could be induced at a temperature of 44°C.

Most research devoted to the inactivation of *Acaris suum* in biosolids focused on alkaline treatment (Pecson, et al., 2007; Capizzi-Banas, et al., 2004; Brewster, et al., 2003),

thermophilic anaerobic digestion (Aitken, et al., 2005; Kato, et al. 2003), or chemical treatment by ammonia (Pecson and Nelson, 2005).

A consensus is emerging challenging the conventionally prescribed time-temperature regimes to achieve pathogen free biosolids. Part 503 of the EPA biosolids regulation on processes to further reduce pathogens (PFRPs) and meet class A pathogen criteria prescribes a conservative treatment time, for sludge with less than 7 % solids, of 5 days at a temperature of 50°C and 1 day at 55°C (US EPA, 1999). Likewise, the often cited research by Feachem et al. (1983), establishing the thermal destruction curves for a series of enteric pathogens, indicates that for thermal treatments to reach negligible levels of these pathogens, the treatment time must be longer than 30 minutes at 65°C, 2 hours at 60°C, 15 hours at 55°C, and 3 days at 50°C.

In recent years, the research conducted by Capizzi-Banas et al. (2004) questioned these overly conservative treatment duration by aiming to define, between 50°C and 60°C, the time required for limed sludge to reach a negligible level of viable *Ascaris* eggs. The inactivation threshold was determined by analyzing inactivation kinetics up to a point where negligible levels of viable *Ascaris* eggs were attained for a range of exposure temperatures. Depending on the experimental situation, the inactivation threshold period was found to fluctuate between 5 and 75 minutes at 55°C and between 1 and 8 minutes at 60°C. It must be noted that the addition of lime destroys sludge pathogens not only through exothermic temperature rise but also by the increase in sludge pH with the consequence of increasing the ratio of uncharged ammonia; these two factors may act synergistically to reduce treatment duration and increase pathogen inactivation.

In another set of experiments by Aitken et al. (2005), the inactivation kinetics of spiked poliovirus and eggs from *Ascaris suum* in thermophilic batch reactors containing anaerobic biosolids at temperatures from 49 to 55°C was evaluated. The researchers found that the strong correlation between the inactivation rate and temperature is associated with the Arrhenius relationship linking activation energies and protein denaturation over this temperature range. The study was critical of the conservative EPA time-temperature requirement; it concluded that, for instance at 53°C, the EPA time-temperature equation required more than a 2 orders of magnitude greater time to achieve a 3 log reduction of viable *Ascaris* ova than was predicted by the inactivation rate measured in their study. This and other studies on the inactivation of pathogens further support the case for revising the current EPA time-temperature relationships.

2.2. Electrokinetic Technologies

This section will review the general mechanisms of electrokinetic treatment as well as some important electrochemical reactions occurring therein. The electrokinetic (EK) process has been utilized for decades for the remediation of contaminated soil, and has been proven to be a successful and cost effective method. Many bench and pilot scale studies, summarized by Acar et al. (1995), utilizing EK processes had been effectively used for removal of various heavy metal ions (e.g., Cd, Cr, Pb, Hg, Ni, Cu, Zn), anionic pollutants (e.g., Cl^- , NO_3^- , SO_4^{2-} , CN^-), radionuclides, and several organic compounds (e.g., phenol, benzene, toluene, and trichloroethylene). Removal of up to 90-99 % of some pollutants from soil has been observed under optimum conditions. Over the year different approaches to improve the conventional electrokinetic application have yielded

greater efficiencies in contaminant removal. EK technology offers the potential of unique all inclusive method for the simultaneous dewatering, metal removal, and disinfection of wastewater sludge in one operational unit in a cost-effective manner (Elektorowicz, et al., 2008; Huang, et al., 2008; Elektorowicz et al., 2007; Safaei, 2007; Esmaeily, 2002; Elektorowicz, 1995).

2.2.1. Theoretical Aspects of the Electrokinetic Phenomena

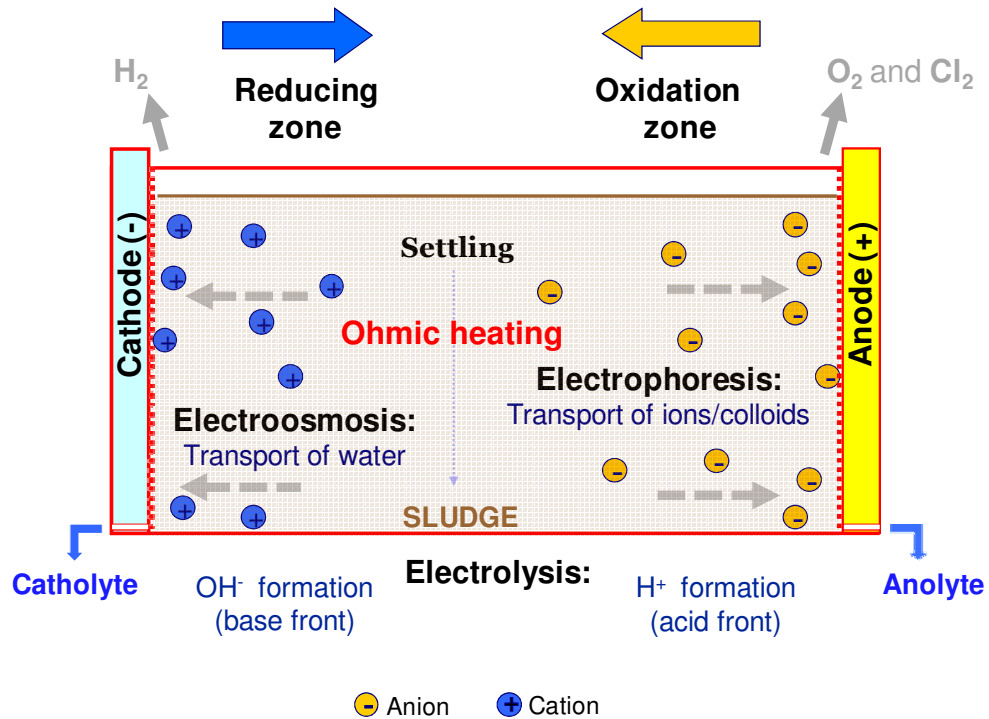
The underlying electrokinetic mechanisms include (Rajeshwar and Ibanez, 1997):

- Electroosmosis: the movement of a liquid adjacent to a charged solid surface when an electric field is applied;
- Electrophoresis: the movement a charged particle (e.g., ions) in an electric field;
- Streaming potential: the production of an electric field due to the movement of an electrolyte under a hydraulic potential;
- Sedimentation potential: The production of an electric field due to the movement of charged particles caused by gravity.

Of these four EK mechanisms, the electroosmosis and electrophoresis processes are the predominantly observable phenomena; with the streaming and sedimentation potentials having only minor contributions, and thus will not be further elaborated on.

When an electric field is produced by the application of a direct current (DC) source between an anode(s) and cathode(s) placed in contact with a conductive medium (e.g., sludge or soil), one or more of these mechanisms can occur and be utilized for the

removal of pollutants. Figure 2.6 illustrates the broader aspects that may be encountered during the EK phenomena.



(Adapted from Elektorowicz et al. (2008))

Figure 2.6 Overview of the electrokinetic phenomena in a sludge matrix

During the electrokinetic process, the application of electric potential produce electrolytic reactions at the electrodes causing oxidation reactions at the anode that decreases the pH and reduction at the cathode which increase the pH (Elektorowicz, 1995). The hydrogen ions (H^+) generated at the anode form hydronium cations (H_3O^+) in the presence of water and advance through the medium toward the cathode principally by electrophoresis (i.e., ionic migration) under the force of the electrical gradient. Fluid advection, due to the prevailing electroosmotic flow, and diffusion, due to the developed chemical gradient, are also factors involved in ionic migration in a soil matrix (Acar and Alshwabkeh, 1996). The negatively charged hydroxyl ions (OH^-) generated at the cathode advance toward the

anode by electrophoresis and diffusion; however, its transport through the medium is masked by neutralization caused by the advance of H_3O^+ towards the cathode (Acar and Alshwabkeh, 1993). In a soil medium, the observed migration of the base front is thus much slower than the advance of the acid front. Consequently, the acid front dominates the changes in the medium's pH (Alshwabkeh and Acar, 1996). Because of the acidification of the medium, desorption and solubilization of the cationic metal species can be facilitated. These metals can then move by electrophoresis towards the cathode, where they can be removed and collected. Negatively charged organic compounds, inorganic anions, and anionic metal complexes will migrate towards the anode. Furthermore, the applied electric field induces an electroosmotic flow of fluid towards the cathode initiated by the dipolar interactions between the water molecules and the soil solids (Acar, et al., 1995); this phenomenon may perhaps also contribute to the transport of uncharged organic molecules out of the medium.

The following chapters outline the fundamentals of the electrokinetic phenomena and tie together the elements into a concise representation.

2.2.1.1. Principal of Electrophoresis

Electrophoresis is the migration of charged particles in a solution under the influence of an electric field. Different particles with different charges and/or sizes migrate with different velocities. The electrostatic force (F) exerted on a particle in solution is proportional to the net charge of the particle (q) and the electric field strength or voltage gradient (E) (Kok, 2000):

$$F = q \cdot E \quad (1)$$

The direction of the force is to the electrode with a charge opposite to that of the particle. Its movement is opposed by viscous drag forces in the solution, which increase proportionally with the electrophoretic velocity (v_e) of the particle. For a spherical particle, the viscous force is given by Stokes' equation:

$$F = 6\pi\eta \cdot r \cdot v_e \quad (2)$$

Where η is the viscosity of the solution and r is the effective radius of the particle. The effective radius determining the mobility is the radius of the moving particle together with its hydration shell: the cloud of water molecules bound to it. After a very short time, equilibrium is reached and the particle then moves at a constant velocity through the solution:

$$v_e = \frac{q \cdot E}{6\pi\eta \cdot r} \quad (3)$$

To better compare the behavior of specific ions in solution subjected to different field strengths, an ionic mobility constant can be defined as:

$$\mu_i = \frac{v_e}{E} \quad (4)$$

Where the dimension of ionic mobility (μ_i) is given in $\text{m}^2 \cdot \text{V}^{-1} \cdot \text{s}^{-1}$. From the equations above, the mobility of any spherical particle can be defined by:

$$\mu_i = \frac{q}{6\pi\eta \cdot r} \quad (5)$$

Thus at a given electric field strength and viscosity, the extent to which the different ions or charged particles will migrate in a solution is related to both their charge (q) and effective radius (r). The application of the above equation to a sludge medium requires the simplifying assumption of spherical sludge flocs.

In Table 2.2, the mobility of a number of simple inorganic ions in water at infinite dilution (i.e. with an ionic strength approaching zero) and 25°C are given.

Table 2.2 Mobility of some inorganic ions

Cations	μ ($10^{-9} \text{ m}^2 / \text{V} \cdot \text{s}$)	Anions	μ ($10^{-9} \text{ m}^2 / \text{V} \cdot \text{s}$)
H ⁺	362	OH ⁻	205
Li ⁺	40	Cl ⁻	79
Na ⁺	52	HCO ₃ ⁻	46
K ⁺	76	NO ₃ ⁻	74
NH ₄ ⁺	76	SO ₄ ²⁻	83
Ca ²⁺	62	PO ₄ ³⁻	72

(Adapted from Andrews (1983))

The unusually high mobilities of the H⁺ and OH⁻ ions is due to the fact that, in addition to mass transport, these ions have the ability to move virtually by rearranging the electronic structure of adjacent water molecules.

The concentration of solute (its ionic strength) has a significant effect on the electrophoretic mobility. In an electrolyte solution an ion is surrounded by other ions. The excess of oppositely charged ions around a certain ion can be represented as a diffuse ionic cloud, with a charge just neutralizing that of the central ion. When the ionic strength of the solution (I_s) [mol/l] increases, this ionic cloud will be denser. When subjected to an electric field, this ionic cloud surrounding the central ion will migrate in a direction opposite to that of the central ion; thus, the mobility of an ion decreases when the ionic strength of the solution is increased. This decrease in mobility is found to be approximately proportional to $I_s^{0.5}$ (Friedl, et al., 1995).

Since the electric field only exerts a force on charged species, the observed mobility of weak acids and bases will depend on their dissociation equilibrium which in turn depends on the pH of the solution. Moreover, amphoteric compounds, such as amino acids which

contain both positively and negatively charged functional groups, can migrate towards the positive or negative electrode depending on the pH of the solution. At low pH, the effective mobility approaches the mobility of the cation, and at high pH, that of the anionic species (Kok, 2000).

Another factor influencing the mobility of charged species is their potential complexation with ions present in the electrolyte solution. For instance, in a solution rich in chloride or hydroxide, metal ions may migrate towards the anode (positive electrode). In this case the metal cation effectively behaves in solution as a negative metal oxide or chloride complex (Kok, 2000).

2.2.1.2. Electrolysis

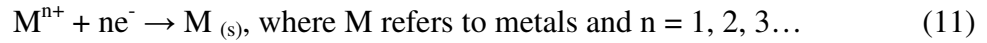
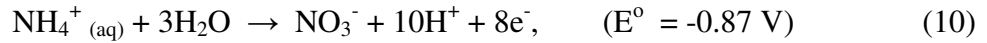
The passage of electrical current through an aqueous solution is always associated with electrochemical reaction at the electrodes. The most predominant of which is the hydrolysis of water, as it constitutes the bulk of the solution. Water at the positive electrode, or anode, is oxidized to oxygen and protons according to the oxidation half-reaction (Ebbing and Gammon, 2008):



At the negative electrode, or cathode, water is reduced to hydrogen and hydroxide anions according to the reduction half-reaction:



Secondary reactions may exist at the electrodes depending on the concentrations of available ions, the pH of the solution, and their electrochemical half-cell potential. Several possible electrochemical reactions under standard condition are enumerated below (Ebbing and Gammon, 2008):



Chemical species whose oxidation half-reaction potential (E°) is larger (i.e., less negative oxidation potential) are the most readily oxidized.

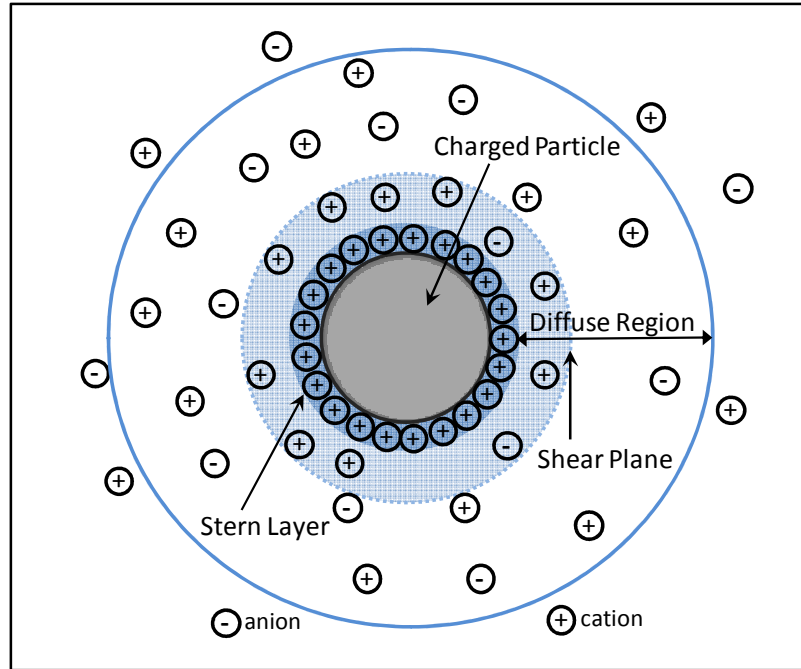
According to Faraday's law, the number of moles (n) of ions produced at an electrode is directly proportional to the amount of charge (C) generated, with $n = C/F$, where F is the Faraday constant ($96\,485 \text{ C/mol e}^-$). If we take the example of the electrolysis of water, a current of 1 A , in C/s , passing through a cell for a period of 1 hour will generate:

$$1 \frac{\text{C}}{\text{s}} \cdot 3600 \text{ s} = 3600 \text{ C}, \text{ therefore, } n = \frac{3600 \text{ C}}{96485 \frac{\text{C}}{\text{mol e}^-}} = 0.037 \text{ mol e}^- \quad (12)$$

By the stoichiometry of water half-reactions above, each proton and hydroxide ion has one electron equivalent, consequently, after one hour about 37 mmol of H^+ and OH^- , or 37 mg H^+ and 629 mg OH^- respectively, are produced in a two electrode cell. Depending on the volume of the sludge and its buffering capacity, the pH at each electrode can alter dramatically. Furthermore, from the same stoichiometric equation, the flux of O_2 is one quarter the flux of H^+ at the anode and the flux of H_2 is half the flux of OH^- at the cathode. The amount of gas produced can be significant and was found to influence the electroosmotic flow regime in soil matrices (Alshawabkeh, et al., 2004), presumably by the formation of gas bubbles at the electrodes' surfaces creating obstacles to the flow of ions and liquids.

2.2.1.3. Principal of Electroosmosis

Electroosmosis is the movement of a liquid (i.e., generally water) induced by an excess positive charge on a porous media when subjected to an electric field (Eykholt and Daniel, 1994). When an aqueous solution of electrolytes is in contact with charged colloidal and humic solids, there is a charge separation between the solution and the particles. As colloidal and humic particles are usually negatively charged at standard pH (Acar, et al., 1995), in order for the system to remain electrically neutral, the electrolytic solution develops a net positive charge with a buildup of positive ions close to the particles attracted by electrostatic forces (Figure 2.7). This ionization effect creates an electric double layer (or potential difference) which defines the zeta potential (Ohshima, 2006). The electrolytic solution surrounding the particles is present as two fractions: an inner region where the counter ions are strongly bound, called the Stern layer, and an outer diffuse region where the ions are weakly attracted. The thickness of the electrical double layer around the charged particle is determined by the amount of counter ions recruited to balance out the surface charge. Within the diffuse region there is a theoretical boundary inside which the ions and the particles form a stable unit. This boundary between the stagnant ions and the mobile ions is called the shear plane. The summation of charges constituting the electrostatic potential (i.e. surface charge + adsorbed ions + diffuse ions) within the shear boundary defines the strength of the zeta potential (Hiemenz and Rajagopalan, 1997).



(Adapted from Hiemenz and Rajagopalan (1997))

Figure 2.7 Schematic representation of the distribution of ions around a charged particle in solution.

At a given field strength, the electroosmotic mobility, μ_{eo} , is described by the Smoluchowski equation (Smoluchowski, 1914):

$$\mu_{eo} = \frac{\varepsilon_0 \varepsilon_r \zeta}{\eta} \quad (10)$$

where ε_0 is the permittivity of vacuum, ε_r is the relative permittivity of the liquid, and ζ is the zeta potential; it is seen that the electroosmotic mobility is also inversely proportional to the viscosity.

When a voltage gradient is applied, the electric field exerts a force on the excess positively charged ions in the diffuse double layer. The mobile ions adjacent to the shear plane, together with the water molecules associated with them, migrate in the direction of the cathode and induce the solution between the particles to move in the same direction by imparting a strain field or drag by the viscosity of the fluid (Acar and Alshawabkeh,

1993). Generally in a soil medium, the wider the electrical double layer, the broader the extent of the drag reaches into the pore fluid, the more uniform will be strain field, and the greater the electroosmotic flow (Acar, et al., 1995). The velocity (v_{eo}) of the electroosmotic flow is proportional to the electric field strength, and is defined similarly to that of the ionic mobility (Kok, 2000):

$$v_{eo} = \mu_{eo} \cdot E \quad (13)$$

where (μ_{eo}) is the dimension of electroosmotic mobility also measured in $m^2/V \cdot s$. This formulation is analogous to the one used to describe the flow of fluids through a volume of soil given by Darcy's law, whereby the fluid velocity is linearly proportional to a driving force as expressed by (Mitchell, 1991):

$$Q' = k_h \cdot \frac{\Delta h}{\Delta l} \quad (14)$$

where Q' is the specific fluid discharge (m/s), $\Delta h/\Delta l$ is the hydraulic gradient, and k_h is the hydraulic conductivity (m/s).

If the electroosmotic mobility is greater than the ionic mobility of the ions in solution, then these ions will migrate towards the cathode with a flux (J) reflecting an apparent mobility (μ_{app}) (Kok, 2000):

- For cations: $J_c = (\mu_{eo} + \mu_i) \cdot E = \mu_{app} \cdot E \quad (15)$

- For anions: $J_a = (\mu_{eo} - \mu_i) \cdot E = \mu_{app} \cdot E \quad (16)$

- For neutral particles: $J_n = \mu_{eo} \cdot E \quad (17)$

The composition of electrolytes and the nature of colloidal matter in the sludge will thus greatly affect the electrokinetic flow.

The application of an electrical potential gradient results in a current intensity which is a function of the medium's conductivity; this current intensity establishes the amount of ionic species that can be displaced through Faraday's Law. However, Pomes et al. (2002), working on electrokinetic remediation of soils, demonstrated that at high solute concentration, a non-linear relationship exists between the ionic strength of the solution and the current intensity; this means that the presence in solution of higher concentration of ionic species (particularly others than the pollutants) does not improve the EK process. For instance, a solution concentration five times higher (e.g., 0.01 M and 0.05 M) gives concentrations at the cathode about five times higher, but this trend cannot be extrapolated when a concentration of 0.14 M is used. The influence of the solution's concentration on electroosmosis is thus not an obvious one, and possibly due to a slight modification of the zeta potential for the system studied (Pomes, et al., 2002).

2.2.2. Previous Studies on EK Treatment of Biosolids

Although applications of EK technology towards soil remediation are numerous, relatively few studies can be found with applications towards the treatment of wastewater sludge. In recent years, EK applications have extended to include the treatment of industrial sludges and biosolids. In one particularly notable study, EK experiments conducted by Yuan and Weng (2006), using processing fluids to enhance the removal of heavy metals from industrial wastewater sludge, showed removal efficiencies varying between 43.4 % and 78 % by using 0.024 M of citric acid and a voltage gradient of 1.25 V/cm. Subsequent analysis of the binding forms of heavy metals with the sludge matrix revealed a transformation from a more difficult extraction type (residual and sulfate

fraction) to an easier extraction type (exchangeable, sorbed, and organic fraction) after the EK treatment.

Effect of EK application on wastewater sludge was studied by a number of students at Concordia University under the supervision of Dr. Elektorowicz. In a study conducted by Esmaily (2002), EK was applied for the removal of water, metal, and organic compounds, together with Fecal Coliform (FC) elimination in biosolids. The result of this research showed an average removal of 84 % for zinc, 100 % for Cd and Pb, and 91 % for iron. The results also demonstrated a negative growth of FC in units with voltage regimes between 0.5 and 1.5 V/cm (Esmaily, et al., 2006). It was demonstrated that an essential factor controlling the transfer of metals from an immobile solid phase to a mobile fluid phase is the pH gradient developed in the system (Elektorowicz, 1995). These results were verified at the pilot-scale level by Abdoli (2009) through the use of a newly designed system (Elektorowicz and Oleszkiewicz, 2009) which demonstrated maximum Pb and Zn removal efficiencies of about 75 % and 90 %, respectively, with the application of a relatively low voltage gradient, and a maximum dewatering capability of 70 % TS using a higher voltage gradient.

In another research, Huang et al. (2008) used five different combinations of biosolids: primary, combined primary and secondary, attached growth secondary, waste activated and anaerobically digested sludges. The EK units were run on a voltage regime between 0.5 and 2 V/cm, for 6 to 9 days. The treated biosolids were evaluated for presence of FC and *Salmonella*. An 11 log-reduction for *Salmonella* was observed in the unit containing the anaerobically digested sludge. No FC were observed in any of the units after the EK treatment. The highest total solids content of 98 % TS was achieved with the lowest

voltage gradient in combination with the addition of a sludge conditioner. An average reduction of 50 % for volatile solids (VS) was observed; exceeding the 38 % VS reduction precondition for achieving a stable biosolid that meets the vector attraction reduction requirement (US EPA, 1999).

The research performed by Safaei (2007) assessed the optimal condition for the inactivation of *Clostridium perfringens* and Reovirus in anaerobically digested biosolids by studying the synergetic effects of different enhancement agents, such as a di-ammonium phosphate conditioner and two commercial biocides in conjunction with EK technology. Optimal inactivation results were demonstrated with a 4.5 log reduction in *C. perfringens* and a complete inactivation of Reovirus.

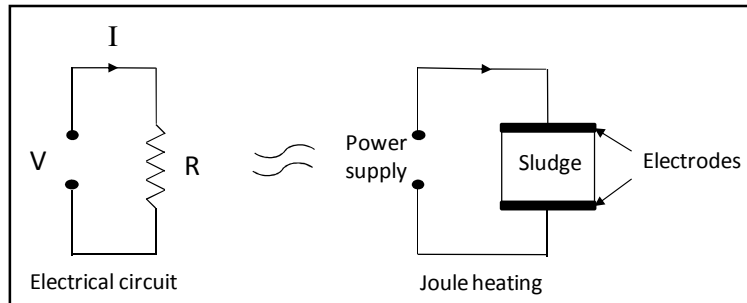
The author of the present thesis formerly assessed the application of an enhanced EK process at the laboratory of Dr. Dwight D. Bowman in Cornell University with both anaerobically digested and mixed primary and secondary sludges, using the optimally derived biocide concentrations, from Safaei (2007), and di-ammonium phosphate on the inactivation of *Ascaris suum* ova. The inactivation results, measured as the percentage of viable embryonated ova, were for the most part not statistically different from either control treatments: one with the addition of conditioners but with no applied voltage, or the other with the application of voltage alone. However, a 3 log reduction in *Ascaris suum* viability did occur in the region of the anode of both anaerobic and mixed biosolids subjected to the highest concentration of conditioner (13 mg/l and 40 mg/l, respectively), and a voltage gradient of 1.5 V/cm. Although the temperature inside the bench-scale unit was not measured directly, it was hypothesized that ohmic heat generation in proximity of the anode, evidenced by the amount of vapour condensation inside these enclosed

units, due to increases in that region's resistivity was sufficient to produce the observed inactivation results. Another factor that may have contributed to the observed inactivation result is the formation of reactive chemical species from the oxidation of ammonium and other compounds in the anode zone. The former assumption was the motive which led to the present research with the aim to deliberately induce ohmic heating in the sludge and to define the temperature range wherein the inactivation of *Ascaris ova* can be observed to occur.

2.2.3. Thermal Treatment by Ohmic Heating

Although the principle of ohmic heating has been known for a few centuries, it is only in the last 30 or so years that it has been considered a viable means of thermally treating sewage sludge. Ohmic heating presents the potential of heating fluids by generating heat within them and as such this method appears ideally suited to heating viscous products contain particulates like wastewater sludge, leading to a much more uniform internal heat distribution which in turn will produce more uniform pathogen inactivation (Sun, 2005). In a conventional heating system, such as oven heating and drying methods, the thermal conductivity of the medium controls its heating rate. In an ohmic heating process, electrical conductivity is the controlling factor. The ohmic heating technique offers a significant advantage over conventional thermal processes because the conventional heating of sludge relies on the build-up of a time dependent thermal gradient in the liquid/solid slurry. Conduction is a relatively slow process; therefore, materials in close contact with the heat sources will be over treated compared to material distant from the heat source which may not obtain an adequate high temperature exposure (De Alwis, 1990).

Figure 2.8 Conceptual model of ohmic heating



(adapted from Li (2004))

Some insight on the operation of an ohmic process can be drawn by using the experience from the resistance heating of metals. Ohmic heating occurs when an electric current passes through an electrical conductor of finite resistance, or reciprocally of finite conductance; this is illustrated in Figure 2.8 using the analogy of a closed electrical circuit. In this instance, the sewage sludge can be considered as a conductive electrolytic solution: a mixture of organic and inorganic ions in solution together in an array of charged solid particles. Provided this conductive solution has uniform resistance, the resultant heat generation will also be uniformly distributed throughout the solution. As shown in Figure 2.8, if an electrical potential or voltage (V) is applied at the ends of two electrodes, the passage of electric current (I) through a conductor or an electrically conductive material of electrical resistance (R), it will obey Ohm's Law:

$$I = V/R \quad (18)$$

When a current is passing through a resistive medium, the power (P), in watts, dissipated as heat in the conductor, due to the electrical resistance of the medium, is given by Joule's Law:

$$P = I^2 \cdot R = V^2/R \quad (19)$$

The heat generated in a material can be altered by either changing the current flow, the voltage potential, or the bulk resistance (Raj and Hunter, 1991). The resistance of an electrically conductive (electrolyte) solution can be given by:

$$R = \rho L/A \quad (20)$$

where ρ is the specific electrical resistivity (Ohm·m), L and A are the respective length and cross-sectional area of the cell.. Conversely, the conductance G is given by:

$$G = \kappa A/L \quad (21)$$

where κ is the specific electrical conductivity (ohm⁻¹·m⁻¹ or siemens· m⁻¹). The electrical conductivity of the solid/liquid fraction of the sludge slurry is the composite of two factors: the conductivity of the solids and the conductivity of the liquid solution containing a considerable amount of dissolved ionic species (Samaranayake, 2003).

The ohmic heating of fluids is better illustrated using the equivalent field form of the equations (De Alwis, 1990). In this respect, the power dissipated per unit volume (W), in W·m⁻³, can be defined in terms of the voltage gradient (E), in V·m⁻¹, and the current density (J_{CD}), in A·m⁻² (Petersen, et al., 2004):

$$W = E^2 \cdot \kappa = \frac{J_{CD}^2}{\kappa} \quad (22)$$

Assuming conductivity is constant, the amount of heat generated increases proportionally to the squared value of the applied voltage gradient or the current density.

Whenever the current lines are parallel within the cell, a heating power is delivered homogenously within the solution. The distribution of heat generation will thus depend on the local values of current density and electric field strength (De Alwis and Fryer,

1992). At a constant applied voltage, the critical property influencing the rate of heating is the electrical conductivity, which in turn depends on two critical factors: the temperature and ionic strength of the solution (Wang and Sastry, 1997).

The dependence of the conductivity on temperature is most often approximated by a linear function for temperature changes less than 40 degrees (Petersen, et al., 2004):

$$\kappa = \kappa_0 [1 + a(T - T_0)] \quad (23)$$

where κ_0 is the conductivity at the temperature T_0 , and a is the temperature coefficient of variation. This coefficient is expressed as the percentage increase in conductivity for a temperature change of 1°C, and can be determined experimentally for a given solution using the following equation (Barron and Ashton, 2005):

$$a = \frac{(\kappa - \kappa_0) \cdot 100}{\kappa_0 (T - T_0)} \quad (24)$$

The temperature compensation slope for most naturally occurring waters is generally in the range of 1.8 to 2.0 % per °C. Concentrated salt, acid, and alkali solutions have slopes of about 1.5 % per °C. (Aquarius Technologies PTY Ltd., 2000).

The increase in electrical conductivity with temperature leads to a phenomenon called the autothermal effect. Take the example where a fluid is subjected to a constant potential gradient, an increase in temperature due to ohmic heating increases the electrical conductivity. The increase in conductivity results in a higher current flow, which in turn, boosts the heating generation term (W); this increases the local temperature even further, which again contributes to intensifying the current density, and so on, in a positive feedback loop (Sastry and Palaniappan, 1992).

The increase in electrical conductivity with temperature is largely explained by related changes in the viscosity and degree of ionic disassociation of the electrolyte. The conductivity of a solution is dependent on the sum of the conducting properties of all the electrolytes present in the solution (Atkins & de Paula, 2002):

$$\kappa = \sum_{i=1}^n \mu_{ep_i} \cdot |q_i| \cdot c_i \cdot N_A \quad (25)$$

where μ_{ep_i} is the electrophoretic mobility (synonymous with ionic mobility), q_i is the effective charge of the ions, c_i is the concentration of the ions, with the index i referring to the different ions in the solution, and N_A is Avogadro's constant.

In combination with the standard approximation of the ionic mobility (μ_i), seen in equation (5), we get (Atkins and de Paula, 2002):

$$\kappa = \frac{1}{\eta} \sum_{i=1}^n \frac{q_i^2 \cdot c_i \cdot N_A}{6\pi \cdot r_{hi}} \quad (26)$$

where η is the viscosity of a solution and r_{hi} is the hydrodynamic radius of the individual ions. As seen from equation (26), the conductivity is expected to be inversely proportional to the viscosity. The viscosity, η , of a liquid decreases with temperature and is inversely related to temperature; by fitting experimental data for the viscosity of water as a function of temperature, the following equation can be obtained (Knox and McCormack, 1994):

$$\eta = 2.761 \times 10^{-3} \cdot \exp\left(\frac{1713K}{T}\right) \quad (27)$$

Although equation (27) accounts for a significant part of the observed temperature dependence of conductivity, the ionic strength of an electrolyte in relation to the degree of ionic dissociation of the electrolytes in solution is also implicated in this phenomenon. The chemical disassociation which influences the effective charge and the hydrodynamic

radius of the different solutes is also temperature dependent. The dissociation constant is related to the temperature via the Arrhenius equation (Atkins and de Paula, 2002) which gives the temperature dependence of the rate of a chemical reaction. The Arrhenius equation is commonly generalized for many chemical reactions as a doubling in the reaction rate for every 10°C increase in temperature. This may especially influence the conductivity of solutes that are not fully ionized at room temperatures.

The elaboration of a theoretical account of temperature on conductivity can be seen to tie directly to the influence of ohmic heating on the EK processes of electroosmosis and electrophoresis through changes in the viscosity of the solution and its chemical composition.

In studying ohmic heating as a method of food sterilization, Sastry and Palaniappan (1992) found that the use of high solids concentrations is favourable to rapid heating. This is because particle-liquid mixtures heat at rates which depend on the relative conductivities of the phases and on the volume fractions of the respective phases. As the solids concentration increases, the parallel conduction paths through the fluid are increasingly restricted, forcing a greater proportion of the total current to flow through the particles. They, thus, concluded that sterilization by way of ohmic heating is most suited for high particle concentration mixtures. Their findings, therefore, have some important implication on any variety of particle-liquid mixtures, as is the case with biosolids.

The principal mechanisms of microbial inactivation in ohmic heating are thermal in nature. Recent research indicates that a mild electroporation mechanism may occur

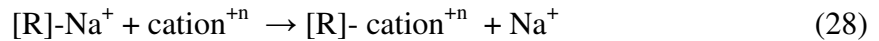
during ohmic heating. The principal reason for the additional effect of ohmic treatment may be its low frequency (50-60 Hz), which allows cell walls to build up charges and compromise their integrity by the formation of micro-pores in the cell walls (USFDA, 2000).

One of the main challenges in ohmic heating is controlling the divergence of electrical energy through Faradic reactions (i.e., electrochemical reactions) at the electrode-solution interface (Amatore, et al., 1998). The main Faradic reactions that take place can include the electrolysis of the solution and the corrosion of the metal electrode, either directly or by the electrochemical generation of corroding chemicals (e.g., H^+) (De Souza, et al., 1995).

2.2.4. Ion Exchange Textiles

Ion exchange is widely used as a technology in the removal of metals. It has been proven effective in removing heavy metals such as cadmium, lead, and mercury. The ion exchange mediums generally consist of cationic and anionic exchange resins or textiles. There are also amphoteric exchangers that are able to exchange both cations and anions simultaneously. These can be further subdivided into strong acid and strong base, or weak acid and weak base exchange media. The ion exchange media can be unselective or have binding preferences for certain ions or classes of ions, depending on the chemical structure of the functional groups. During the cationic exchange process, multivalent cations with larger atomic radii and atomic charge will preferentially adsorb onto the media and displace sodium atoms linked with the functional group embedded in the

medium. In an aqueous environment, the following reaction occurs instantly, where [R] is the exchange media (Peavy, et al., 1985):



The process of ion exchange is generally reversible and the ion exchange media can be regenerated by saturating the media with an excess of the original ions; in the example above, this can be achieved with a solution of brine water.

The use of ion exchange resins and textiles in the treatment of water and wastewater is pervasive, however, its use in conjunction with electrokinetic treatment is lacking. Choudhury (1998) and Elektorowicz et al. (1996a) have experimented with the use of ion exchange textiles in the electrokinetic removal of lead and nickel from natural clay soils. The results obtained demonstrated good removal efficiencies and the potential for the application of ion exchange textiles in soil remediation. The principal obstacle of the standard EK method is related to the solubilization of these metals in the pore water phase and the generation of insoluble hydroxides at the cathode resulting in a significant fraction of the contaminants being cut-off from electrokinetic transport. This problematic was alleviated with the incorporation of the chelating agent: Ethylenediaminetetraacetic acid (EDTA). In another study by Abdoli (2009), cationic and anionic exchange textiles were applied to electrodes during the electrokinetic treatment of biosolids with optimal results in heavy metal removal compared to trials without the use of such textiles.

2.3. Innovative EK Technology

The use of EK towards sludge treatment is a relatively new technology with a growing body of research, mainly focusing on dewatering and heavy metal removal. This study aims to contribute to this field of research by addressing the additional dimension of pathogen control and elimination through the optimal application of enhanced EK techniques towards the inactivation of *Ascaris suum* ova, a standard indicator of the quality of biosolids. The thesis develops a unique EK treatment for the purpose of achieving exceptional quality biosolids by manipulating the applied electrical gradient and sludge conditioner to induce ohmic heating within the sludge for a predetermined period of time sufficient to achieve a near complete inactivation of the pathogen, and in addition, to improve the extraction of water, metals and other ions from the biosolids.

3. Experimental Methodology

This research was performed in four experimental phases:

- I. The first phase consisted of designing the EK reactor cells (both bench and pilot scales) and the *Ascaris* egg chambers, and elaborating the experimental conditions for each test. The collection of sludge from the Auteuil WWTP and the grinding of the sludge conditioners used.
- II. The second phase consisted of a series of bench-scale trials to evaluate three different conditioners (i.e., ammonium nitrate (AN), di-ammonium phosphate (DAP), and urea) for their efficiency on dewatering and heating rates. The best conditioner was chosen and further testing was performed at different concentrations and voltage gradients to investigate the empirical relationships between these two parameters.
- III. The third phase implemented the optimal conditions of the latter stage on a series of bench-scale experiments with *Ascaris suum* ova. A series of ohmic heating screening tests were conducted at target temperatures, ranging between 40°C and 70°C, in order to determine the minimal temperature at which 99.9 % inactivation of the pathogen was attained. A parallel set of convective heating tests, using a hot plate, was conducted as a control reference. A further control trial was performed to examine the effect of the applied electric current on *Ascaris* inactivation in the absence of heat, by placing the cell in an ice bath.
- IV. The last phase of the study consisted of implementing the target inactivation temperature established in the previous phase towards subsequent bench-scale and pilot-scale experiments to evaluate the performance of biosolids under enhanced

EK treatment in terms of the broader physical and chemical parameters: pH, total solids content (TS), volatile solids content (VS), heavy metal content (Cd, Cr, Cu, Fe, Pb, and Zn), and ion content (NH_4^+ , NO_3^- , and PO_4^{3-}), in addition to *Ascaris* ova inactivation. For the bench-scale trials, two replicate conditions were implemented: one without the application of ohmic heating and the other without the addition of conditioner, as control conditions. For the pilot-scale tests, similar parameters of conditioner concentration and voltage gradients as the bench-scale were implemented toward two pilot-scale tests in order to evaluate those same physical, chemical, and biological performances when the dimensional and electrical variables are scaled-up. A final pilot test assessed the implementation of multi-functional electrodes consisting of a secondary layer of ion exchange textiles.

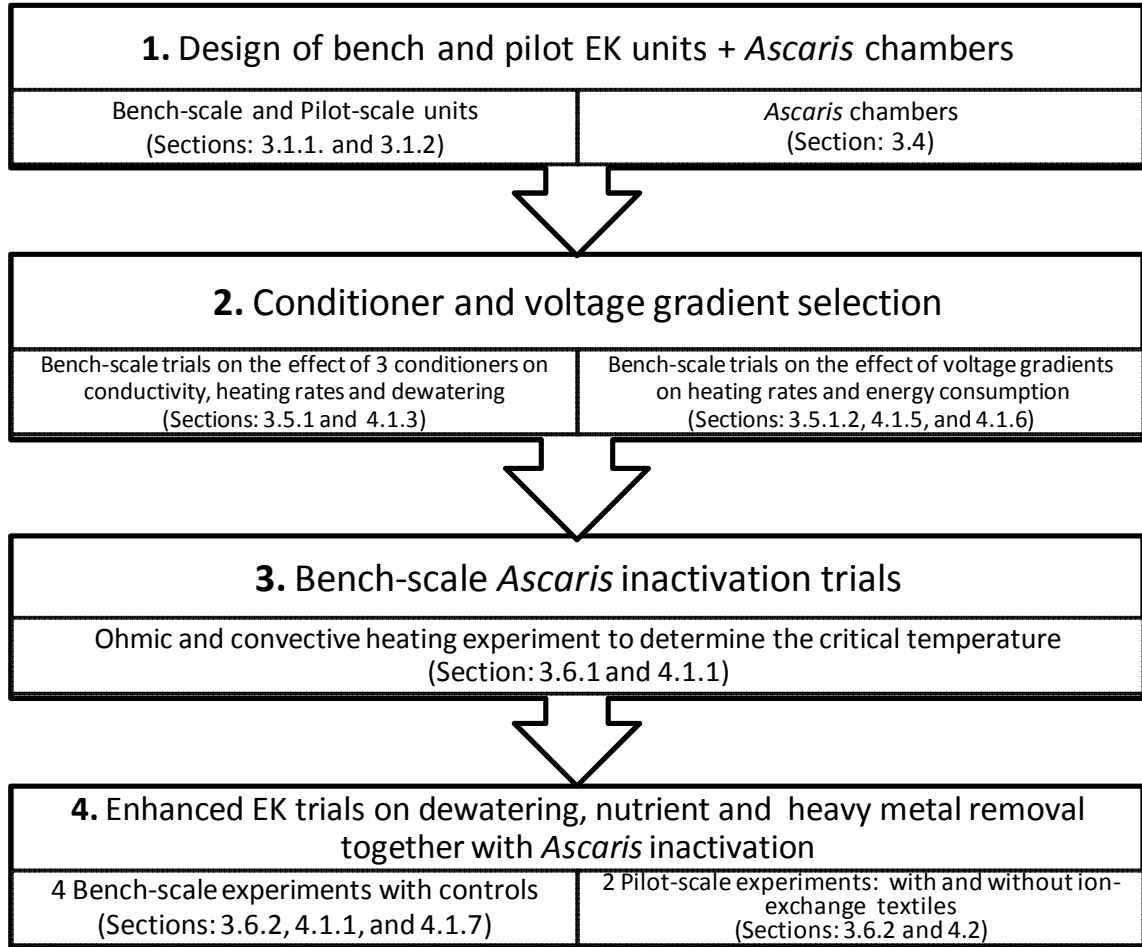


Figure 3.1 Flow chart of experimental methodology

3.1. Set-up of Bench and Pilot Units

The set-up essentially took the form of an electrolytic cell. An electrolytic cell has three defining parts: an electrolyte and two electrodes (a cathode and an anode). The electrolyte can be any liquid with soluble ions (e.g., wastewater sludge).

3.1.1. Bench-Scale Units

The bench-scale EK units consisted of rectangular clear Plexiglas cells (Figures 3.2 and 3.3) with internal dimensions of 23 cm (length) by 5 cm (width) by 7.5 cm (height). Two types of cells, permeable and impermeable, were utilized during the bench scale

experiments. For the ohmic heating trials and *Ascaris* inactivation trials (phases 2 and 3), the cells were impermeable in order to maintain constant volume conditions of 700 (± 7) ml of sludge in each experimental run. At each extremity, a flat 0.5 mm steel plate electrode was inserted. The distance between the electrodes was 23 cm and the effective geometric surface area of each electrode involved in ohmic heating was constant at 30 cm² with that volume. Figure 3.4 illustrates the two types of steel electrodes used. To minimize heat losses, strips of foam insulation (1.5 cm thick) were fixed to the exterior of the cell with masking tape and the top wrapped with cellophane. Three glass red-dye thermometers (-10°C to 100°C), spaced at 5.75 cm intervals and embedded in a Plexiglas support, were inserted into the cell to monitor heating rates.

For the combined heating, dewatering, and *Ascaris* inactivation trials (phases 2 and 4), the cells were rendered permeable by creating two 0.5 cm diameter holes at the base of both ends of the cell. The steel plate electrodes were perforated with eleven 0.5 cm diameter holes and covered with 200 stainless steel mesh to allow the sludge liquors (“Anolyte” from the anode and “Catholyte” from the cathode) to flow out of the cell, but retain the particulate matter. The effective surface area of each electrode was thus reduced to 26.5 cm². The sludge liquors were collected by gravity into 300 ml beakers placed at either end, under the cell.

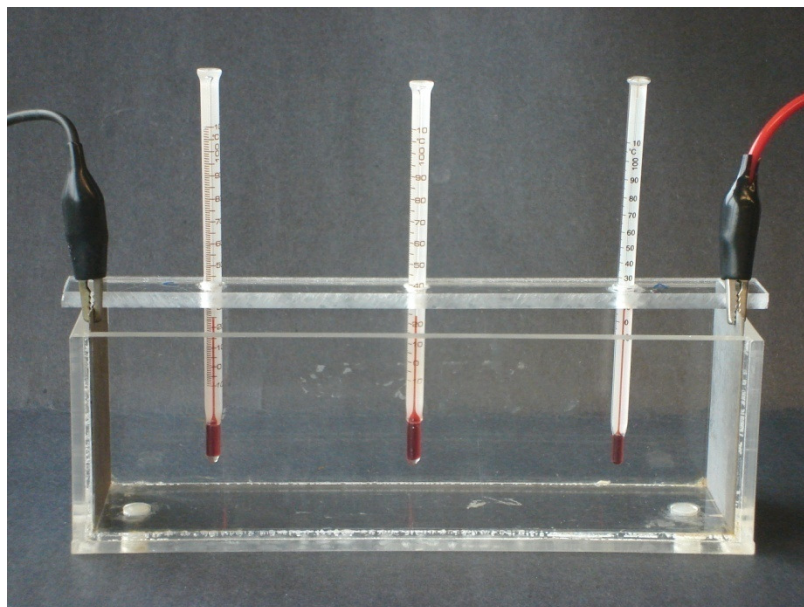


Figure 3.2 Bench-scale EK unit

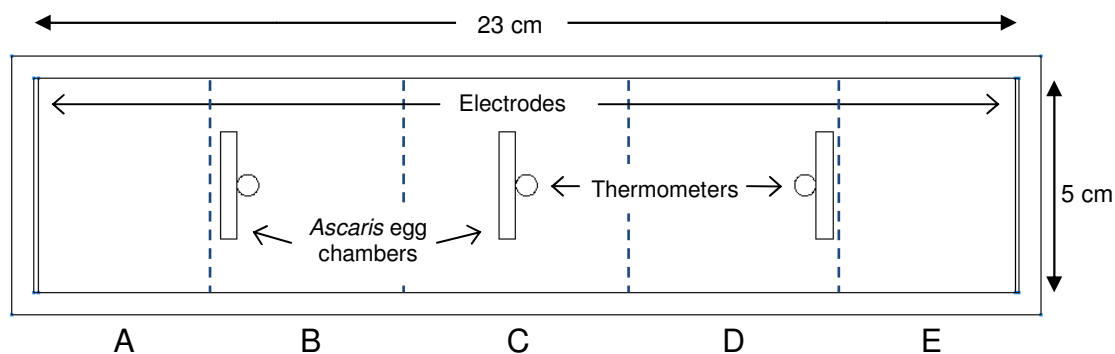


Figure 3.3 Diagram of bench-scale EK unit

The electrodes in the cells were connected, either single or in parallel, to a power supply. The DC power supply, Lambda model GEN 150-10, was operated under constant voltage conditions. The unit possessed a maximum voltage and current capacity of 120 V and 10.5 A, respectively. The AC power supply was an analogue Variac, model 130, with a maximum output of 115 V and 15 A at 60 Hz. The voltage gradients applied during the sets of bench-scale experiments were 2, 2.5, 3, 4, and 5 V/cm. When the two or more cells were connected in parallel with the power supply, digital multimeters were

connected in series with each cell to be able to monitor the variations in amperage. The current density at the electrode surface with a surface of $A = 30 \text{ cm}^2$ can be calculated by $J = I/A = 33.3 I$, in mA/cm^2 .

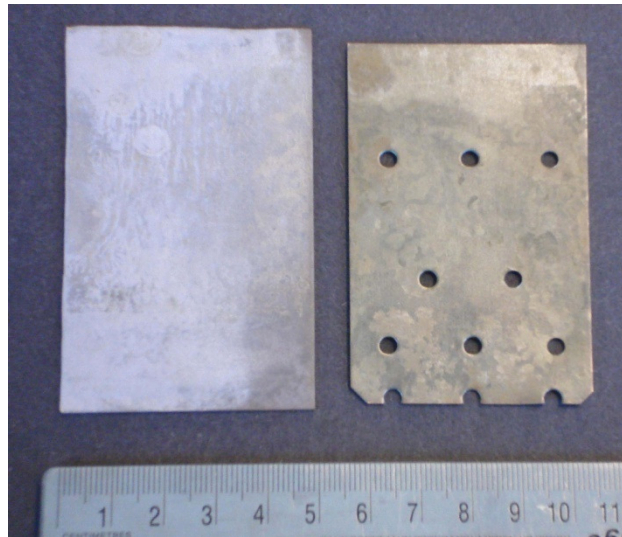


Figure 3.4 Steel plate electrodes (left: inactivation trials, right: dewatering trials)

3.1.2. Pilot-Scale Units

The pilot scale EK unit consisted of an insulated 35 liter Coleman[®] cooler with the lid removed. The internal dimensions were 55 cm in length and 28 cm in width (Figure 3.5). An initial sludge volume of 26 liters was used for the two pilot tests; this volume produced in a sludge depth of 18 cm. The electrodes used for the tests consisted of two perforated stainless steel pipes of 5.1 cm diameter each fixed at both ends of the unit. The extraction of the accumulate anolyte and catholyte inside the hollow electrodes was done with peristaltic pumps. The liquors were collected inside 20 liter plastic containers. Ten thermometers (8 digital and 2 mercury) were fixed to Plexiglas strips on the top of the unit and inserted into the sludge to a depth of 5 cm from the bottom. The temperatures were monitored at 4 points between the electrodes and at 6 points, offset 11 cm from the

center row (see diagram in Figure 3.5). Only half the unit was monitored with the assumption that the current densities and therefore the temperatures are symmetrically distributed with respect to the electrode axis. Electrical power during the heating phase was supplied by a common low-frequency (60 Hz) sinusoidal alternating current delivering a potential of 120 V with a maximum current capacity of 30 A. Throughout this period, the amperage was monitored by an open clamp digital multimeter. During the subsequent dewatering phase, the electrodes were connected to the DC power supply (Lambda model GEN 150-10).

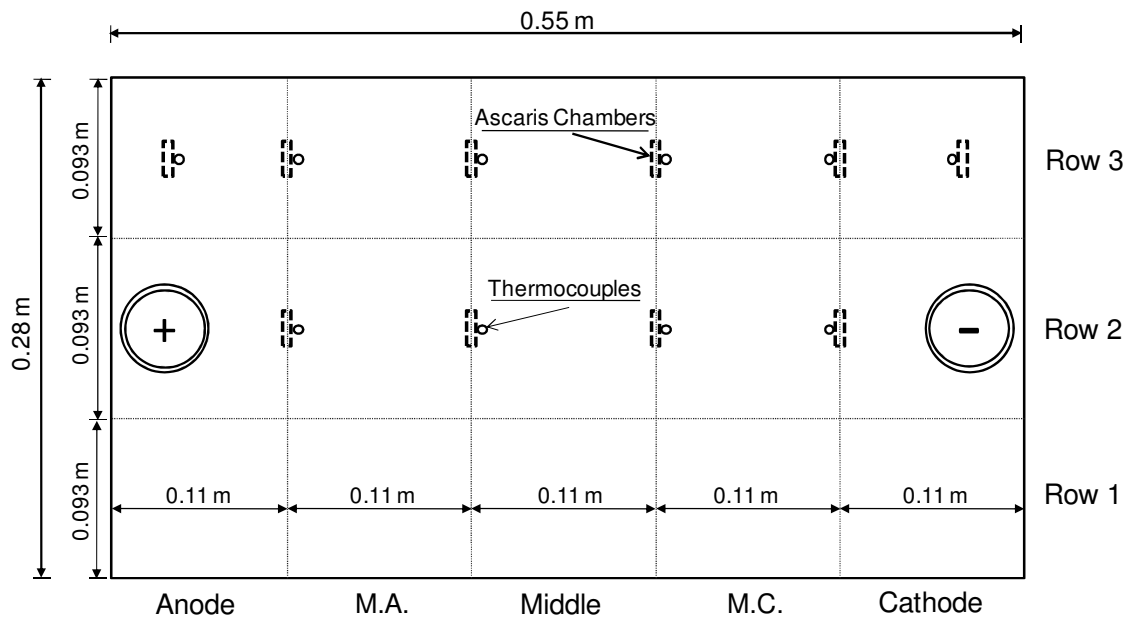


Figure 3.5 Diagram of the pilot-scale EK unit

3.2. Equipment and Materials

The following section outlines the equipment and materials used during the set of experiments, together with their properties and construction method.

❖ Bench EK Reactor Cell

- Plexiglas rectangular reactor cell (length = 23 cm, width = 5 cm, height = 7.5 cm)
- Foam insulation (thickness = 2 cm)
- Steel plate electrodes (width = 5 cm, height = 8 cm, thickness = 0.5 cm)
- Perforated steel plate electrodes (1.06 cm² net reduction in surface area)
- 8 beakers (300 ml)

❖ Pilot EK Reactor Cell

- Coleman[®] 32 liter cooler (length = 55 cm, width = 28 cm, height = 30 cm)
- Perforated hollow cylindrical stainless steel (type 302) electrodes (height = 30 cm, $D_{out} = 5.12$ cm, $D_{in} = 5$ cm)
- Two plastic containers (20 liters)
- Two Fisher Scientific low flow peristaltic pumps
- Flexible polyethylene tubing (5 m)
- Cation exchange textile (with sulfonic functional group (0.5 meq/g))
- Anion exchange textile (with tertiary amine functional group (1.6 meq/g))
- Stainless steel mesh 200

❖ Conditioners

- Diammonium phosphate (DAP) pellets
- Ammonium Nitrate (AN) pellets
- Urea pellets

❖ ***Ascaris suum* Ova**

- Unembryonated ova, in a 50,000 eggs/ml solution, obtained from the Department of Microbiology and Immunology at Cornell University (Ithaca, NY.)

❖ **Apparatus and equipment**

- Mechanical shaker (Burrell model 75)
- DC 1500W power supply (LAMDA model: GEN 150-10)
- AC power supply (VARIAC model 130)
- pH meter (Denver Instrument Model 215)
- Digital multimeter (Kyoritsu Kew Mate 2000)
- Atomic absorption spectrometer (Perkin Elmer, Analyst 100)
- Analytical balance (Accumet model AR25)
- Mercury filled glass Thermometer (Fisher Scientific)
- Digital thermometer (Accutemp)
- HACH DR 2800 Portable spectrophotometer
- HACH HQ30D Portable meter with standard 1 m conductivity probe
- Aluminum weighing dishes
- Autoclaving biohazardous Plastic bags
- Grinder (Hamilton Beach)
- Funnels
- Nylon mesh 25 microns (Miami Aqua-culture inc.)
- Filter papers (Whatman 40 and Sartorius Folded 12.5)
- Centrifuge ISE HN-SII (International Equipment Company)
- Centrifuge tubes (15 and 50 ml)

- Erlenmeyer flasks (50, 250, 1000 ml)
- Digital stirred hotplate (Corning)
- Standard sieves (Newark no. 100 and 450)
- Folded filter paper (HACH 892-57)
- Vortex mixer (Fisher)
- Filter paper (Whatman 40, FSSP 9751058)
- Fine pipetter (ThermoFisher 0.1-1 ml)
- Graduate cylinder (25, 50, 100 ml)
- Laminar air flow hood-Class II A/B2 (Forma scientific)
- Muffle furnace (Fisher Scientific)
- Cell culture flasks (Corning 25 cm²)
- Micromaster Phase contrast microscope (Fisher model CK)
- Isotemp® Incubator (Fisher model 304)
- Mortar and Pestle

❖ Reagents

- AA standard solution Cd (SCP, 140-052-241)
- AA standard solution Cr (SCP, 140-001-291)
- AA standard solution Cu (SCP, 140-001-291)
- AA standard solution Fe (SCP, 140-001-261)
- AA standard solution Pb (SCP, 140-001-821)
- AA standard solution Zn (SCP, 140-001-301)
- HACH High range Nitrogen Ammonia AmVer® Test 'N Tube™ Reagent set

- HACH Total Phosphate Test 'N Tube™ Reagent set
- HACH Nitrate NitraVer® Test 'N Tube™ Reagent set
- Distilled Water (Produced in the Concordia laboratory)
- Formaldehyde (reagent grade, 37% v/v)
- House bleach (Chlorox, 5.25% v/v sodium hypochlorite)
- Hydrochloric acid (reagent grade, 34-37 % v/v)
- Magnesium Sulfate Anhydrous (powder/certified)
- Perchloric acid (reagent grade, 1N)
- Sodium Hydroxide (reagent grade, 1N)
- pH buffer solution (pH= 4, 7, 10)

❖ **Software**

- Partial Differential Equation Toolbox in MATLAB® version 7 (R14)

3.3. Chemical and Physical Characteristics of Biosolids

The mixed primary and secondary municipal sludge obtained from the WWTP in Auteuil was stored in refrigerators at 4°C. An initial sludge analysis was performed on well mixed samples to obtain a base line reference for its physical and chemical properties. The results are presented in Table 3.1. These constitute intrinsic concentrations present in the wastewater sludge at the time it was sampled; no additional elements, apart from the conditioners, were added to the sludge prior to the experiments.

Table 3.1 Biosolid characteristics

Elements	Values	Units
Biological		
<i>Ascaris suum</i> ova	ND*	<i>Ascaris ova</i> /4 g TS
Physical		
Total Solids (TS)	3.84	%
Volatile Solids (VS)	67.9	%
pH	6.03	-
Chemical		
Metals		
Cd	1.14	mg/kg dry TS
Cr	30.54	mg/kg dry TS
Cu	214.49	mg/kg dry TS
Fe	4062.04	mg/kg dry TS
Pb	231.67	mg/kg dry TS
Zn	487.02	mg/kg dry TS
Macro-Nutrients		
Ammonium (NH ₄ ⁺)	6152.98	mg/kg dry TS
Nitrate (NO ₃ ⁻)	874.44	mg/kg dry TS
Phosphate (PO ₄ ³⁻)	331.90	mg/kg dry TS

*(ND: Not Detected)

3.4. *Ascaris suum* egg Chamber Design and Placement

The use of chambers to contain *Ascaris suum* eggs during the inactivation experiments drastically reduces the number of eggs required and facilitates their sampling from biosolids. One type of chamber or another have successfully been employed as an alternative to spiking (Capizzi-Banas, et al., 2004; Brewster, et al., 2003), as the later method requires many orders of magnitude more eggs, depending on the volume of biosolids, with poor egg recovery. A comprehensive study aimed at determining the embryonation ability of *Ascaris suum* eggs deposited in permeable nylon bags compare with that of free eggs in wastewater sludge treated with lime, demonstrated a slight increase in the viability of the enclosed eggs subjected to the same treatment, seemingly by offering some degree of protection (Eriksen, et al., 1995). Therefore, if there is a bias

with the use of chambers, it is in underestimating the effectiveness of the treatment by overestimating the relative viability of *Ascaris suum* ova.

The design of the chamber used during this study was inspired by the garden cloth packets and sentinel chambers utilized by Brewster and Oleszkiewicz (2003) in their study of *Ascaris suum* inactivation in biosolids using a modified alkaline treatment. The chambers utilized for the purpose of this thesis consisted of a fine nylon mesh sac, with a mean pore size of 25 μm , locked inside a slotted plastic chamber (25 mm in width by 30 mm in height), with a gap width of 1 mm. Figure 3.6 shows each component of the chamber. The nylon mesh sacs were fabricated by folding the nylon cloth in half and sealing the two halves together in approximately 20 mm intervals with the use of a soldering gun. The sootier line was verified for holes and cut with scissors. The formed sac was thus impermeable to *Ascaris suum* eggs, but permeable to the sludge liquor. The sac could be secured inside the plastic chamber by shutting the two halves of the chamber over the open top portion of the sac; thus, effectively sealing the contents of the sac.

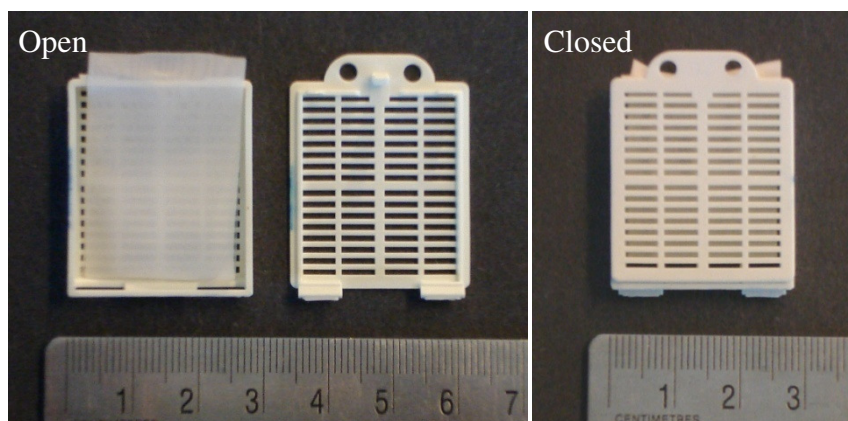


Figure 3.6 *Ascaris suum* egg chambers (open and closed) with nylon mesh

Each batch scale ohmic heating experiments utilized three chambers per EK cell placed adjacent to the base of each glass thermometer by suspending each cell with nylon string and securing them to the Plexiglas thermometer support. The chambers were spaced 5.75 cm from each other along the length of the unit and 2 cm from the bottom. This configuration was believed to adequately capture the temperature variance from the anode through the cathode regions (see Figure 3.3).

For the pilot scale study, a total of ten chambers were distributed along half of the pilot unit between the anode and the cathode (see Figure 3.5). The current densities were logically assumed to be symmetrically distributed along the electrode axis, and thus the heat distribution would be similarly distributed between the two halves. Two rows of chambers were distributed at 11 cm intervals along the length of the unit for a total of 8 chambers, and the two rows were offset by 11 cm. Two additional chambers were placed at 6 cm from the electrodes adjacent to the lower row of chambers. Each chamber was positioned 5 cm from the bottom by fastening the chamber to a prepositioned plastic rod glued to the Plexiglas support. For each chamber a digital thermocouple was secured next to it to precisely monitor the temperature experience by the *Ascaris* eggs and the temperature distribution throughout the unit.

3.4.1. Preparation of *Ascaris suum* eggs

The *Ascaris suum* eggs, collected from the intestinal content pigs by sequential sieving, were obtained the Department of Microbiology and Immunology at Cornell University (Ithaca, NY). 750,000 eggs were shipped in a 15 ml vial in 0.5 % formalin and at 4°C. The egg batch was subsequently stored in a refrigerator at 4°C. No other chemicals were

used prior to the experiments. This single 15 ml batch of eggs was used for all the inactivation experiments. Prior to each experiment, a control sample was obtained from the batch and incubated to obtain a baseline viability count.

For each *Ascaris* EK inactivation trial a 700 ml volume of sludge was used; the sludge was taken from 20 liter containers kept in storage at 4°C in a refrigerator. To the sludge was added 13 g/l of AN and mixed in a 1 liter beaker on a stirred hotplate. The temperature of the sludge was adjusted to room temperature with the aid of a thermometer. After approximately 5 minutes of mixing and heating, the sludge was poured in the reactor cell.

From the well mixed stock solution of 50 000 eggs/ml, 100 µl was pipetted into the fashioned nylon mesh sac, amounting to approximately 5000 eggs/sac. To the sac was added an additional 1 ml of conditioned biosolids. The sac was then placed into the screened chamber (see Figures 3.6). Three such chambers, labeled A (anode) through C (cathode), were utilized for each batch test. The chambers were suspended by means of nylon strings from the Plexiglas thermometer support and placed adjacent to each thermometer. The whole was immersed into the sludge filled cell to a depth of 2 cm from the bottom. Finally, a specified voltage gradient was applied to the electrodes in order to ohmically heat the sludge to predefined ranges of temperatures.

3.4.2. Procedure for Collecting and Processing *Ascaris suum* eggs from Chambers

A modified standard operating procedure (SOP), based on the Tulane Method (Bowman, 2003), for collecting *Ascaris* eggs from a small volume of sludge was obtained from Dr.

D.D. Bowman from the Department of Microbiology and Immunology at Cornell University (Ithaca, NY).

To isolate the *Ascaris suum* eggs deposited in the biosolids, the biosolids are processed by sieving the contents of the nylon mesh sack through a standard 100 mesh sieve. The material caught on the sieve was discarded, and the filtrate transferred in a 50 ml centrifuge tube and centrifuged.

After centrifugation, the tubes were decanted. After centrifugation and decanting, there should be no more than 4 or 5 ml of packed sediment in the tube. If more sediment than this is present, the sediment was split between necessary tubes, resuspended in water, and the tubes filled to 50 ml and centrifuged again.

To the appropriate volume of packed sediment, about 10 ml of a magnesium sulfate solution with specific gravity of 1.20 was added to the tubes. The sediments were resuspended in the magnesium sulfate solution by breaking it up with two applicator sticks while on a vortex mixer. Care was taken in order to prevent the sample from splashing out of the top of the tube by cover it with parafilm. After the pellet is resuspended and mixed, the tube is filled with 50 ml of the magnesium sulfate solution and centrifuged again.

After the second centrifugation, the material floating on the tubes was passed through a standard 450 mesh sieve. The filtrate this time was discarded, and the eggs and any other debris on the sieves were transferred from the top of the sieve, via a small paper cup, to a 25 ml cell culture flask. The flask was filled to 10 ml with distilled water, and to each flask was added 50 μ l of 37 % formaldehyde to prevent mold growth. The flasks

containing the eggs were finally stored in an incubator at 28°C for between 21 and 28 days, during which period the larvae matures.

At the time of the analysis, the flasks were removed from the incubator and 100 µl of house bleach (5.25 % sodium hypochlorite) was added to the flask to clear away the brown external uterine layer in order to better observe the enclosed larvae. The content of the flask was transferred to a 15 ml centrifuge tube and centrifuged. The supernatant was discarded and the pellet transferred by pipetting it onto a glass slide. A cover glass was positioned on top and placed under the phase contrast microscope at x100 magnification. The eggs were then counted and scored as embryonated (i.e. viable), or unembryonated (i.e. inactivated), distinguished by the absence of a motile first stage larva. This distinction is illustrated in Figures 3.7 and 3.8, representing viable and inactivated ova, respectively. The viability percentage was calculated by dividing the number of viable eggs by the total number of eggs counted (US EPA, 1999), which was in the neighborhood of 1000 eggs in order to obtain up to 3 log magnitude inactivation results. Whether the embryonated eggs were infective to pigs had not been determined in this study.



Figure 3.7 Example of viable (embryonated) *Ascaris suum* ova (x200 magnification)

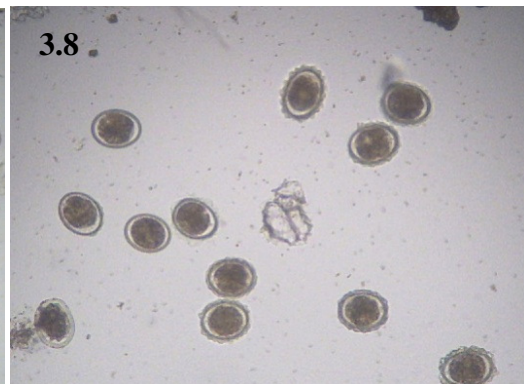


Figure 3.8 Example of inactivated (unembryonated) *Ascaris suum* ova (x200 magnification)

3.5. Experimental Parameters and Variables Studied

In order to carry out the *Ascaris suum* inactivation experiments by enhanced EK treatments, several key biosolids variables needed to be examined. The principal means of inactivation was by the action of heat on the helminth eggs. To carry the inactivation, the temperature of sludge was elevated by the process of ohmic heating, a process by which the passage of an electric current through a conductor (e.g. an electrolytic solution) generates heat. As discussed in section 3.2.3, the heat generated per unit volume of solution will be proportional to the square of the applied electric field multiplied by the conductivity of the solution. Therefore, for the purpose of obtaining a reasonable heating rate at a practical voltage gradient, it was fundamental to study the behavior of these two parameters: the conductivity and voltage gradient. Ultimately, the goal was to be able to more precisely control the application of enhanced EK processes.

3.5.1. Conditioners

The addition of a conditioner to a biosolid, as a means to enhance the EK activity, has a significant impact on its conductivity. The ionic nature of the conditioning compounds used enables them to substantially contribute to the electrolyte load in the sludge, and consequently, to its ability to conduct electric current.

Preliminary studies were thus conducted by comparing the effects of adding crushed AN, DAP, or urea pellets to the wastewater sludge. Typical characteristics of these conditioners are listed in Table 3.2. The conditioned sludges were analyzed for conductivities with respect to conditioner type and concentration, and for heating rates and dewatering ability when subjected to an applied voltage gradient of 3 V/cm.

Table 3.2 Typical composition and solubility of conditioners used

Conditioner	Molecular Form	% N	% P ₂ O ₅	Solubility (lb cond./ 100 gal water)	Physical State
AN	NH ₄ (NO ₃)	34	-	1617	Solid (pellets)
DAP	(NH ₄) ₂ HPO ₄	18-21	46-54	574	Solid (granules)
Urea	CO(NH ₂) ₂	46	-	902	Solid (pellets)

(Adapted from Havlin et al. (1999))

3.5.1.1. Temperature Impact on Conductivity

As explained in section 2.2.3, the conductivity of an electrolyte solution is temperature dependent. As a general rule, for most aqueous solutions, there is a 1.8 % to 2 % change in conductivity per degree Celsius (Aquarius Technologies PTY Ltd., 2000). Since biosolids contain an important fraction of colloidal and organic mass, this can influence the conductivity-temperature dynamic. To obtain accurate temperature curves, several parameters were evaluated for their impacts on this relationship. The parameters studied included the effects of the conditioner type, its concentration, and of the water content on the conductivity/temperature relation.

3.5.1.2. Voltage Gradient Impact on Temperature

As seen in section 2.2.3, small changes in voltage gradients will have an important impact on the heating rates attainable, given the same conductivities. However, this exponential relationship will be altered due electrical energy being diverted away from heat generation towards electrolysis and other electrochemical processes. Therefore, part of this research involved studying the energy efficiencies at applied voltage gradients between 2 and 5 V/cm. Duplicate tests were conducted with both AC and DC to observe

their influence on heating rates and energy efficiencies. The purpose of which was to find the optimal electric parameter, in terms of energy efficiency, to apply towards the ohmic heating process.

3.6. *Ascaris suum* Ova Inactivation Experiments

The inactivation trials of *Ascaris suum* ova were studied at both the bench-scale and pilot-scale phases. Preliminary bench-scale ohmic and convective heating experiments were conducted to determine the inactivation dynamics with respect to temperature; the units utilized for this set of experiments operated under constant volume and used the solid steel plate electrodes. The optimal inactivation parameters were subsequently applied towards further bench and pilot scale EK experiments for the purpose of evaluating the physical and chemical performance of biosolids in terms of dewatering, metal and ion removal, together with the *Ascaris* inactivation under enhanced EK treatment. These units operated under variable volumes by allowing the discharge of the sludge liquors.

3.6.1. Bench-Scale Treatment of *Ascaris suum* Eggs

The bench scale experiments were designed to assess the efficacy of an enhanced EK treatment on the inactivation of *Ascaris suum* ova and to define the temperature at which 99.9 % inactivation occurs. The EK enhancement, in this situation, consisted of the combined application of a high voltage gradient together with a moderate amount of conditioner. All the inactivation experiments were carried out with the same 20 liter batch of biosolids to minimize the amount of independent variables; however, the degradation and mineralization of the biosolids over time, even in cold storage, does introduce

confounding factors. The chosen conditioner was AN with a concentration of 13 g/l of sludge. This amount produced an average sludge conductivity of 16.57 ± 0.18 mS/cm. The applied voltage gradient for the purpose of heat generation was set at 2.5 V/cm. These combined to generate a mean ohmic heating rate of 1.38 ± 0.04 °C/min. The research aimed at defining the temperature at which complete inactivation is achieved; to this end, a temperature range between 40°C and 70°C was selected with a test conducted for every 5°C interval. Once the target temperature was attained, it was maintained constant for 10 minutes by lowering the voltage gradient to 0.5 V/cm. The *Ascaris* egg chambers were then removed from the heated biosolid and processed as described in section 3.4.2.

A parallel set of control experiments were performed, at the same temperatures and exposure time, using convective heating. The same concentration of conditioner (13 g/l) was added to one liter of sludge in a one liter beaker and placed on a stirred hotplate to be heated to the target temperatures. Once reached, the heated sludge was transferred to a second stirred hotplate that was preset to the target temperature. An *Ascaris* egg chamber was suspended inside the sludge while being continuously stirred to keep the temperature uniform throughout and maintained there for 10 minutes. Still another control trial involved subjecting the eggs to the same EK treatment with respect to the applied conditioner and electric field, as formerly described, with the exception of limiting the temperature rise to 30°C, a non-lethal range. This was carried-out by using cooled biosolids and reducing the heating rate by immersing the cell in an ice bath. Thus, the duration of the electrical exposure of this control trial was comparable to that of the 65°C ohmic heating trial.

Table 3.3 Designed treatment conditions for bench-scale EK experiments

Treatment conditions	Abbreviation	Electrical parameters	Target temperature
No heat / no AN conditioner	NH(0)	0.5 V/cm for 72 hours	Ambient T°
No heat / 13g AN/l	NH(13)	0.5 V/cm for 72 hours	Ambient T°
Ohmic heat / no AN conditioner	H(0)	2.5 V/cm until target T° & 0.5 V/cm for the balance	55°C
Ohmic heat / 13g AN/l	H(13)	2.5 V/cm until target T° & 0.5 V/cm for the balance	55°C

Once the critical inactivation temperature identified, another series of enhanced EK experiment were designed to detect the effects of ohmic heating and AN conditioner on the biological, chemical, and physical parameters of the biosolids. Four bench-scale units were operated in parallel; in one of the four initial conditions outlined in Table 3.3. One pair of units were subjected to ohmic heating at an initial voltage gradient of 2.5 V/cm, and subsequently declining to 0.5 V/cm after the target temperature was reached; one with no conditioner added and the other with 13 g AN /l. The other pair was run in the absence of ohmic heating and maintained a voltage gradient of 0.5 V/cm for the length of the experiment. Again, one unit had no conditioner added and the other had 13 g AN /l. Three *Ascaris* egg chambers were placed per EK unit, as described in section 3.4.1. Prior to the application of electricity, the sludge liquor in the units was allowed to drain out by gravity for 2.5 hours, by which time no appreciable flow could be observed. The total accumulation of liquor from each unit amounted to about 50 ml. During the experiment, the amperages and temperatures in the units, together with the volumes of anolyte and catholyte collected, were monitored at frequent intervals throughout a 66 hour treatment. A higher sampling frequency of every 3 minutes was, however, maintained during the initial heating phase. At the end of the treatment, the *Ascaris* chambers were removed and

the dewatered biosolid in the units were subdivided into 5 equal portions (labeled A through E, see Figure 3.3) at 4.6 cm intervals for physical and chemical analysis. Each chamber was processed and analyzed according to the method described in section 3.4.2.

3.6.2. Pilot Scale *Ascaris suum* ova Inactivation Experiments

In contrast to the bench-scale unit, the pilot-scale unit was a more heterogeneous environment in terms of the electrical parameters. Therefore, the ohmic heat generation would predictably be unevenly distributed. The aim was thus to examine the effect of this variation on the inactivation performance of the enhanced EK treatment. To this end, 10 *Ascaris suum* egg chambers were distributed throughout the unit as described in the pilot-scale arrangement in section 3.1.2. The treatment parameters for the 2 pilot trials are detailed in Table 3.4. A concentration of 13 g AN /l was used for both tests, resulting in an average conductivity of 16.82 ± 0.05 mS/cm.

Table 3.4 Designed treatment conditions for pilot-scale EK experiments

Treatment conditions	Ion exchange textile	Electrical parameters	Target temperature
Ohmic heat / 13 g AN/l	no	2.5 V/cm until target T° & 0.5 V/cm for 70 hours	55°C
Ohmic heat / 13 g AN/l	yes	2.5 V/cm until target T° & 0.5 V/cm for 70 hours	55°C

To this end, 338 g of AN in pellet-form was crushed and added to 26 liters of biosolids; the mixture was stirred continuously for 10 minutes to insure a good dissolution of the conditioner. Several conductivity measurements were taken at various points and depths to guarantee uniformity. The electrodes were made impermeable to solids by fixing a stainless steel mesh around the electrode, including its base, and immersing them into the conditioned sludge. Flexible 8 mm polyethylene tubing was inserted into each electrode

and connected to two low flow peristaltic pumps. The pumps were turned on and the sludge liquors were extracted into two graduated 20 liter containers, marked anolyte and catholyte to denote their respective origins. The removal of sludge liquor continued until such a time at which the extraction rate was deemed negligible; this occurred after approximately 4 hours, amounting to about 250 ml of liquor in each container. The Plexiglas supports with chambers and thermocouples were then inserted, and the electrodes connected to an electrical outlet providing 120 VAC with a 30 Amps capacity. This power supplied the pilot unit with an effective voltage gradient of 2.5 V/cm. The amperage delivered to the electrodes was monitored using a digital multimeter (Kyoritsu Kew Mate 2000) with an open clamp probe. When the specified temperature was attained, the electrical cable was disconnected from the wall-mount and immediately reconnected to the DC power generator with the voltage set to supply a voltage gradient of 0.5 V/cm to the unit. The duration of the enhanced EK treatment lasted a total of 70 hours, after which the *Ascaris suum* eggs and biosolids were processed and analyzed accordingly. Figure 3.9 below illustrates the general layout of the pilot unit moments before electric current is applied.

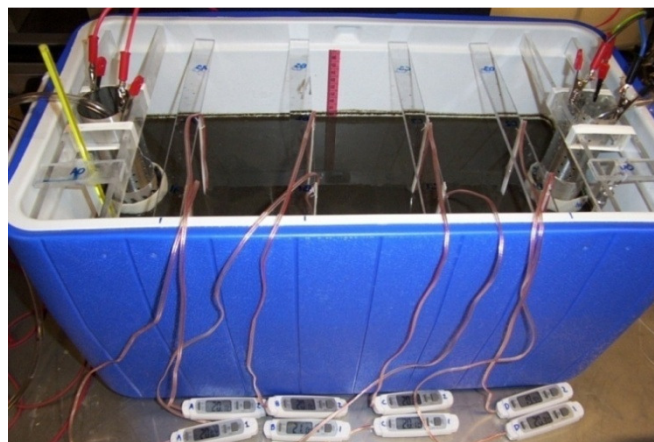


Figure 3.9 General layout of the pilot-scale EK unit

In the second pilot test the same parameters were implemented, with the exception that anionic and cationic exchange textiles were used during the experiment. These textiles were obtained from the “Institut des textiles de France” and were of the non-woven synthetic polymer variety. The cation exchange textile, CAMDS[®], was of the strong acid category consisting of a sulfonic group (R-SO₃⁻) as its main functional group. The anionic exchange textile, Plexinone[®], was a strong base type exchanger consisting of three bound methyl groups (R-3CH₃⁺) as its primary functional group. Both textiles have an ion exchange capacity of 0.6 meq/g. Each textile was cut approximately 20 cm by 16 cm to match the depth and the circumference of the perforated electrode. No conditioning of the textiles was required, except to be placed in a dish containing distilled water for a few hours before the experiment. As defined in US patent 12/571,482 (Elektorowicz and Oleszkiewicz, 2009), the multifunctional electrodes consisted of perforated stainless steel tubes, a stainless steel mesh, and an ion exchange textile. An anion exchange textile was used on the anode and a cation exchange textile was used on the cathode. Figure 3.10 illustrates this multifunctional electrode. The biosolids were then subjected to the same preliminary dewatering conditions, specified above, together with the same regimens of conditioner concentration and applied electrical fields.



Figure 3.10 Multifunctional electrode

The electrical, temperature, and volumetric parameters were recorded with the same frequency as the bench-scale experiments during the 70 hour run. At the end of the treatment, the *Ascaris* egg chambers were removed for processing, as described in section 3.4.2, and the resulting dewatered biosolids were divided into 15 equal portions (see figure 3.5), labeled, and stored in 500 ml plastic containers to be analyzed as described in section 3.7.

3.7. Measurements and Analyses

This section outlines the general analytical methods used to obtain data for the biological, chemical, and physical parameters studied.

3.7.1. Electrical Parameters and Temperature Measurements

Since the applied EK process was based on a constant voltage gradient technique, the electrical measurements consisted of setting the DC power generator at a specified voltage, and taking joint measurements of the amperage value displayed on the generator and the temperature values of the three thermometers.

When more than one EK unit was used during a trial, these were each connected to the generator in parallel and the amperage monitored with digital multimeters connected in series with each unit. For the AC trials, both voltage and amperage were monitored with multimeters connected in parallel and in series, respectively. Every electrical and temperature data reading was taken at three minute intervals; except for the experiments conducted with voltage gradients of 4 and 5 V/cm where each parameter was logged at one minute intervals.

3.7.2. pH Analysis

The partitioned samples were homogenized, and approximately 5 g from each sample were placed in 50 ml centrifuge tubes and weighted. To this 5 g, 40 ml of distilled water was added. The sludge mixtures were then put on a rotating mixer for about 3 hours. The sludge mixture was filtered using Sartorius Folded filter papers. The collected filtrates were subsequently used for both pH and macro-nutrient analyses. Before the pH measurements, the pH meter was calibrated with three buffer solutions of pH: 4, 7 and 10. The pH probe was inserted into the filtrate and the stabilized value documented.

3.7.3. Heavy Metal Analysis

The metal concentrations of the samples were measured by standard method 2540-E (Eaton, et al., 1995). The metals were extracted from the biosolids by an acid digestion. The biosolids samples were initially oven dried at 105°C for 24 hours and subsequently ground to a powder. Approximately 5 g of oven-dried sludge was weighted and added to a 50 ml plastic centrifuge tube and mixed with 30 ml of 37 % HCl and capped tightly. The suspension was then cured for 24 hours with continuous shaking to allow desorption of the metal species from the sludge matrix. The suspension was filtered through a Whatman 40 Filter paper. Dilutions were made from the filtrates and metal standards prepared. The same concentrated HCl solution was used to make all the dilutions and standards. The samples were then measured using an Atomic Absorption Spectrometer (Perkin Elmer, Analyst 100). Analyses were performed for cadmium, chromium, copper, iron, lead, and zinc. The results given in mg/l were converted to mg/kg dry TS.

3.7.4. Ion Analysis

The sludge samples for the ions analyses were prepared in a similar fashion as for the pH analysis, described in section 3.7.2. As most of the analytical techniques were pH sensitive and required the samples to be within a pH range of 6 to 8, the filtrated samples were adjusted to this range with NaOH (1N) and Perchloric acid (1N). All macro-nutrients were measured using a HACH DR 2800 instrument and HACH reagent sets following the manufacturer's methods. As the sets can only detect concentrations within a narrow range, all the samples were diluted 10 times before measurements.

For the nitrogen-ammonia analysis, a 0.1 ml of diluted sample was added to each vial of AmVer™ reagent Test 'N tube for high range ammonia nitrogen. The contents of one ammonia salicylate reagent powder pillow and one ammonia cyanurate reagent powder pillow were added to each sample. The vials were capped tightly and shaken thoroughly to dissolve the powders. The vials were left to react for 20 minute. An orange color develops if ammonia is present. After which, it was inserted into the HACH DR2800 and the resulting concentration displayed in mg/l of $\text{NH}_3\text{-N}$.

For the nitrate analysis, 1 ml of diluted sample was added to a NitraVer X Reagent A vial. The vial was capped and inverted 10 times to mix the contents. The contents of one NitraVer X Reagent B powder pillow were added to the vial, inverted 10 times, and left to react for 5 minutes. A yellow color develops if nitrate is present. The prepared sample vial was inserted into the HACH DR2800 and the resulting concentration displayed in mg/l of $\text{NO}_3^- \text{-N}$.

For the phosphorous-phosphate analysis, 5 ml of diluted sample was added to a total phosphorus test vial together with the contents of one potassium persulfate powder pillow. The vial was shaken to dissolve the powder. The vial was then inserted into the a well heater preset to 150°C for 30 minutes; after which the vials were removed from the reactor and left to cool to room temperature. Once cooled, the contents of one PhosVer 3 powder pillow were added to the vial, shaken for 30 seconds, and left to react for 2 minutes. A blue color develops in phosphate is present. The prepared sample vial was inserted into the HACH DR2800 and the resulting concentration displayed in mg/l of PO_4^{3-} .

3.7.5. Percent Total Solids (%TS) and Volatile Solids (%VS) Analyses

The Standard Method 2540G (Eaton et al., 1995) was used to measure total solid (TS) content of the treated and untreated sludge samples. The sludge samples were place in an aluminum weighing dish, weighed, and transferred in a drying oven at 105°C for 24 hours. After this period, the samples were placed in a desiccator for 15 minutes to cool to room temperature. The percent dry TS content was calculated based on the following formula:

$$\text{TS}\% = \left(\frac{M_{\text{dry}}}{M_{\text{wet}}} \right) \times 100 \quad (28)$$

Where M_{dry} is the mass of dry biosolids and M_{wet} is the mass of wet biosolids.

The analysis for volatile solids was determined based on the Standard Method 2540E (Eaton, et al., 1995). The dried samples obtained for TS analysis were incinerated in a furnace at 550°C for 2 hours. The remaining solids after this duration consisted of mostly

the fixed total, dissolved, and/or suspended solids, while the weight loss was due to the volatile portion. This portion can be roughly considered as the organic content of the solid mixture.

The percentage of organic matter can be calculated using the following formula:

$$VS\% = \left(\frac{M_{105} - M_{550}}{M_{105}} \right) \times 100 \quad (29)$$

Where M_{105} is the mass of samples after drying at 105°C and M_{550} is the mass of residue after incineration at 550°C.

4. Results

This section presents the data obtained from the measurements and analyses performed during the laboratory experiments. It is divided into two parts: the results from the series of bench-scale experiments, followed by the results of the pilot-scale experiments.

4.1. Results of Bench-Scale Experiments

The sets of bench-scale experiments had a threefold objective: (1) optimization of conditioner and electrical parameters; (2) optimization of the temperature parameter in the inactivation of *Ascaris* ova; and (3) evaluation of the performance of the chosen parameters on the removal efficiency of heavy metals and ions. This section will initially outline the results of *Ascaris suum* ova inactivation by heat treatments, followed by a study of the effect of variable electrical parameters and conditioner type, and ending with the results of the comparative EK tests on the physical and chemical properties of the treated biosolid.

4.1.1. Inactivation Experiments of *Ascaris suum* Eggs

As outlined in section 3.6.1, screening experiments on *Ascaris* inactivation were carried out for the temperature range between 40°C and 70°C, at targeted 5°C intervals and subjected to that temperature for 10 minutes. The results of 30 distinct *Ascaris suum* egg viability analyses are illustrated in Figure 4.1:

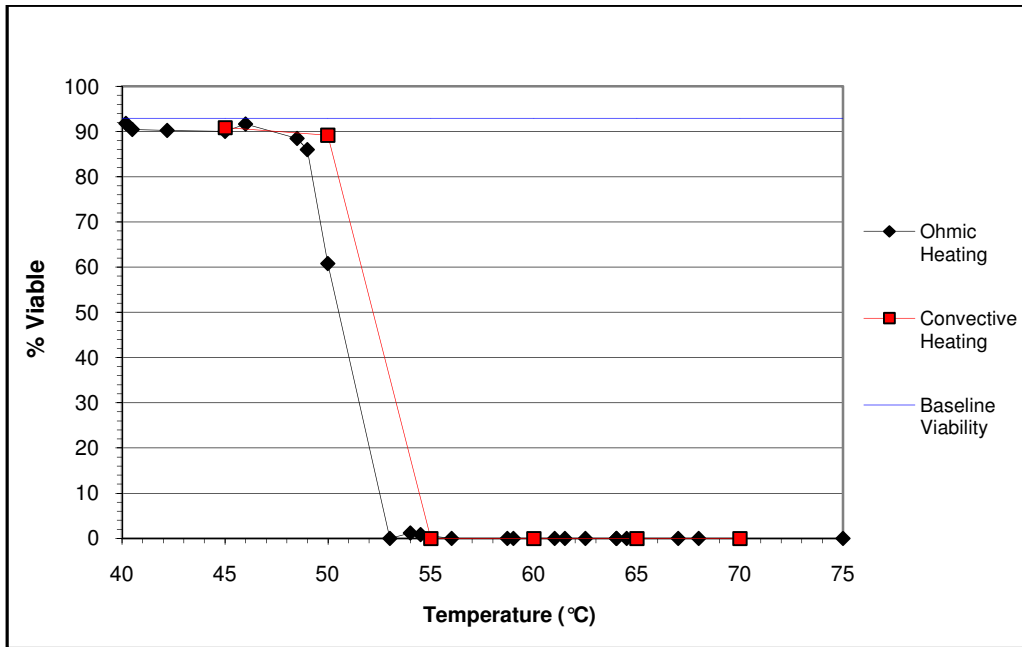


Figure 4.1 Percentage of viable *Ascaris suum* eggs as a function of temperature during bench-scale experiments comparing the inactivation of egg between ohmic and convective heating trials.

The graph combines both ohmic and convective heating results, together with the control no treatment reference. This background viability was verified on three separate occasions in parallel with the inactivation trials and subjected to the same egg processing technique (section 3.4.2) to negate its potential to inactivate *Ascaris* eggs. The viability results showed an average value of 92.92 % with a variance of 0.08 %. The ohmically heated sludge was subjected to an electrical field strength of 2.5 V/cm and an AN concentration of 13 g/l (yielding a mean conductivity of 16.57 ± 0.18 mS/cm). The curve of the ohmically heated sludge exhibits a better distribution of data points because although the average heating rates was relatively uniform between the trials, local temperature distribution across the cells did vary significantly; sometimes as much as 5°C along the unit. These uneven temperature distributions in the unit were detected by the three thermometers placed at each *Ascaris* chamber locations; so the temperature experienced by each egg chamber could be precisely monitored. It is observed that the

critical range of temperature for *Ascaris* egg inactivation stands between 50°C and 55°C (examples of which are illustrated in Figures 4.2 and 4.3, respectively), with a complete inactivation obtained at 55°C and beyond.

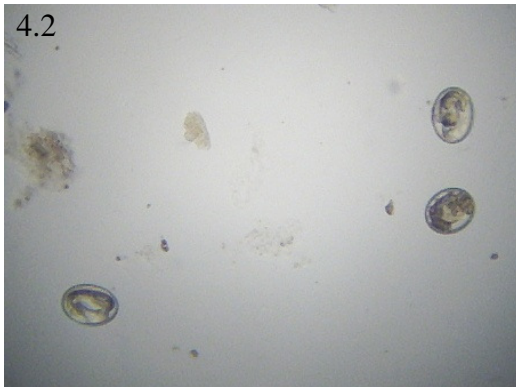


Figure 4.2 Example of *Ascaris suum* ova subjected to 50°C for 10 minutes during bench-scale EK experiments. (x200 magnification)

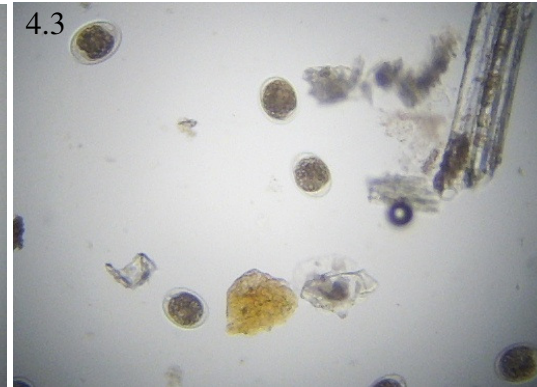


Figure 4.3 Example of inactivated *Ascaris suum* ova subjected to 55°C for 10 minutes during bench-scale EK experiments. (x200 magnification)

The inactivation curve for ohmic heating is similar to the conventional heating curve except for a slight shift to a lower critical temperature of 53°C. It is uncertain that the presence of the electric field at this temperature range exerted a positive role in the inactivation of the *Ascaris* ova as only two data points are available in the circumscribed critical inactivation range for the convectively heated sludge. According to the graphical results in Figure 4.1, the ohmic heat treatment appears to outperform the convective heat treatment by showing an earlier onset in inactivation and a comparative 29 % more inactivated egg when expose to 50°C for a 10 minute period and the same conditioner concentration.

While these results established heat as the principle inactivating agent, the combination of electricity and conditioner may have a disinfecting activity. To determine if the application of electric current in conjunction with the AN conditioner had an influence

on the viability, a control trial was conducted with the *Ascaris* eggs subjected to the same conditioner concentration and the same electrical field intensity for a duration of 30 minutes (analogous to the 65°C inactivation trial), with the exception that the ohmic heating throughout the unit was limited to a mean temperature of 30°C (near that of its incubation temperature) by maintaining the unit in an ice bath. The average viability result of this control trial was 91.77 % with a variance of 1.27 %. Statistical analysis was performed using a two-sample t-test, assuming unequal variance, in the EXCEL[®] Analysis ToolPak to determine if a significant difference existed between the mean viability results of eggs subjected the combined effect of the applied conditioner and electrical gradient, and the control no treatment condition; with a *p* value <0.05 considered significantly different. The count data (viable or nonviable) were assumed to have a binomial distribution. The data were, therefore, transformed to achieve asymptotic normality (a precondition of the t-test) using the formula (Neter et al., 1996):

$$Y' = 2 \cdot \arcsin \sqrt{Y}$$

where *Y* is the percent viability of the sampled eggs divided by 100. This transformation is recommended when the response variable is a proportion (Nelson and Darby, 2001).

The exposure of *Ascaris* eggs to the electrical gradient of 2.5 V/cm and 13 g/l of AN conditioner did not have a significant impact on their mean viability result compared to the control no treatment condition (*t* = 1.69, *p* = 0.23). It is, therefore, presumed that the presence of the combined electrical field and conditioner did not have a significant impact on the viability of the ova, implying that temperature is the effective parameter in the inactivation of *Ascaris* for this particular set of experiments.

Most of the other data point could not be subjected to statistical analysis because of the heterogeneous conditions under which the eggs were subjected. All three *Ascaris* chambers placed within the same bench-scale unit and subjected to the same experimental test conditions experienced vastly different environments in terms of pH, temperature, oxidation potential, oxygen levels, reactive chemical species, etc. Thus very few duplicate conditions existed with which to apply towards further statistical analysis.

Table 4.1 Results of *Ascaris suum* inactivation for the bench-scale EK trials

Treatment conditions	<i>Ascaris suum</i> viability (% embryonated)			Maximum temperature attained (°C)		
	Anode region	Middle region	Cathode region	Anode region	Middle region	Cathode region
No heat / no AN conditioner	92.7	91.4	88.4	21	21	21
No heat / 13g AN/l	91.2	92.1	90.4	20	20	20
Ohmic heat / no AN conditioner	90.9	90.3	6.4	46	43.5	44
Ohmic heat / 13g AN/l	0	0.8	0	57.5	54.5	55
Baseline <i>Ascaris suum</i> viability	92.9	92.9	92.9	N/A	N/A	N/A

N/A: not applicable.

Table 4.1 contains the *Acsaris* inactivation results of the EK treated sludge. The anode, middle, and cathode regions correspond to positions along the bench-scale units (Figure 3.2). The target temperature for subsequent heat treatment was selected from the results of the *Ascaris* inactivation screening trials defined in the third experimental phase; that is to say, the target temperature was set at 55°C for the duration of 10 minutes. The subsequent parameters of applied voltage gradient and AN conditioner concentration remained the same; the only modification being that the sludge liquor was allowed to drain out of the EK cells during these trials and the *Ascaris* eggs remained in the units for the entire length (66 hours) of the experiment. To this end, perforated electrodes were

used, reducing the effective surface area by about 1 %. The occurrence of drainage impacted other parameters that during the screening experiments remained relatively constant. It is important to note that the time to reach 55 °C during this set of experiments had almost doubled, from an average of 22 minutes during the screening tests to 43 minutes for the analogous conditioned heat treated sludge [H(13)] (the complete set abbreviations and treatment parameters referred to here are summarize in Table 3.3). Although the applied voltage gradient and AN concentration were the same, the change in sludge volume due to electroosmotic dewatering altered the flow of electrical current reflected in the lower registered amperages which remained relatively constant throughout the heating phase. As for the unconditioned heat treated sludge [NH(0)], due to its low inherent conductivity (3.49 mS/cm) in the absence of conditioner, the heating of the sludge, at the set voltage gradient of 2.5 V/cm, was so low, that even after 2.5 hours, the temperature had only increased by about 20 °C to reach an average of 44.5 °C. The voltage gradient was lowered to 0.5 V/cm after 3 hours, effectively ending ohmic heating, due to concerns that the sustained high electric field would bias the *Ascaris* inactivation results. The target temperature of 55 °C was not attained as shown in Table 4.1. The inactivation results of this latter test, in general, conform to the screening test results for *Ascaris* ova subjected to the temperatures in the range of 40 to 45 °C. However, the inactivation result for the ova adjacent to the cathode show a marked reduction in viability, with only 6.4 %, even though the maximum temperature attained was only 44 °C. It is hypothesized that the inactivation phenomena can be explained by two factors: (1) the generation of reactive compounds at the cathode, for instance hydrogen peroxide (H₂O₂), and migration of these towards the egg chamber causing impairment to the

Ascaris ovum; and (2) the conversion of the ammonium (NH_4^+) present in the sludge to the more lipid soluble ammonia gas (NH_3) in an alkaline environment within the generated base front, causing protein denaturation inside the ovum.

The *Ascaris* inactivation trials conducted during the two pilot-scale experiments demonstrated a complete inactivation of all *Ascaris* ova in the 10 chambers placed along the middle and the low half of the pilot unit (see Figure 3.5). This result was not unexpected as the mean temperature distribution in the unit increased past the intended 55°C to 60.9°C and 60.2°C for pilot tests 1 and 2, respectively. Even those egg chambers placed perpendicular to the electrodes, effectively on the margins of the current lines, showed 100 % inactivation. The highest temperatures attained during the ohmic heating process were in the immediate vicinity of the tubular electrodes where current densities and, thus, heat generation are the greatest; the maximum temperatures recorded in these zones at the end of the heating phase were 72°C and 79°C for pilot test 1 and 2, respectively. Heat diffusion from the electrode region appeared sufficient to inactivate *Ascaris* ova adjacent to the electrodes where heating capacity is minimal.

4.1.2. Effect of Conditioner Type on Dewatering, Conductivity and Heating Rate

Preliminary tests were conducted with the purpose of discerning the best conditioner to apply for all subsequent enhanced EK trials. The conditioner's performance was evaluated on its ability to attain suitable heating and dewatering rates. Three batches of sludge were prepared with 13 g/l of the specified conditioner (i.e. AN, DAP, and urea), and subjected to ohmic heating by applying an electric field strength of 3 V/cm, and 0.5 V/cm thereafter. The results of these trials are illustrated in Figure 4.4 below:

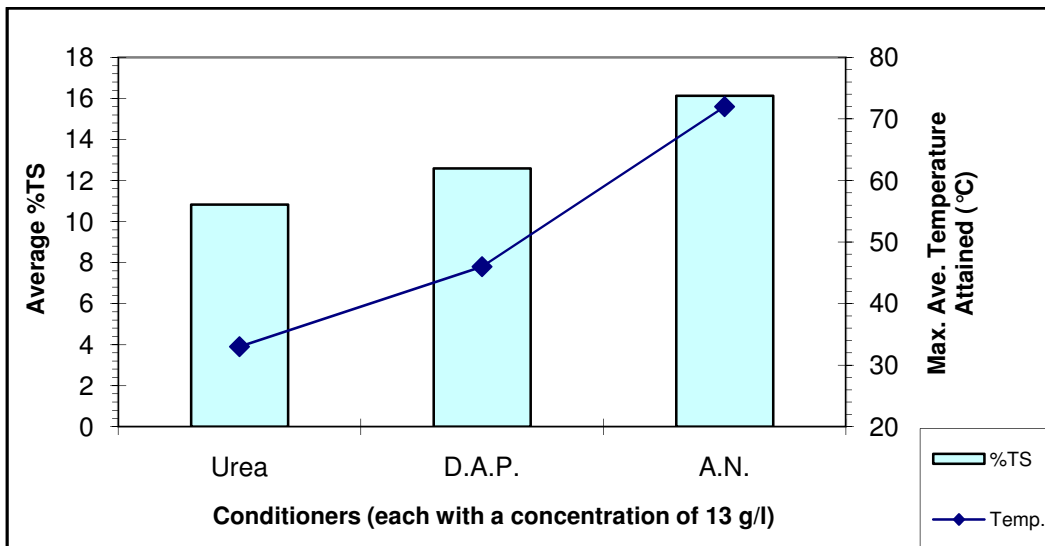


Figure 4.4 Sludge temperature and final % TS vs. conditioner type with 3 V/cm for 45 min and 0.5 V/cm for 67 hrs

The AN conditioner clearly outperformed the other two in terms of both the maximum averaged temperature obtained after 45 minute of ohmic heating and the average total amount of water extracted after 67 hours, expressed in percent total solids (% TS). The temperature was the most variable parameter observed with a nearly 30°C difference between the best and worst competing conditioner. Consequently, the AN conditioner was selected for all subsequent experiments.

The variable results observed amongst the conditioners can be partially explained by analyzing each one's conductivity in relation to one another and to their concentration. A linear relationship can be plainly observed in Figure 4.5.

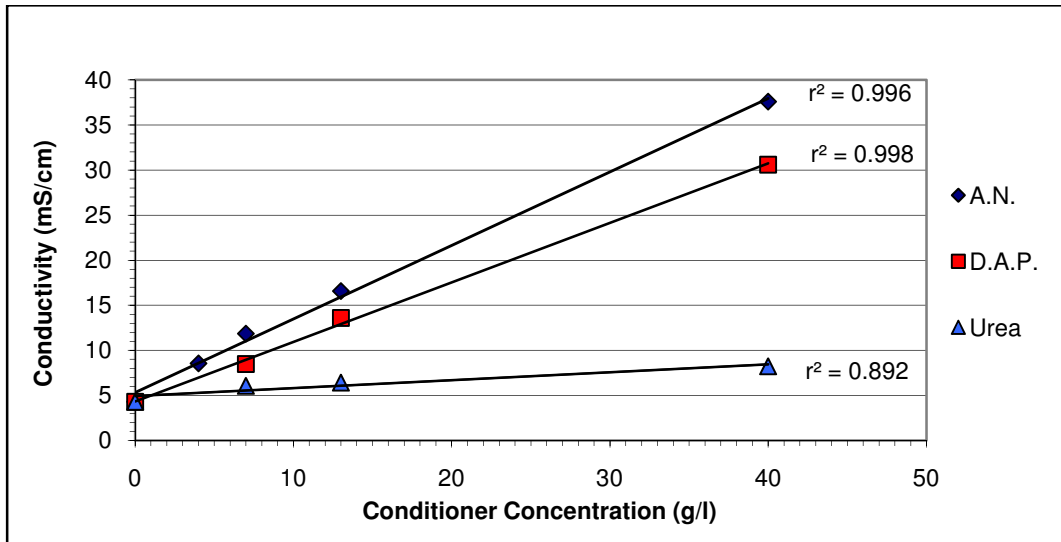


Figure 4.5 Sludge conductivities at room temperature as a function of the type and concentration of conditioners

These conductivity results demonstrate a correlation between the performances of the conditioners as witnessed in the preliminary trial and their conductivity values at 13 g/l. A linear relationship was also demonstrated, by the r^2 values listed, between the amount of conditioner added and the resulting conductivity of the sludge. The better performance of the AN conditioner is also related to its high solubility index facilitating its ionic dissolution in the sludge.

4.1.3. Effect of Conditioner Concentration on Dewatering, Conductivity and Heating Rate

A similar set of trials conducted with the selected AN conditioner was designed to detect the effect of various concentrations of AN on the dewatering capability and on the heating rates achievable. The same parameters as the previous test studying the effects of conditioners were implemented, with the exception of the time period during which ohmic heating was applied. The biosolids sustained an additional 18 minutes at 3 V/cm. The resulting maximum average temperatures and TS attained are given in Figure 4.6.

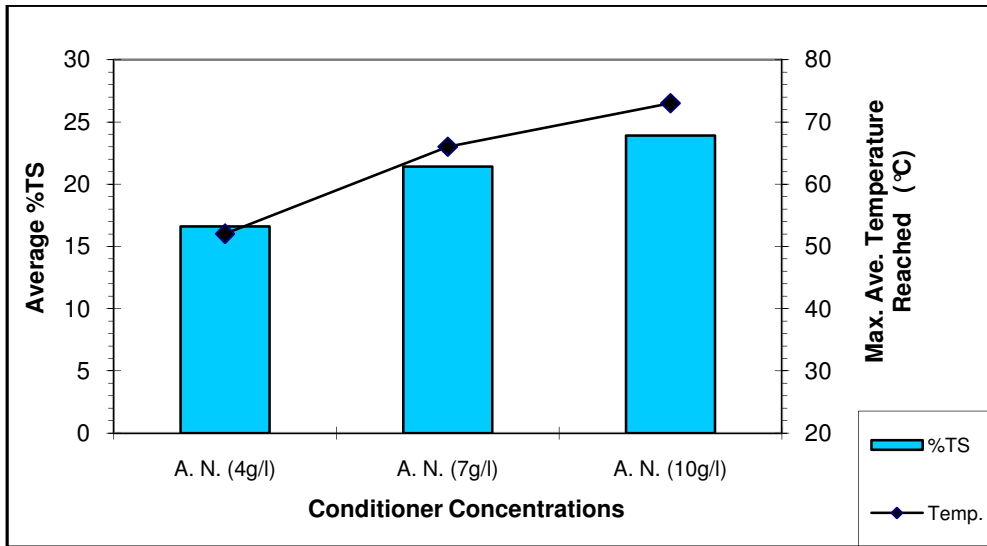


Figure 4.6 Sludge temperature and % TS vs. AN concentration with the application of 3 V/cm for 63 min and 0.5 V/cm for 67 hrs

These results again bear a close relationship with the conductivity profiles of Figure 4.5. The higher average % TS contents achieved during these trials, when compared to the same AN conditioner in Figure 4.4, can principally be ascribed to the additional 18 minutes at the higher voltage gradient.

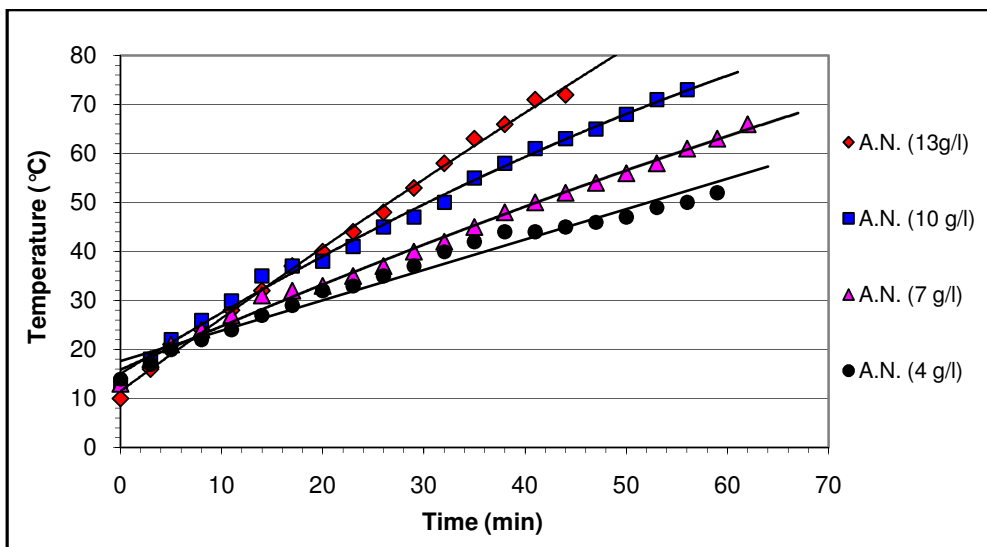


Figure 4.7 Heating rates for the various AN concentrations, each subjected to an electric field strength of 3 V/cm

When comparing the heating rates of all these preliminary trials depicted in Figure 4.7 above, we observe the direct relationship between the conditioner concentration, its conductivity, and the heating rate; as given by Joule's law (equation 22).

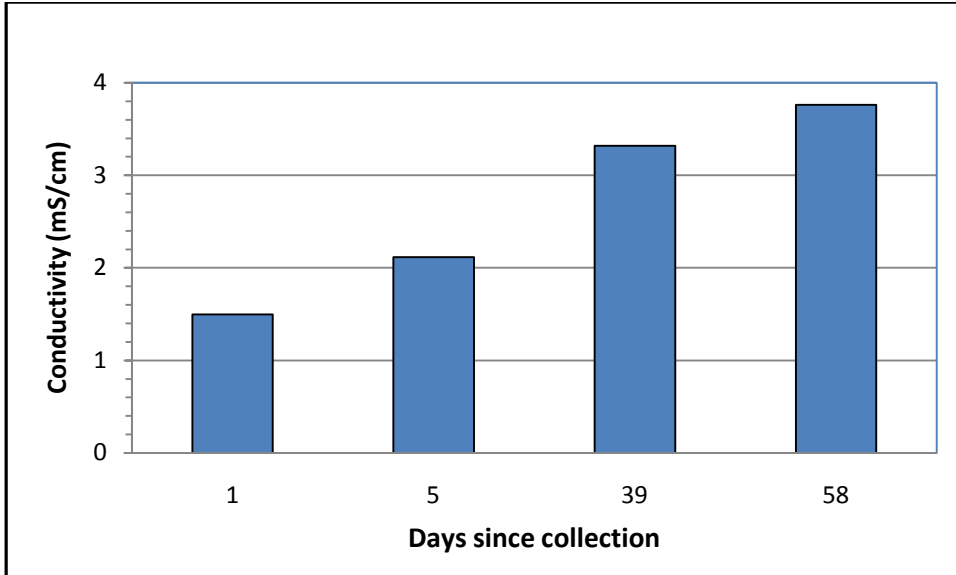


Figure 4.8 Changes in sludge conductivity with time

Although the trend between conditioner concentration and conductivity shows a linear relationship, as expected by the dissolution of ionic compounds constituting the conditioner, the conductivity also demonstrated variability with respect to sludge age (Figure 4.8). As sewage sludge is a highly variable product from day to day, and even hour to hour, its soluble organic and inorganic composition will vary accordingly. With time, the organic matter will degrade, through both biological and physical transformation processes, liberating organic acids and bases. The storage of sludge would, therefore, be a favorable precondition to treatment.

4.1.4. Effect of Temperature on the Conductivity of Various Conditioner Concentrations

As discussed in section 2.2.3 on ohmic heating, the conductivity of an electrolytic solution is temperature dependent; commonly a temperature compensation of 2 % is used for every change in degree Celsius. This relationship was investigated for different sludge batch and for different AN concentration. The conductivity of the sludge was measured for temperatures ranging from about 15°C to 80°C, by convectively heating a beaker containing 1 liter of sludge on a stirred hot plate. The results are illustrated in Figure 4.9. The rates of change in conductivity are seen to be dependent on the concentration of AN conditioner. It can be observed that the rates of change in the conductivity of the sludge with no conditioner added and with 10.45 g AN/l diverged to some extent with a respective temperature coefficient of 2.06 % and a 1.91 % for every 1°C increment. These rates are within the documented range for electrolyte solutions and do demonstrate a slight decrease in the conductivity rate as the concentrations of AN increased (Dobbs, 1978). As a consequence, their respective heating rates would likely be different as well. Considering the linear dependence between the rate of power or heat generation and the conductivity, the positive feedback established between ohmic heating and the resulting increased in conductivity would tend to accelerate the apparent heating rates, as described by the autothermal effect.

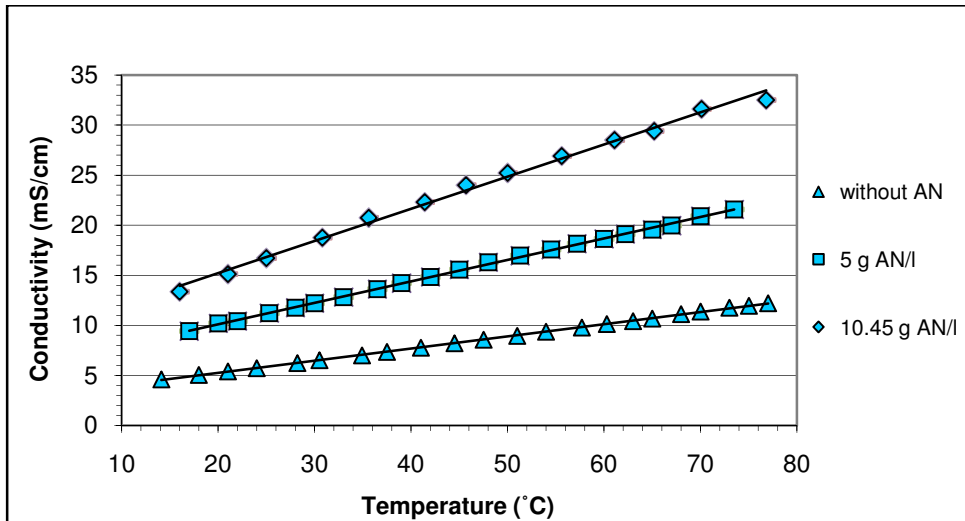


Figure 4.9 Conductivity of sludge as a function of temperature with respect to the AN concentration

The water content of the sludge subjected to the same AN concentrations did not appear to significantly influence the conductivity/temperature curves (Figure 4.10). Even with 40% of the liquor removed by vacuum filtration, the biosolids showed similar temperature coefficients.

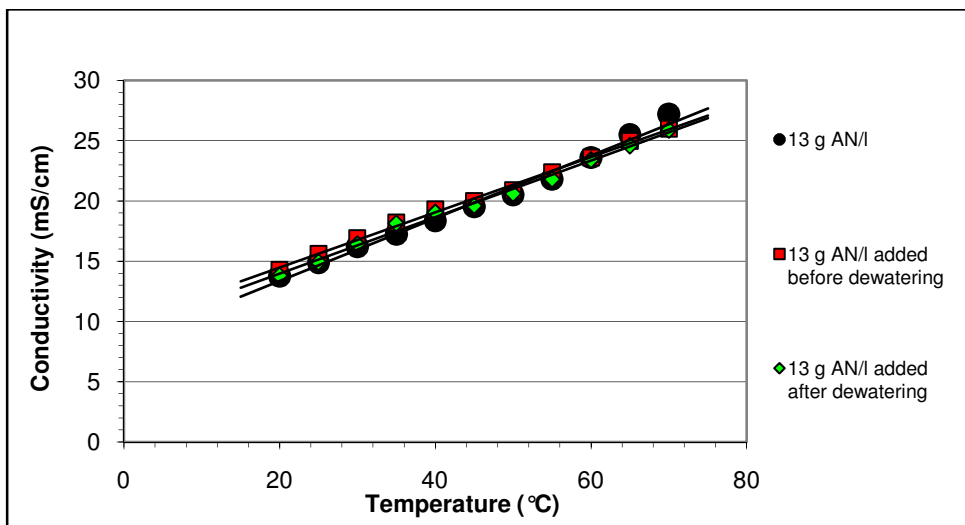


Figure 4.10 Comparison of conductivity and temperature relationship with respect to the water content of the sludge

This would indicate that the dewatering action during the enhanced EK application does not have a direct effect on the heating rate through its influence on conductivity, but rather the simultaneous dewatering will impact ohmic heating through a reduction in the system's volume and mass.

4.1.5. Effect of Applied Voltage Gradients on Heating Rates

The profiles of the electrical current at various applied voltage gradients for the sludge heating trials are shown in Figure 4.13 for the DC tests and Figures 4.15 for the AC tests. The same set of voltage gradients was utilized for both AC and DC experiments. As attempts were made to keep the sludge conductivities between every trials constant, by using the same concentration of the conditioner, the initial amperage is proportional to the applied voltage and follows Ohm's law.

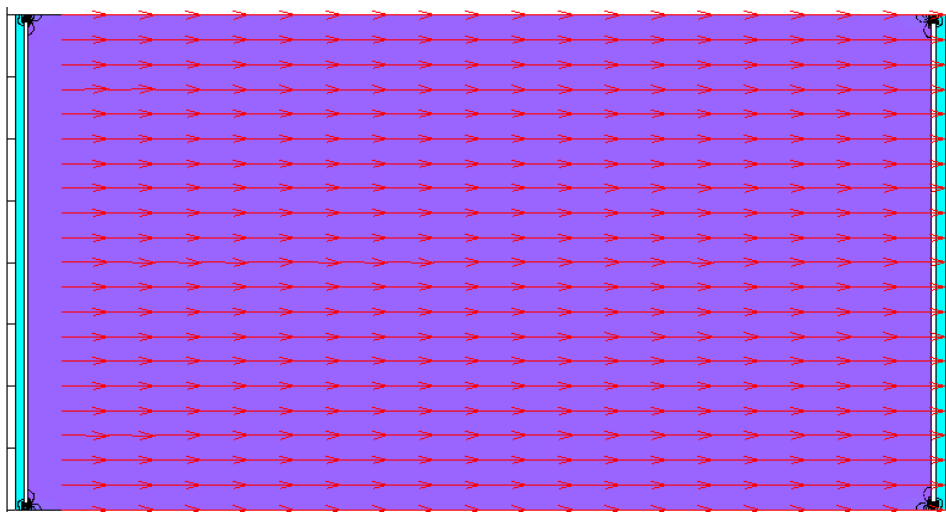


Figure 4.11 1D bench-scale tests: visualization of current lines

Figure 4.11 representing the bench-scale unit is generated, for a purely figurative purposes, using the basic Partial Differential Equation (PDE) Toolbox in Matlab[®] and solving for the Laplace equation, $\nabla \cdot (\sigma \nabla V) = 0$, which defines the 2D physical model for

a conductive media subjected to an electric potential. Dirichlet boundary conditions assign values of the electric potential to the electrodes and a neutral Neumann boundary condition to the outer non-conductive boundaries of the cell. The numerical equations are finally discretized by a built-in Finite Element Method (FEM). The above figure illustrates the resulting current densities uniformly distributed throughout the cell, visualized as current lines (the vector field of the current densities (J_{CD})). Since the current density is proportional the power dissipated as heat, the model exemplifies the uniform ohmic heating taking place in the sludge. The bench-scale experiments, however, did not exactly conform to the model which fails to consider the electrolysis reactions occurring at the electrodes' surface. The generation of the gases at the electrodes creates a zone in the sludge with greater resistance to the flow of charges, thus the heating rates observed at both extremities were slightly higher, producing temperature variations as high as 5°C along the unit; this variation was particularly apparent for the DC trials subjected to the lower range of applied voltage gradients. The AC trials on the other hand produced much more uniform heating rates, due to the absence of visible gas evolution, even at the higher applied voltages.

The temperature profiles associated with the applied electrical field are illustrated in Figure 4.12 for the DC tests and Figure 4.14 for the AC tests. The temperature increase from the power dissipated as heat due to the electrical resistance of the sludge is observed to follow Joule's law ($P = V^2/R$), whereby the increase in heating rates is coupled to the increased applied voltage. This relationship is made apparent in Figure 4.16 with a near square power relationship. From the latter figure, the lowest voltage gradient generating a minimum heating rate can be extrapolated for the given EK unit and test conditions used.

In this instance, any voltage gradient below 0.5 V/cm would be incapable of generating heat in the sludge. Also, the application of alternative current significantly increased the heating rate compared to sludge subjected to direct current; this was particularly apparent at the higher voltage gradients.

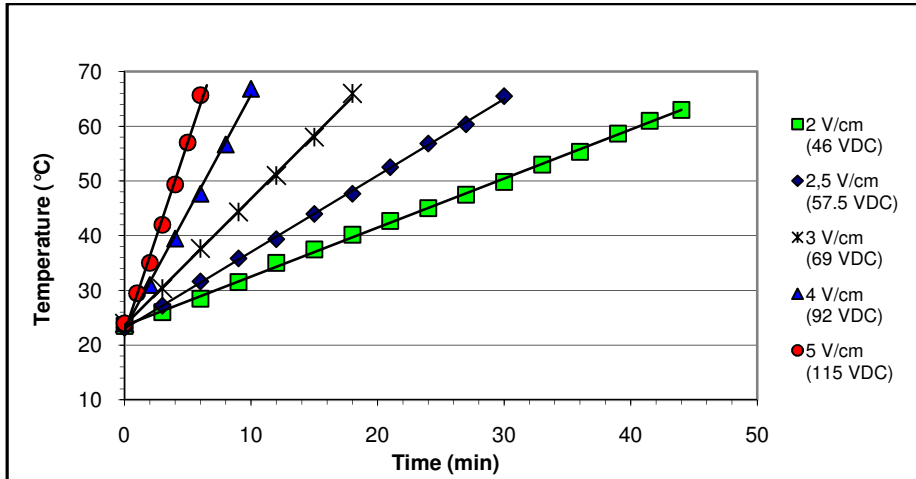


Figure 4.12 Heating rates in sludge as a function of the applied DC voltage gradient (average $\kappa = 16.61 \pm .16$ mS/cm)

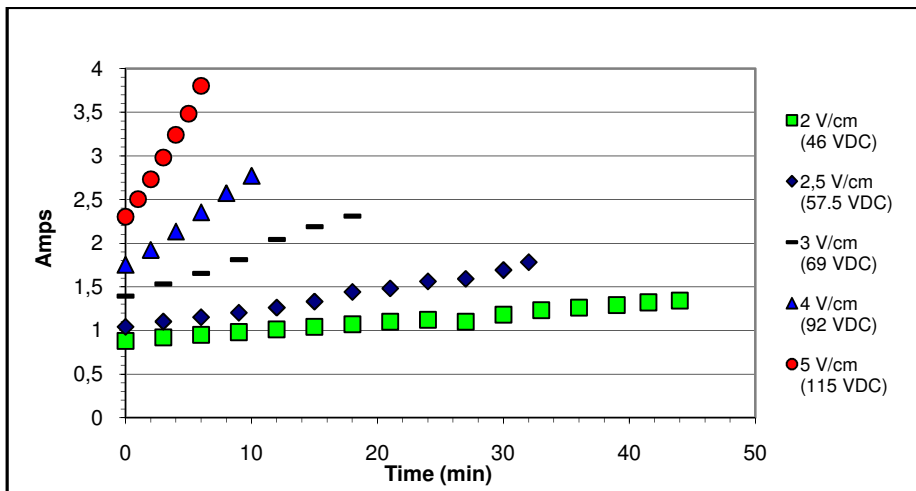


Figure 4.13 Evolution of amperage rates in function of applied DC voltage gradient (average $\kappa = 16.61 \pm .16$ mS/cm)

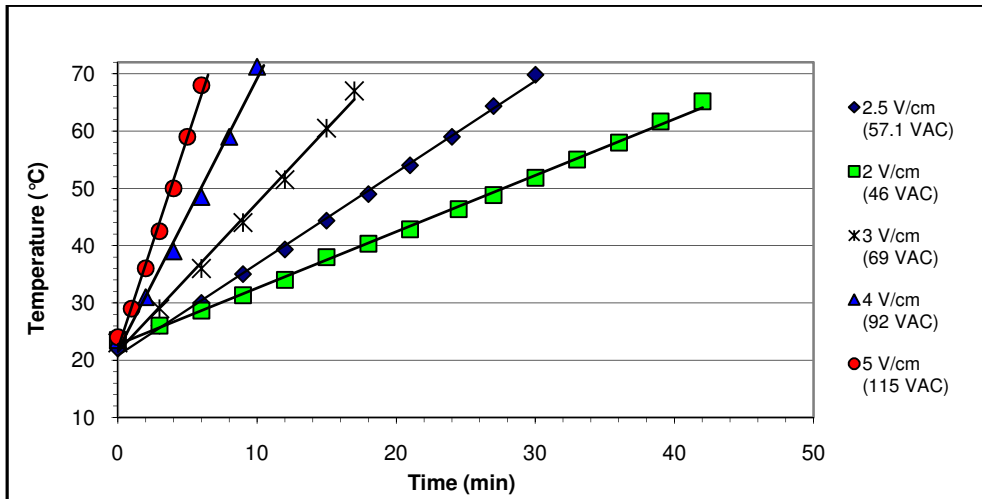


Figure 4.14 Evolution of heating rates as a function of the applied AC voltage gradient (average $\kappa = 16.50 \pm 1.17$ mS/cm)

Figures 4.13 and 4.15 also demonstrate the autothermal effect through the steady increase in the measured electrical current. The increase in temperature due to joule heating raises the electrical conductivity; the increase conductivity results in a higher current flow, which in turn, boosts the heat generation term in equation (22) and further increases the local temperature, which again contributes to intensify the current density and so on in positive feedback loop.

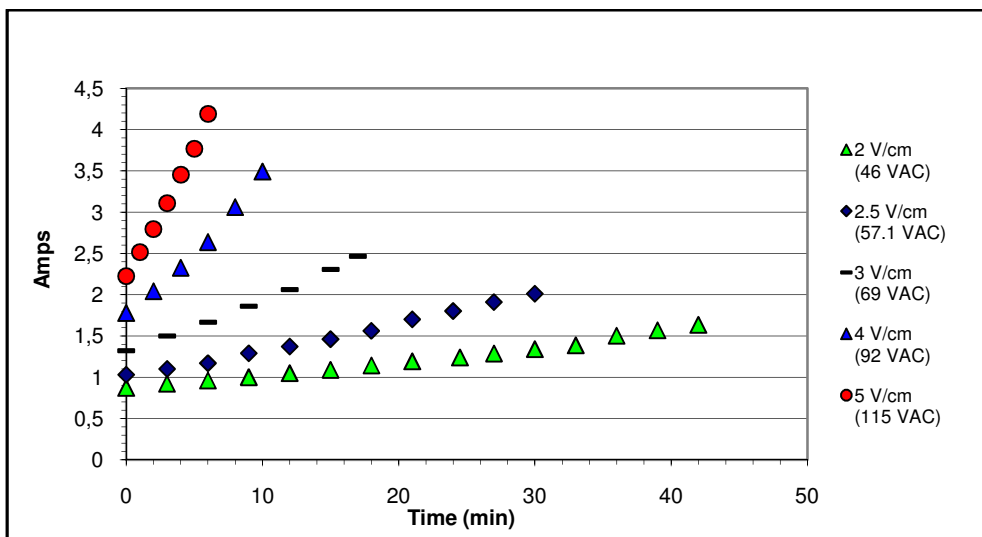


Figure 4.15 Evolution of amperage rates in function of applied AC voltage gradient (average $\kappa = 16.50 \pm 1.17$ mS/cm)

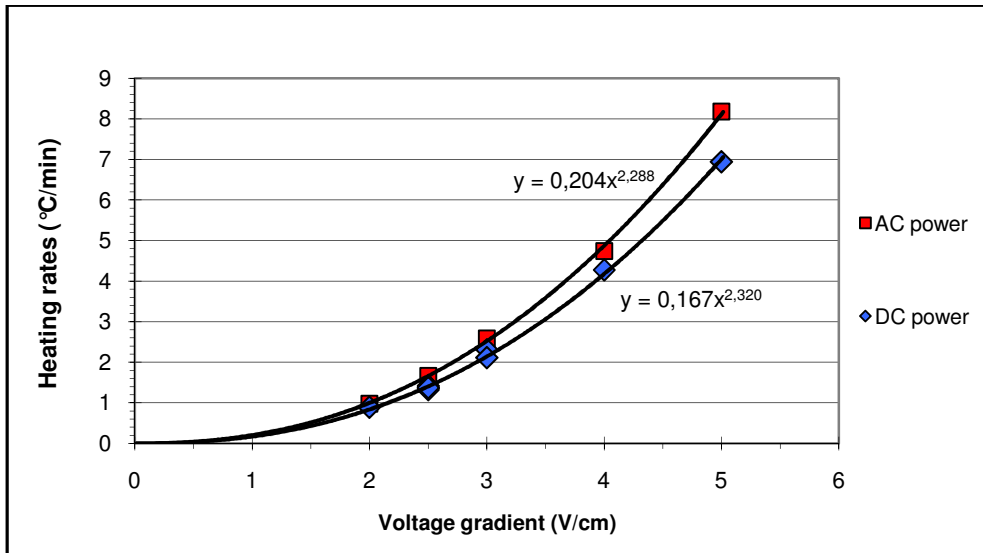


Figure 4.16 Heating rates in function of applied electric DC and AC fields

The divergence between the AC and DC heating rates, in Figure 4.16, is predominantly due to the differences in the proportion of power delivered that was resistively dissipated as heat in the sludge and that was dissipated in Faradic (electrochemical) reactions at the electrode surface, evidenced by the apparent lack of gas production during the AC trials. In this respect, the supply of AC power has an economic advantage over DC power.

4.1.6. Energy Consumption

Since the volume of sludge and the voltage gradient applied across the EK cell was kept constant in these sets of experiments, the energy expenditure is directly related to the time integral of the current, presented in Figures 4.13 and 4.15, across the EK cell. The calculated energy consumption to heat the sludge to 60°C for both DC and AC trials are presented in Figure 4.17. It can be noted that the electrical energy required to heat the sludge during the AC tests was significantly smaller at the lower applied voltage gradients when compared to the DC tests; reaching as much as 7.67 % at 3 V/cm. This

difference was, however, reduced at higher applied voltage gradients, and was insignificant at 5 V/cm.

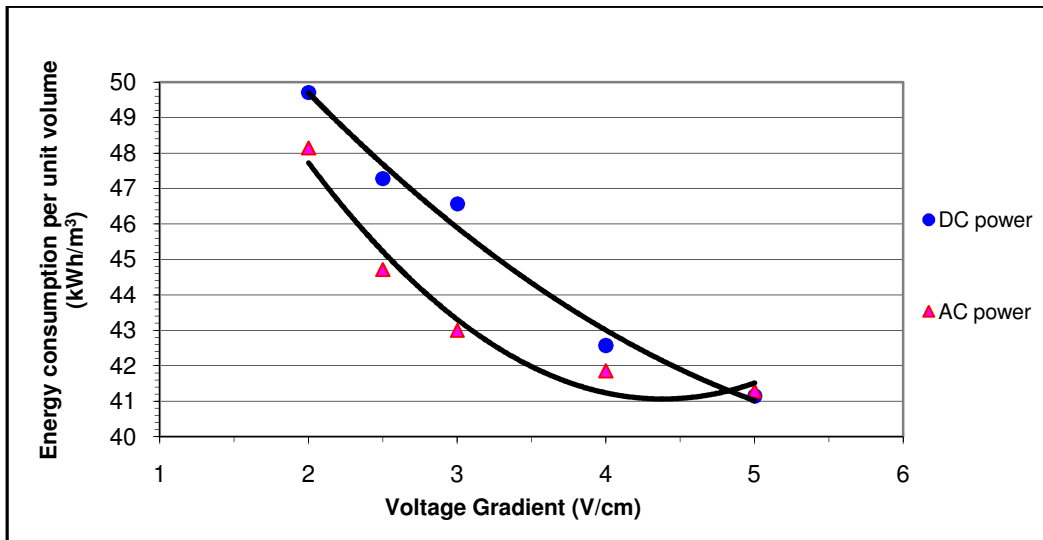


Figure 4.17 Comparison of energy consumption between DC and AC power to reach 60°C (average $\kappa = 16.57 \pm .16$ mS/cm)

4.1.7. Results of the Bench-Scale EK Experiments

The following subsections detail the results of the bench-scale studies and evaluate the physical and chemical parameters of biosolids subjected to enhanced EK treatment. The physical parameters of interest are the volume of sludge liquor collected, the total solids content (TS), the volatile solids content (VS), and the pH. Chemical analyses were performed on the biosolids to determine the residual metal (Cd, Cr, Cu, Fe, Pb, and Zn), and ion (NH_4^+ , NO_3^- , and PO_4^{3-}) distributions along the cell. Two replicate conditions were also implemented in these latter trials: one without the application of ohmic heating and the other without the addition of conditioner, as control conditions. The treatment conditions achieved are described in Table 4.2 below; these did diverge to some extent from the designed conditions of Table 3.3.

Table 4.2 Treatment conditions obtained during the bench-scale EK experiments

Treatment conditions	Abbreviation	Electrical parameters	Maximum average temperature attained
No heat treatment / no AN conditioner	NH(0)	0.5 V/cm for 66 hours	20 °C
No heat treatment / 13g AN/l	NH(13)	0.5 V/cm for 66 hours	21 °C
Ohmic heat treatment / No AN conditioner	H(0)	2.5 V/cm for 2.5 hours, 0.5 V/cm for the balance	44.5 °C
Ohmic heat treatment / 13g AN/l	H(13)	2.5 V/cm for 51 minutes, 0.5 V/cm for the balance	56 °C

4.1.7.1. Sludge dewatering

The sludge liquor collection rate of bench-scale EK experiments with respect to time is shown in Figure 4.18. After an initial 2.5 hour dewatering period by gravitational means, the collected liquor volumes from each cell had stabilized at about 50 ml; a loss of approximately 7.5 % of their respective volumes. The initial flow rates of the liquors (i.e. anolyte and catholyte) are highest for the cells subjected to joule heating. Joule heating in these two instances is the consequence of the application of a higher initial voltage gradient of 2.5 V/cm compared to the control treatments with 0.5 V/cm. Recall that the velocity of the electroosmotic flow is proportional to the applied electrical field (Kok, 2000): $v_{eo} = \mu_{eo} \cdot E$. Although it is not possible to differentiate the influence of heat on sludge dewaterability, heat may have promoted it by decreasing the viscosity of the sludge.

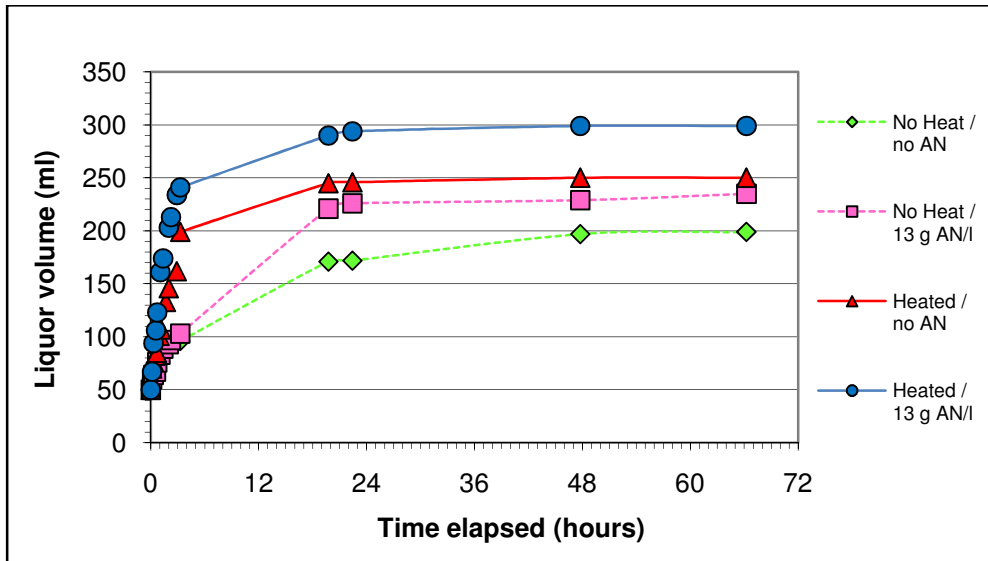


Figure 4.18 Volume of sludge liquor collected during bench-scale EK experiments

When comparing the results of the conditioned sludge, at the point when the voltage gradient was reduced to 0.5 V/cm after only 51 minutes, the heated and conditioned test [H(13)] had almost doubled the total volume of liquor collected compared to the non-heated test [NH(13)]. Another notable effect of heating the sludge is demonstrated in Table 4.3; the heated test condition without added conditioner, H(0), extracted more liquor than the AN conditioned sludge [NH(13)] subjected to a constant voltage gradient of 0.5 V/cm throughout the trial. This is a demonstrable advantage of the application of a higher voltage gradient in the early phase of the EK treatment when resistance to the flow of fluid is at a minimum.

Table 4.3 Total volume of liquor types collected in bench-scale EK experiments

Treatment conditions	Total anolyte collected (ml)	Total catholyte collected (ml)	Total liquor collected (ml)
NH(0)	46	153	199
NH(13)	83	152	235
H(0)	70	180	250
H(13)	117	182	299

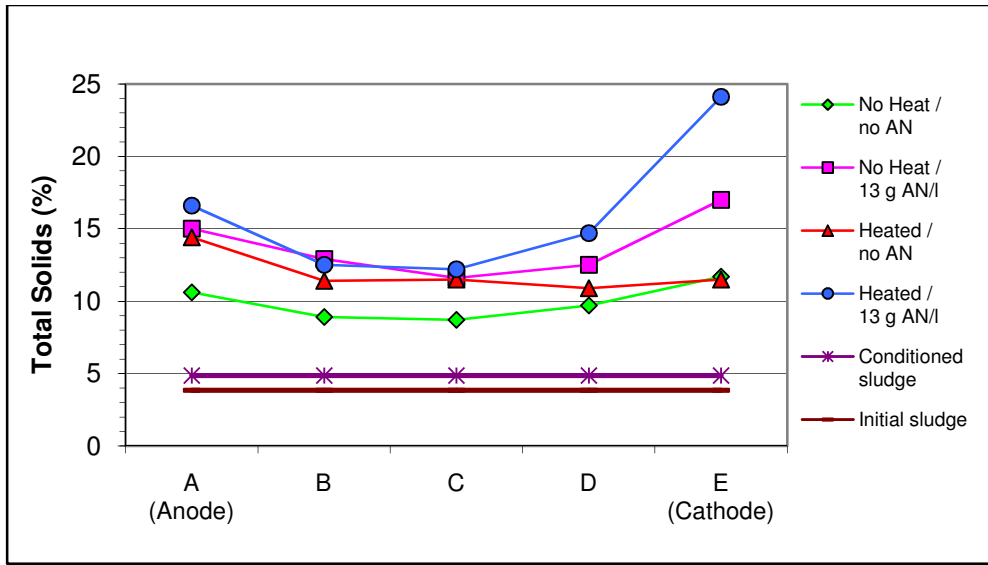


Figure 4.19 Distribution of TS between electrodes in bench-scale EK experiments

The water content profile, expressed in terms of percent total solids (%TS), at the end of the bench-scale EK experiments are displayed in Figure 4.19. The highest %TS reached 24.1 % TS at the cathode area for the ohmically heated and conditioned biosolids [H(13)] compared to only 11.7 % TS for sludge submitted to EK treatment alone [NH(0)], yet more than double the initial %TS. Except for treatment condition H(0), the patterns are virtually similar for the four tests with TS content higher near the electrode regions. The higher water content observed in H(0) at the cathode area is predominantly due to poor drainage caused by the formation calcium carbonate obstructing the fine openings of the stainless steel mesh covering the electrode and possible hydroxide precipitate created inside the base front obstructing the fluid pores; recall that the period of time this treatment condition was subjected to the higher voltage gradient of 2.5 V/cm was more the double that of H(13). This occurrence was compounded by a greater accumulation of liquids in this region as a result of predominate electroosmotic flow towards the cathode. The final average %TS content throughout the unit is depicted in Figure 4.20. The

optimal removal efficiency occurred for test H(13) with an average TS content reaching 16 % after 66 hours. The lowest water removal efficiency occurred for the treatment condition NH(0) with a final average TS content of only 9.9 %. The overall effectiveness of water removal by electrokinetic treatment was optimized by the addition of the AN conditioner. However, this outcome could not have been predicted by looking at the total volume of liquor collected from each cell, illustrated in Table 4.3 and Figure 4.18. These reveal that proportionally more liquor was collected from the two heat treatments conditions independently of conditioner application. This phenomenon suggests that the application of a high voltage gradient with the resulting increase in electroosmotic flow early in the sludge treatment process has a significant impact on the final TS content of the biosolids.

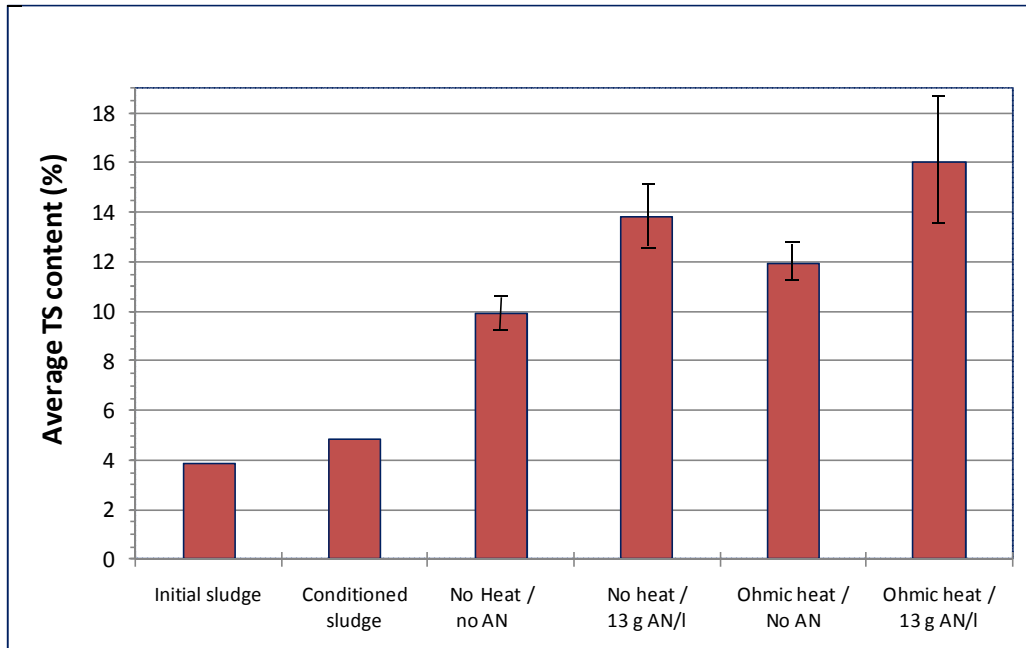


Figure 4.20 Final average of TS content of the bench-scale EK experiments

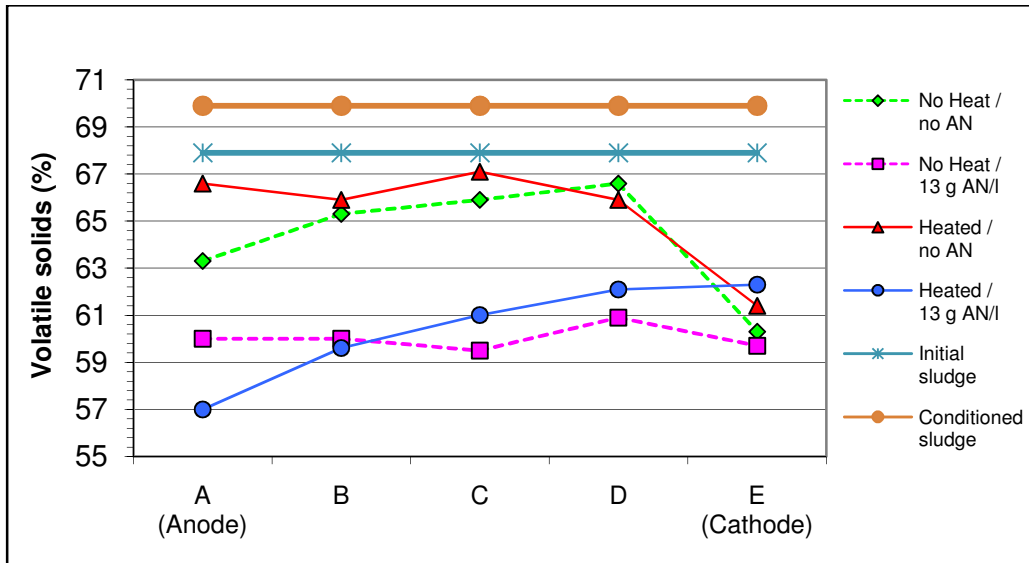


Figure 4.21 Distribution of volatile solids between electrodes in bench-scale EK experiments

Figures 4.21 and 4.22 show a clear difference in the volatile solids content between the conditioned and unconditioned biosolids. The addition of the AN conditioner appeared to increase the mobility and extraction of the organic matter out of the cell by an average of about 15 %. Better drainage of the H(13) treatment may have further helped reduce the overall VS content of the biosolids.

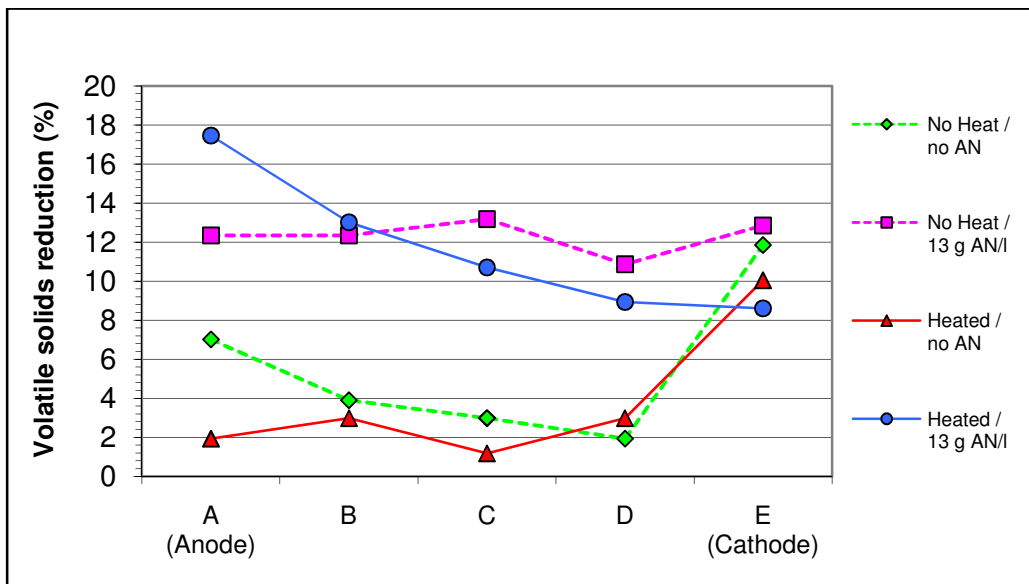


Figure 4.22 Volatile solids reduction in bench-scale EK experiments

4.1.7.2. pH and Ion Distribution

It is essential to measure the pH changes across the cell since the pH is a prominent variable in the chemical equilibriums and the dissolution, precipitation, or sorption reaction in the pore fluid. The soil pH profile for the bench-scale EK trials is illustrated in Figure 4.23. The biosolids' pH values of most sections diverge from the initial value of pH 6.33 to minimum and maximum pH values of 4.50 to 8.95, respectively; achieved by treatment NH(13).

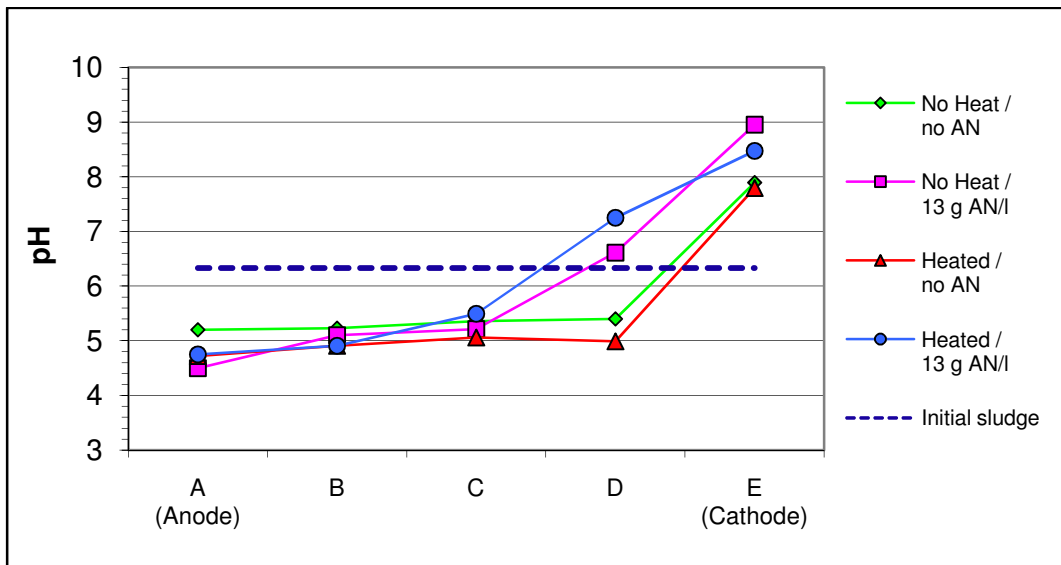


Figure 4.23 pH profiles of the bench-scale EK experiments

The advance of the acid front generated at the anode acidified the biosolids to a greater extent for the unconditioned sludge compared to the conditioned sludge after 66 hours of EK treatment. The conditioned sludge demonstrated a more gradual increase in pH between the anode and cathode; whereas, the unconditioned sludge showed a relatively low steady pH, compared to the initial pH of the sludge, up to section D, adjacent to the cathode zone. This may suggest either a greater migration of hydroxide ion towards the

anode or a higher pH buffering capacity of the AN conditioner when incorporated into the sludge. The decrease of the biosolids' pH mainly depends on the buffering capacity of the sludge and the amount of protons generated at the anode.

As the bench-scale experiments consisted of two sets of conditioned and unconditioned sludge, it was necessary to demonstrate the results of these two sets separately in order to better observe the distribution of NH_4^+ and NO_3^- among the treatments. Although the conditioner did not contain phosphate, it is assumed the increase observed, from 0.34 to 1.55 g/kg TS, with the addition of the AN results from the release of phosphate initially sorbed to the organic fraction of the sludge by ionic exchange mechanisms.

The introduction of 13g/l of AN increased the nitrate concentration in the sludge from an initial concentration of 0.4 g/kg TS to 44.7 g/kg TS. Figures 4.24 and 4.25 show the distribution of nitrate in the EK trials for the unconditioned and conditioned sludge, respectively. Overall, a good reduction in nitrate was observed, with the greatest drop generally occurring near the cathode region. The ohmic heat treatments did considerably better for both conditioned and unconditioned biosolids. Although the heat treatment was not able to remove all the amended NO_3^- from the conditioned sludge to its initial state, over 80 % of this anion was extracted from the system. The extraction of nitrate presumably driven by electrophoretic migration towards the anode, under the ohmically heated condition, had the added assistance of superior electroosmotic movement towards the anode, as seen in Table 4.3, with between 29 % and 49 % greater volumes of anolyte collected.

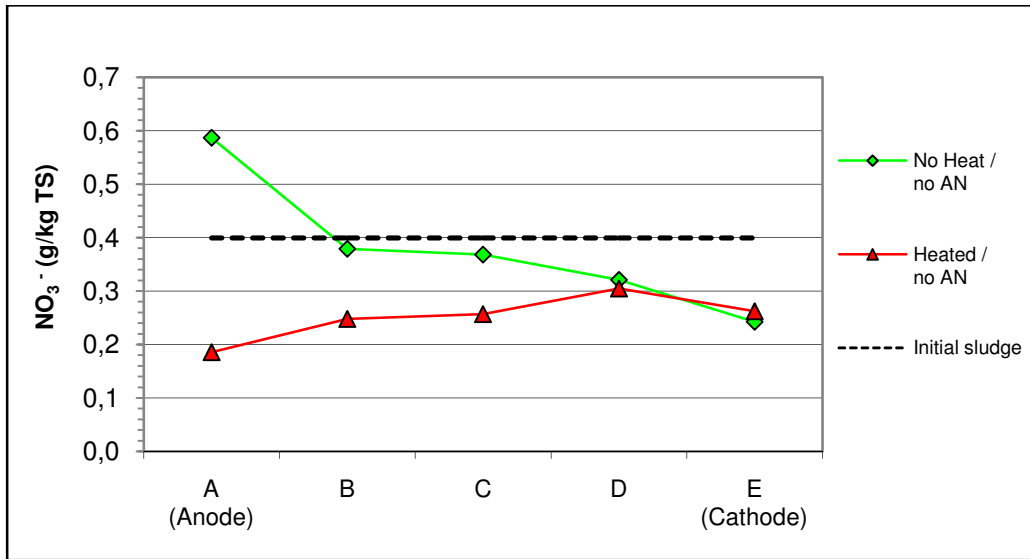


Figure 4.24 Nitrate distributions for the unconditioned sludge in the bench-scale EK experiments

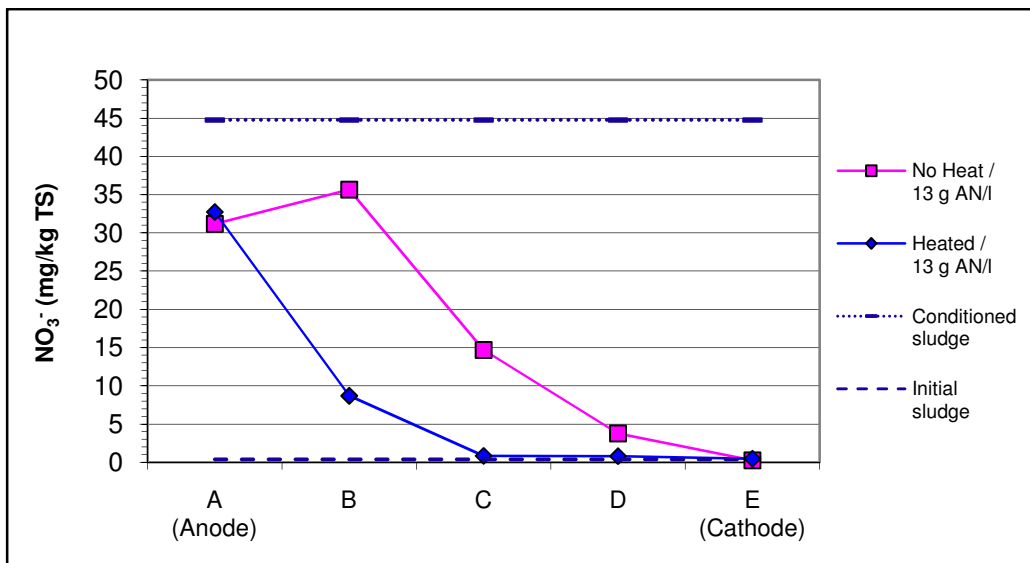


Figure 4.25 Nitrate distributions for the AN conditioned sludge in the bench-scale EK experiments

Similarly, the ammonium concentration rose from 6.2 g/kg TS to 43.8 g/kg TS with the addition of the conditioner. The results presented in Figures 4.26 and 4.27 show a much larger extraction of NH_4^+ from the system for all treatment conditions compared to the former NO_3^- with final mean concentration below the initial sludge value.

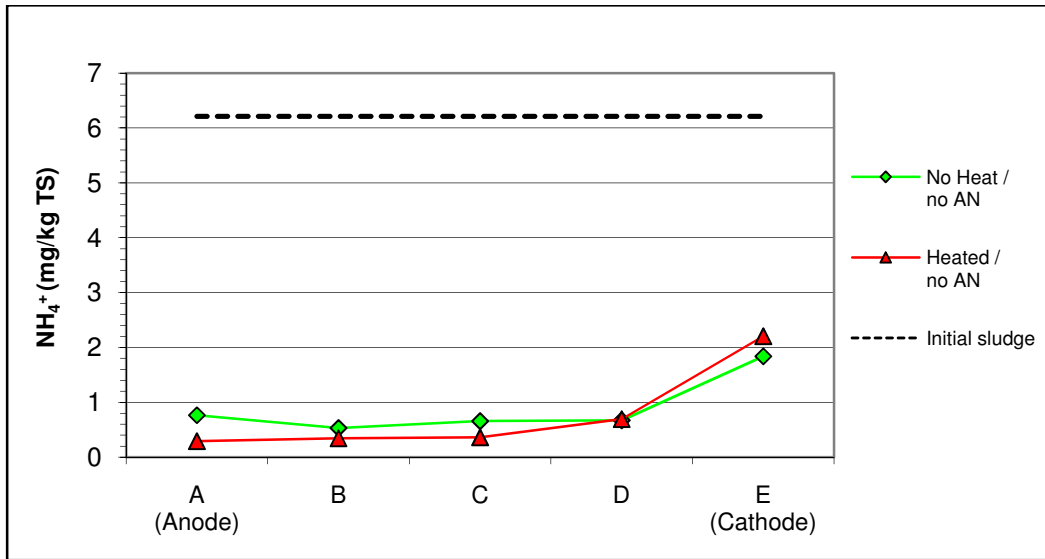


Figure 4.26 Ammonium distributions for the unconditioned sludge in the bench-scale EK experiments

It should be pointed out that for ammonium, the electroosmotic and ion migration occurred in the same direction, towards the cathode, as evidenced from the much larger volume of collected catholyte over the anolyte (Table 4.3). The ohmically heated trials did demonstrate a minor improvement in removal efficiency.

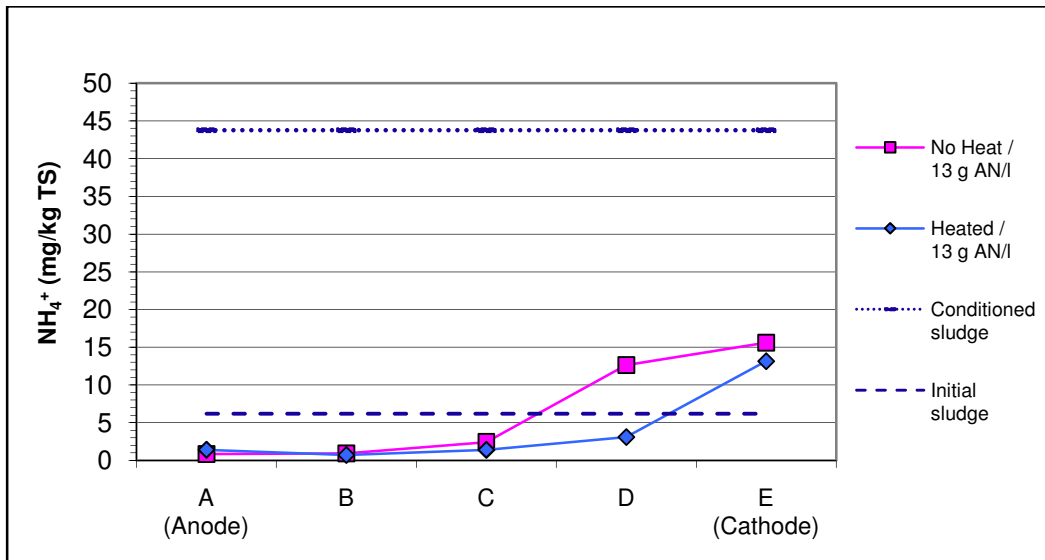


Figure 4.27 Ammonium distributions for the AN conditioned sludge in the bench-scale EK experiments

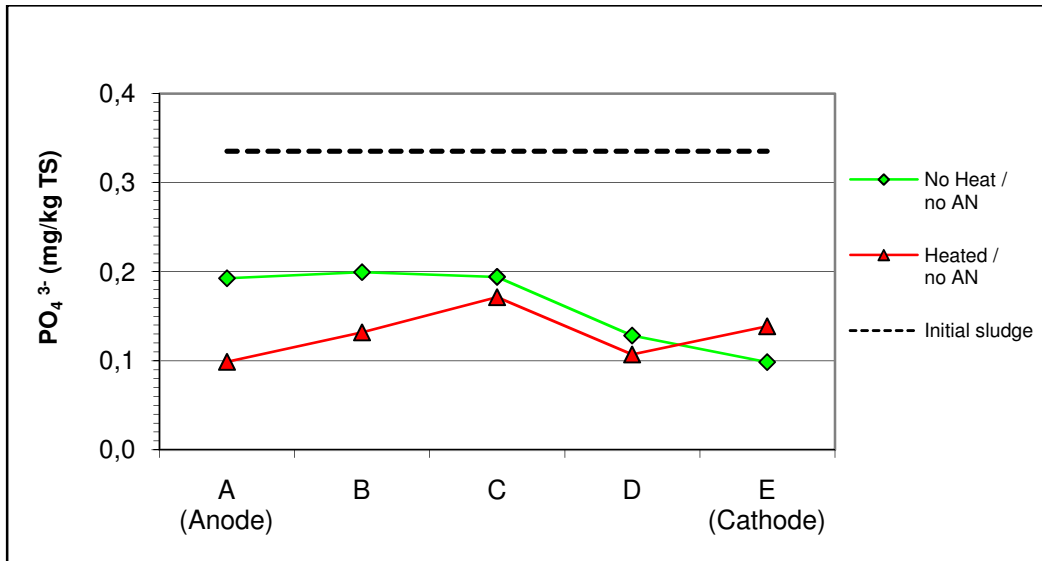


Figure 4.28 Phosphate distributions for the unconditioned sludge in the bench-scale EK experiments

Like the ammonium results, the phosphate showed good removal efficiency from the system to below the initial concentration with all treatment conditions. The resulting concentrations of PO_4^{3-} in the biosolids are presented in Figures 4.28 and 4.29. Again, the application of a high voltage gradient leading to ohmic heating early in the EK process resulted in a greater reduction in final phosphate concentrations.

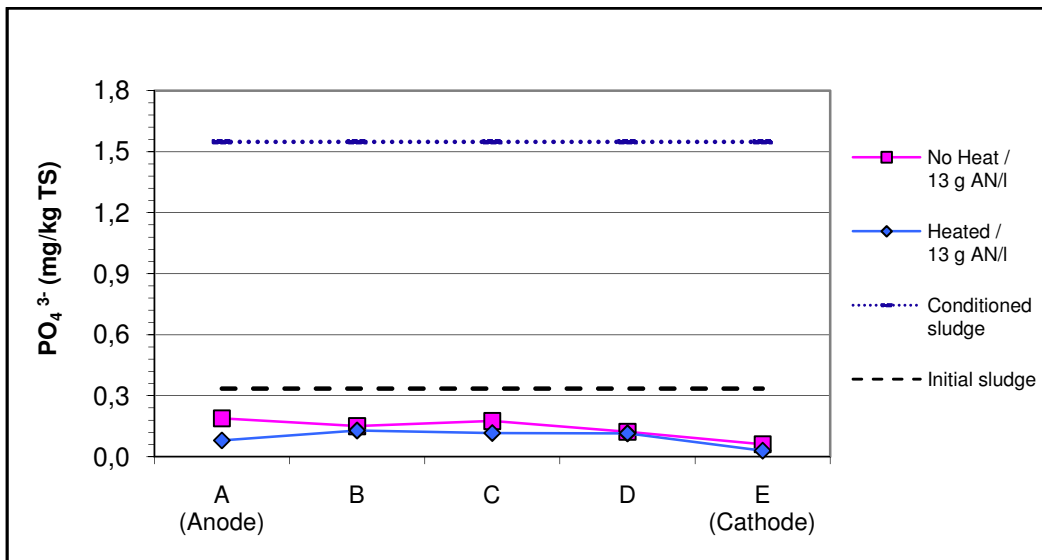


Figure 4.29 Phosphate distributions for the AN conditioned sludge in the bench-scale EK experiments

4.1.7.3. Heavy Metal Distribution

The profiles of heavy metal removal for the bench-scale experiments by EK treatment are shown in Figures 4.30 through 4.35. The nature of the steel electrode composed of Fe and other trace metals greatly influenced the metal content of the biosolids. Electrolysis of the anode released the metal constituents into the sludge to various degrees depending on the applied test conditions. Nevertheless, the removal of these metal species did take place simultaneously due to ion migration and electroosmosis. Both these actions appeared to be slower than the electrolysis process, particularly for tests without the addition of AN conditioner.

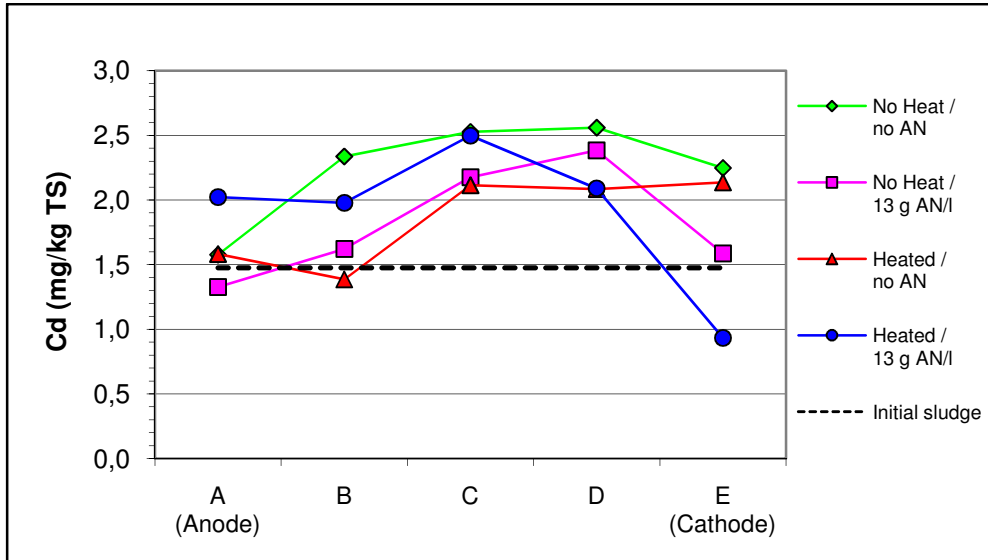


Figure 4.30 Cadmium distribution between electrodes in the bench-scale EK experiments

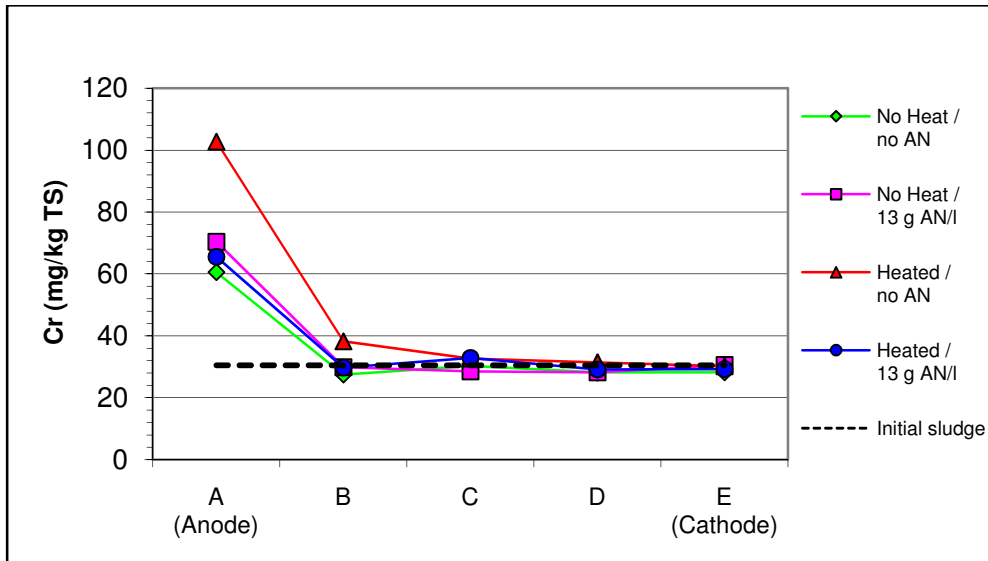


Figure 4.31 Chromium distribution between electrodes in the bench-scale EK experiments

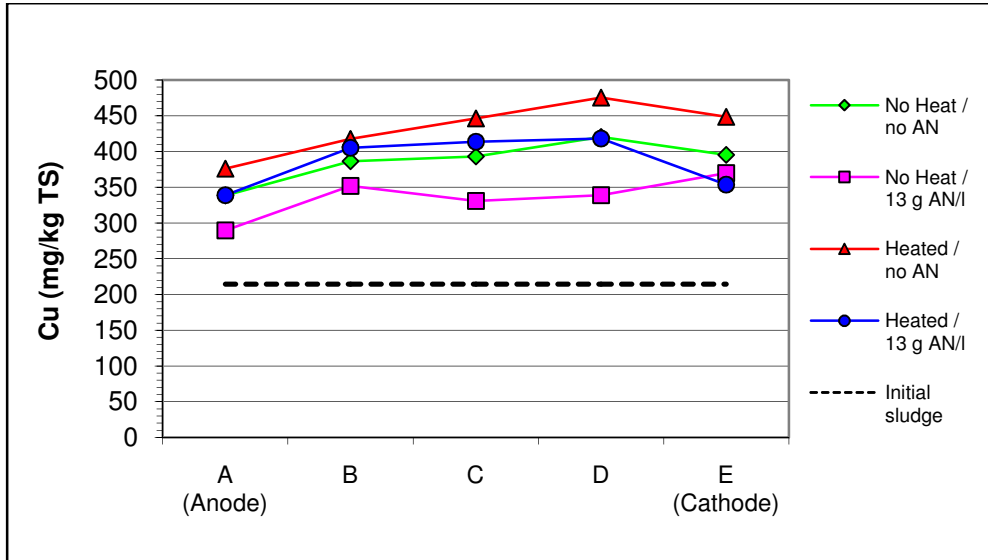


Figure 4.32 Copper distribution between electrodes in the bench-scale EK experiments

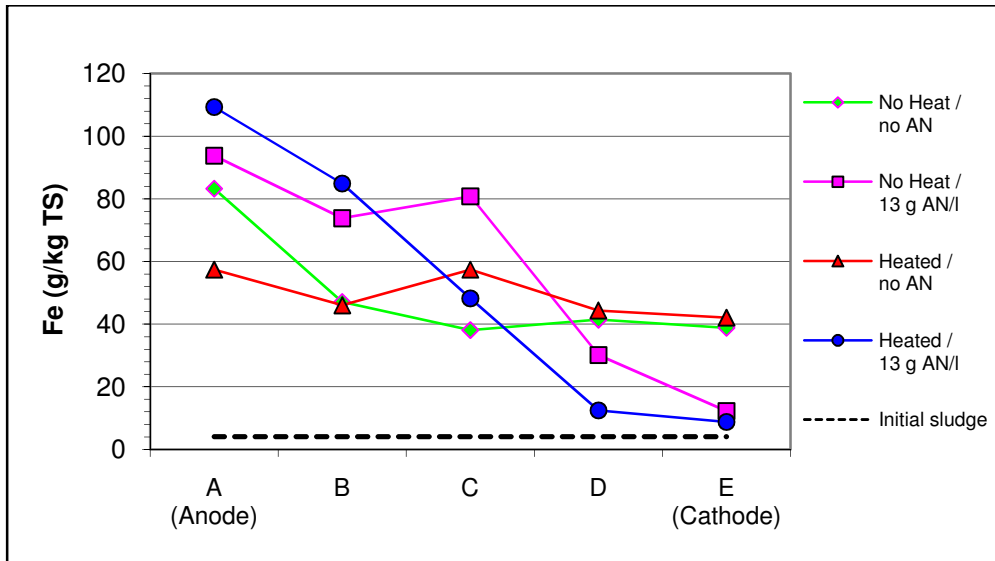


Figure 4.33 Iron distribution between electrodes in the bench-scale EK experiments

Lead showed the widest variation between the treatment conditions. Its ionic speciation is strongly correlated to temperature, oxidation state, and the presence of the conditioner. A movement towards the cathode together with a drainage at the cathode is observed, and in particular with the ohmically heated and conditioned sludge.

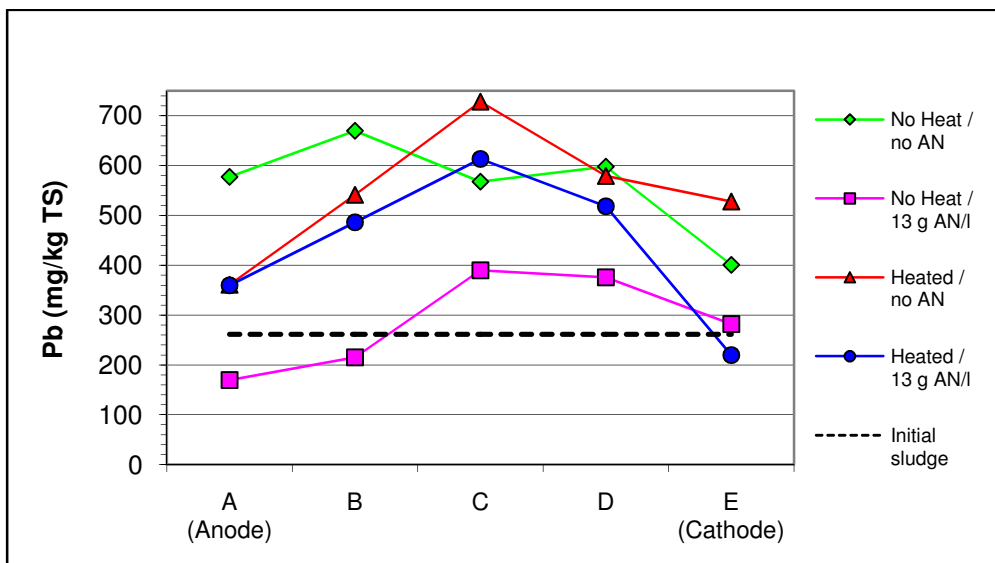


Figure 4.34 Lead distribution between electrodes in the bench-scale EK experiments

Zinc, which does not have a tendency to form metallic species, did demonstrate a relatively uniform distribution and mobility leading to a reduction of 20 % to 50 % compared to the initial concentration in the sludge.

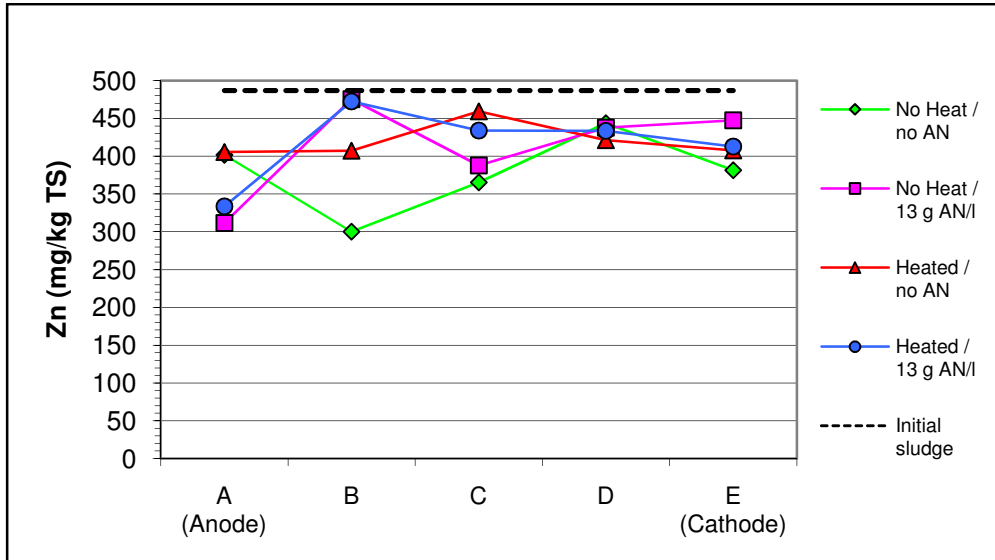


Figure 4.35 Zinc distribution between electrodes in the bench-scale EK experiments

Overall, it can be observed that the application of the AN conditioner influenced the EK process in the following ways: a) stimulated the release of metals from the anode, b) altered the speciation of metals in the sludge, c) enhanced the mobilization of metals present in the sludge, and d) permitted a greater transport of metals through electroosmosis and ionic migration over a relatively short treatment period.

4.2. Results of Pilot Scale EK Experiments

The pilot scale experiments exposed sludge to heterogeneous conditions that were not present during the bench-scale tests. The bench-scale units were designed to obtain a uniform current density throughout the cell by using flat plate electrodes; the pilot unit utilized multifunctional cylindrical electrodes, which simulated a possible field

application of the enhanced Electro-Kinetic Dewatering, Inactivation of pathogens, and Metal removal (EKDIM) technology. In the pilot unit, the electrical field and current densities are unequally distributed throughout. Ohmic heating was achieved by the application of common 120 V alternating current delivering a maximum capacity of 30 A. At this voltage potential, the voltage gradient between the electrodes was approximately 2.5 V/cm, producing an average heating rate in the unit of 1.39°C/min. and 1.18°C/min. during tests 1 and 2, respectively. The maximum average temperatures attained after 27 minutes at the stated voltage gradient were 56.2°C and 55.5°C for tests 1 and 2, respectively.

The current density distribution, together with the current vector field, generated during the pilot-scale trials are illustrated in Figure 4.36. The simulation was generated by means of the PDE Toolbox in Matlab[®] using the same parameters described in section 4.1.5. As the heating power is proportional to the current density, the distribution of the heating rates across the unit differed significantly, with the greatest heat increases adjacent to the electrodes and along their axis. The simulation enables the visualization of the temperature distribution observed during the pilot-scale experiments where the temperature distribution at the end of the heating period accurately reflected the current densities depicted in Figure 4.36. The concentrated high temperature zones adjacent to the electrodes were more significant for test 2 where the presence of the ion exchange textiles formed a layer of additional resistance to the flow of ions and electrons.

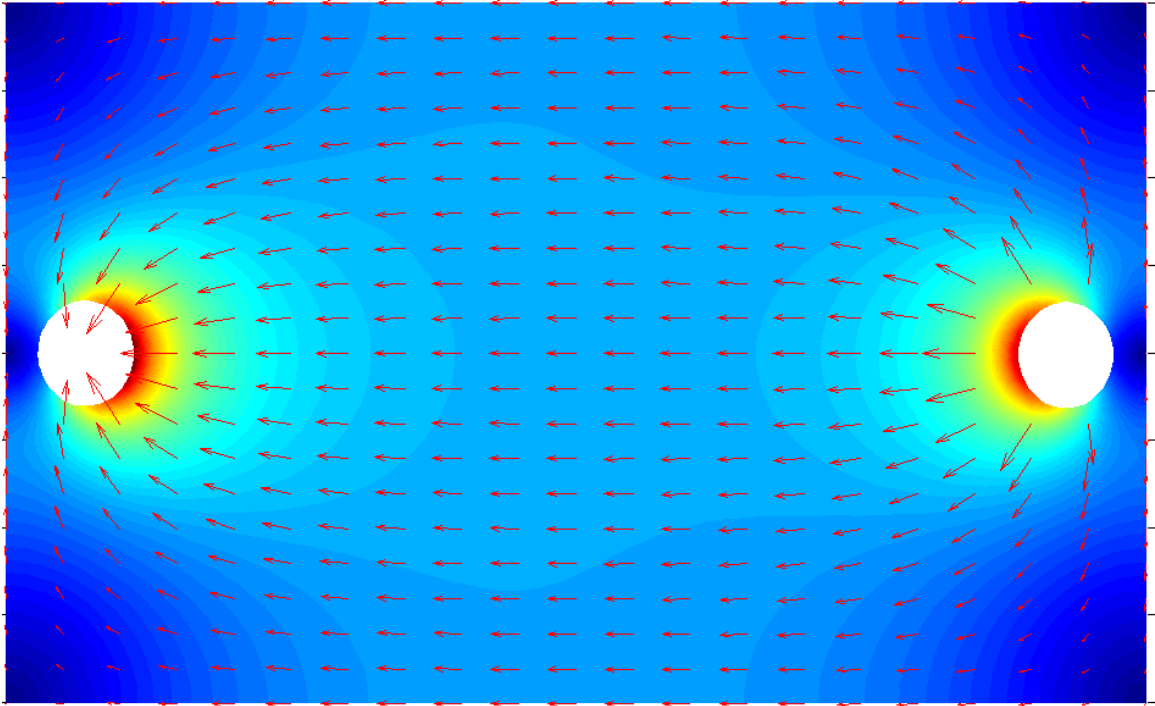


Figure 4.36 Simulation of the distribution of current lines and heat during the pilot-scale EK experiments

During pilot test 2, for instance, the temperature difference between two adjacent thermocouples along row 2 showed an average temperature difference of 24°C; in contrast the temperature difference between the same two thermocouples only showed a difference of 12°C during the heating phase of test 1. Another peculiarity of the pilot tests was the seeming perpetuation of ohmic heating well beyond the reduction of the voltage gradient to 0.5 VDC/cm; the mean temperature of the sludge continued to increase for at least 5.5 hours, reaching an average value of 60.9°C and 60.2°C for pilot tests 1 and 2, respectively, before gradually declining. This phenomenon was not observed during the bench-scale trials where the sludge temperatures immediately began decreasing when the voltage gradients were reduced to 0.5 V/cm.

The results of the pilot-scale experiments subjected to enhanced EK treatment are summarized in the following three sections. The first section discusses the results of

dewatering in terms of the volumes of liquor collected and the percent total solids (TS) distribution. The second section discusses distribution in the pH and the macro-nutrient (NH_4^+ , NO_3^- , and PO_4^{3-}) concentration throughout the unit. The third section contains the results regarding the heavy metals (Cd, Cr, Cu, Fe, Pb, and Zn) distribution and discusses the effects of the various parameters on the mobility of heavy metals.

4.2.1. Sludge Dewatering

Before the application of a voltage gradient, sludge liquor drained passively into the electrodes and was pumped out until such a time when the extraction rate was deemed negligible; this occurred after approximately 4 hours and produced a volume of about 0.5 liter of liquor for each test (a volume loss of less than 2 %). Although no EK control trials were conducted in the absence of an applied voltage gradient, the preliminary dewatering phase did give an appreciable range of extractable liquor in the absence of an electroosmotic gradient. The sludge liquor collection rates for pilot tests 1 and 2 with respect to time are shown in Figures 4.37 and 4.38, respectively, and the total volumes of liquor collected are indicated in Table 4.4.

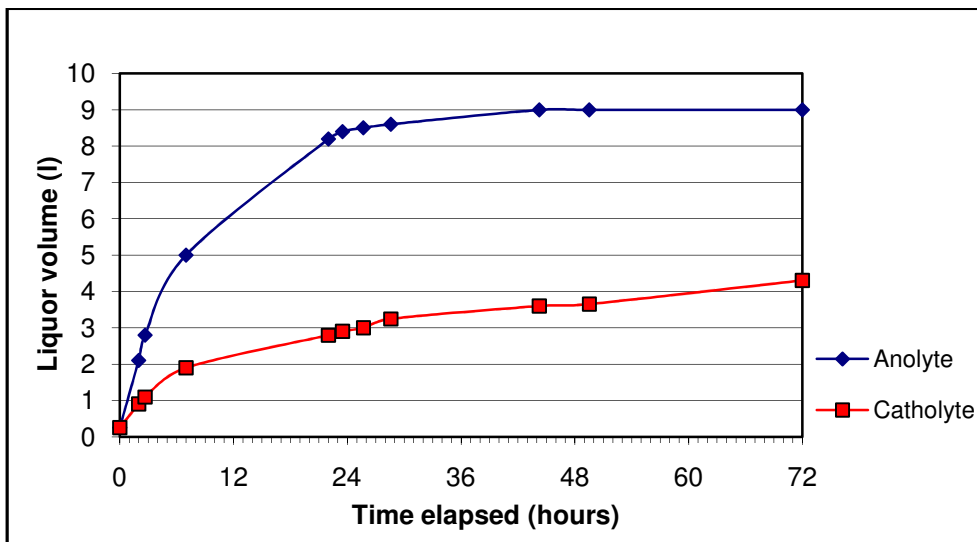


Figure 4.37 Volume of sludge liquors collected during pilot test 1

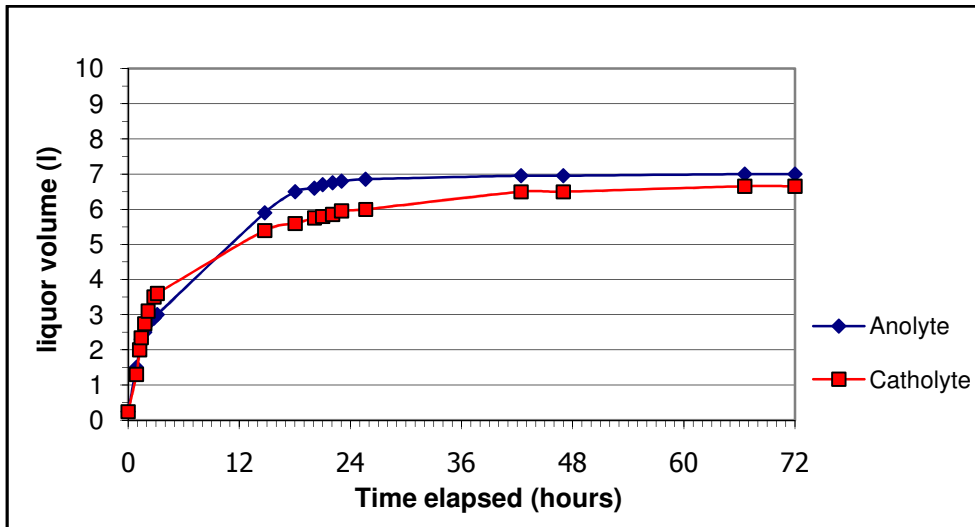


Figure 4.38 Volume of sludge liquors collected during pilot test 2

Electroosmotic dewatering only began after the ohmic heating period, when the units were transferred from AC to DC power. The initial flow rates of the liquors (i.e. anolyte and catholyte) are highest in the early stage of the experiment when the bulk of the water is in the free form and then diminishes as a greater fraction of water is in the interstitial form. There is, however, a noticeable difference in the initial flow rates between the two tests; with a higher rate observed for test 2 compared to test 1.

This occurrence can be due to the preset flow rate of the peristaltic pump initiated in the beginning of the experiments. The pumping rate in test 2 was doubled to 0.5 liter per hour compared to test 1; as the pump's flow rate in the latter did not keep-up with the electroosmotic flow rate of the system and free sludge liquor tended to accumulate inside the electrodes where the drainage tube was inserted. Another distinction between the two pilot tests, as shown in Table 4.4, is twice the volume of anolyte discharged compared to the catholyte during test 1 and an almost equal discharge of catholyte and anolyte during test 2.

Table 4.4 Total volume of liquor collected in the pilot-scale EK experiments

Trials	Total anolyte collected (liters)	Total catholyte collected (liters)	Total liquor collected (liters)
Pilot test 1	9	4.3	13.3
Pilot test 2	7	6.6	13.6

As was observed in the bench-scale experiments, the same fouling problematic occurred at the cathode during the first pilot test with a layer of hydroxide precipitate developing at the electrode surface. This phenomenon was lessened by the application of the ion exchange textile in test 2 where the total volume of liquor collected is roughly the same for both anode and cathode. The multi-component electrodes permitted the free drainage of water transported by electroosmotic flow and also created a barrier to fine particulates transported by electrophoresis. A comparison of the percent TS distribution between the two pilot tests is seen in Figure 4.39. The % TS in the cathode region of row 2 reveals that pilot test 1 attained a 22.1 % TS while the TS content in pilot test 2 reached 17 %. However, the performance at the anode region showed a slight rise in % TS for the second pilot test despite a noticeable decrease in the volume of anolyte collected.

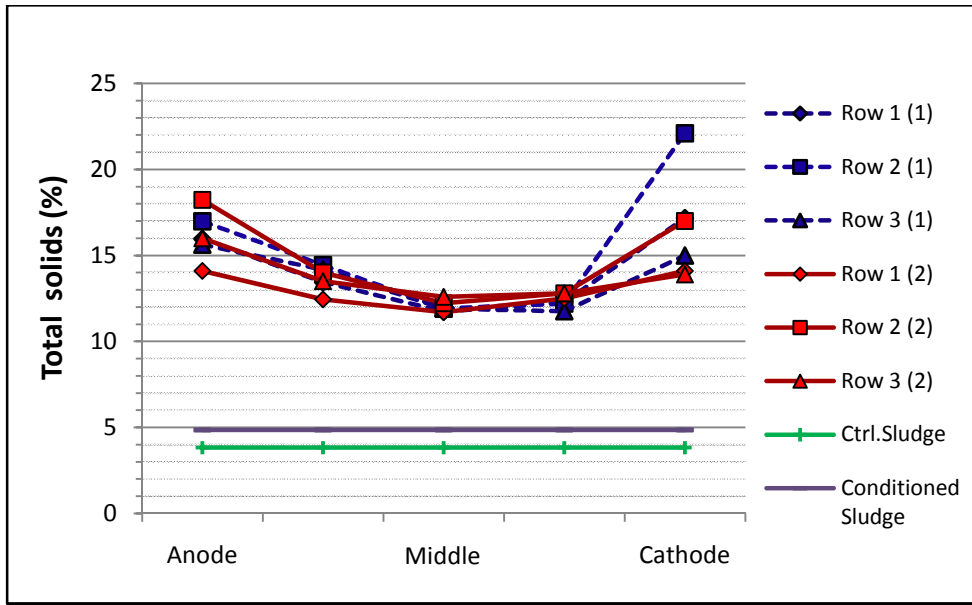


Figure 4.39 Percent total solids distribution in pilot tests (1) and (2)

The distribution of the percent TS content in both tests, ranging between 11.7 % and 22.1 %, is illustrated graphically in Figures 4.39 and 4.40,; while Figure 4.42 visually depicts the physical state of the dewatered biosolids in pilot test 1 after 70 hours of EK treatment. The final average TS percentage of the biosolids in pilot tests 1 and 2 are 14.5 % and 13.9 %, respectively, a value approximately 3 times the original TS content of the initial sludge. The presence of the ion exchange textile did not significantly impact dewatering as slightly more liquor was collected during the second pilot test. The main factor explaining the somewhat lower level of TS in the second test is the dehydration of the ion exchange textile around the electrodes. It is supposed that in the later stages of dewatering, after about 48 hours, when the sludge became more consolidated, the dehydration of textile may have slowed the movement of liquor into the electrode and out of the unit by pumping. The TS distribution pattern illustrated in Figure 4.40, with an upwards of almost 2 % TS difference between the center row and its flanking rows, is due the configuration of a heterogeneous electric field between the tubular electrodes

with a larger gradient developing directly between the electrodes and diminishing away from this central axis (Figure 4.36).

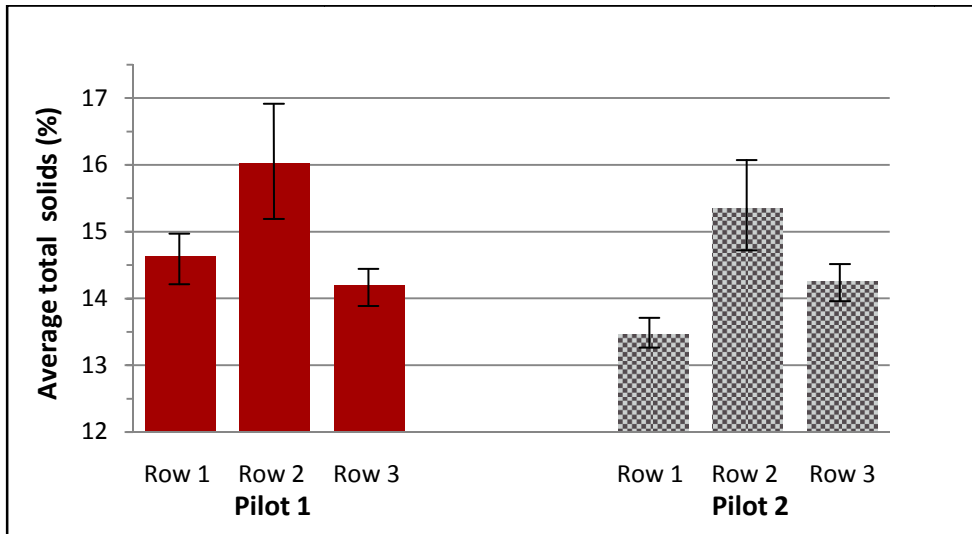


Figure 4.40 Final average total solids of the pilot-scale trials

It can be gathered from Figure 4.41 that there is a clear reduction of volatile solids (VS) concentration between the anode and cathode, with an almost 10 % decrease at the cathode compared to the anode in row 2. As the VS are often taken as a measure of the organic content, these commonly negatively charged species are transported by electrophoresis towards the anode. The overall VS content of the biosolids may have been reduced from its original concentration through both electrophoresis towards the anode and electroosmotic flow towards the cathode with subsequent discharged from the system.

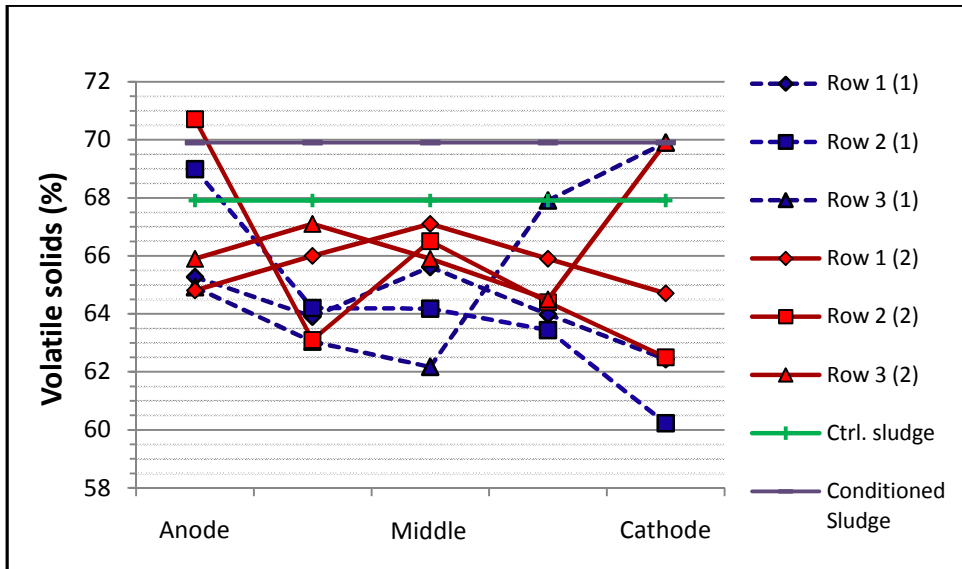


Figure 4.41 Percent volatile solids distribution in pilot tests (1) and (2)



Figure 4.42 Dewatered biosolids of pilot test 1 (after 70 h)

4.2.2. pH and Ion Distribution

The configuration of the electrodes in the pilot tests greatly influenced the biosolids' pH profile, as demonstrated in Figure 4.43. The implementation of tubular electrodes

positioned along the center line (row 2) of the unit resulted in a significant variation in the pH of biosolids in adjacent rows. The pH difference between the anode and cathode was as high as 6 for test 1, whereas a difference of 4.9 was observed for test 2. This distinction can be explained by the presence of the anionic and cationic exchange textiles. Although the textiles are designed to be selective for their respective ions, it would appear that they act as an impediment, particularly at the anode and have a influence on the distribution of H^+ generated at that electrode.

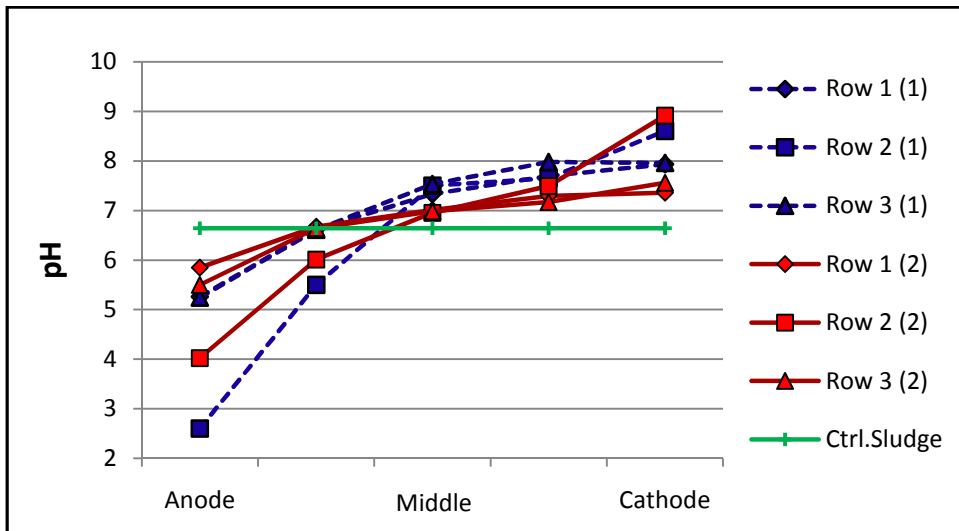


Figure 4.43 pH distribution in pilot tests (1) and (2)

The final concentrations in NH_4^+ and NO_3^- are presented in Figures 4.44 and 4.46. Although the sludge was amended with a significant quantity of these ions, increasing its original concentrations of NH_4^+ by 7.6 times and NO_3^- by 111 times, a good proportion of these were eliminated from the system primarily by ion migration, with electroosmosis engaged in a supporting role depending on the dominant direction of the electroosmotic flow in the sector of the unit.

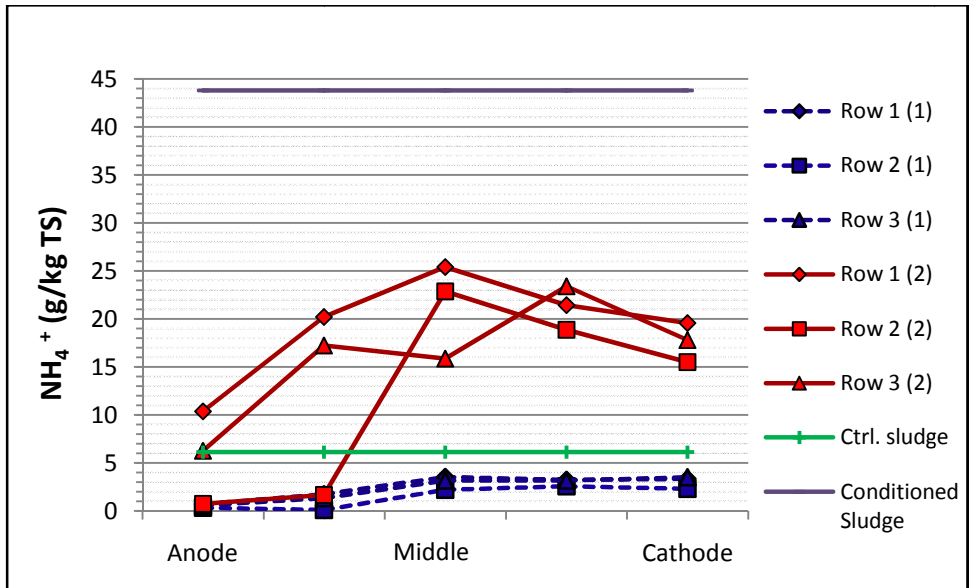


Figure 4.44 Ammonium distribution in pilot tests (1) and (2)

These two ions migrate to their respective electrodes with NH_4^+ towards the cathode and NO_3^- towards the anode.

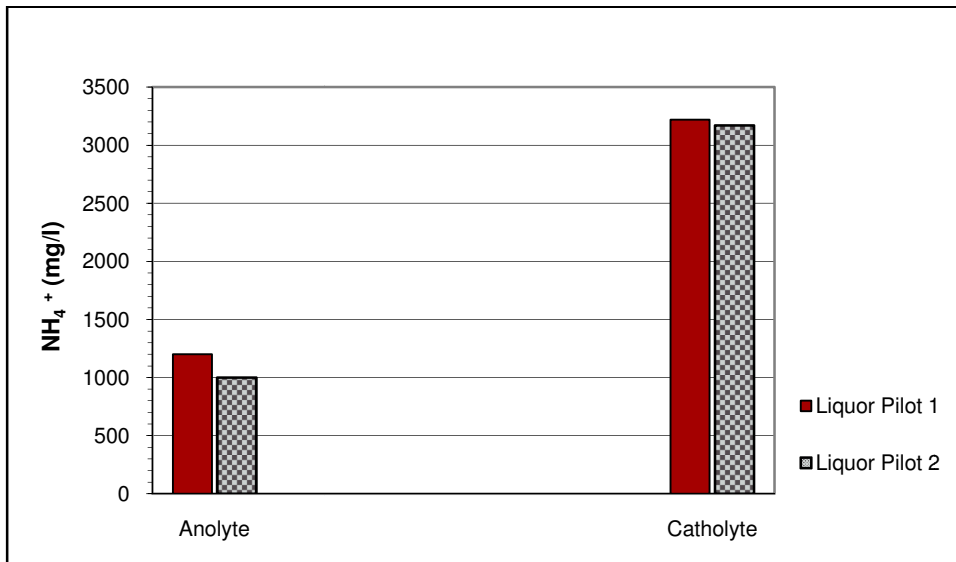


Figure 4.45 Ammonium concentration in the sludge liquor of pilot tests 1 and 2

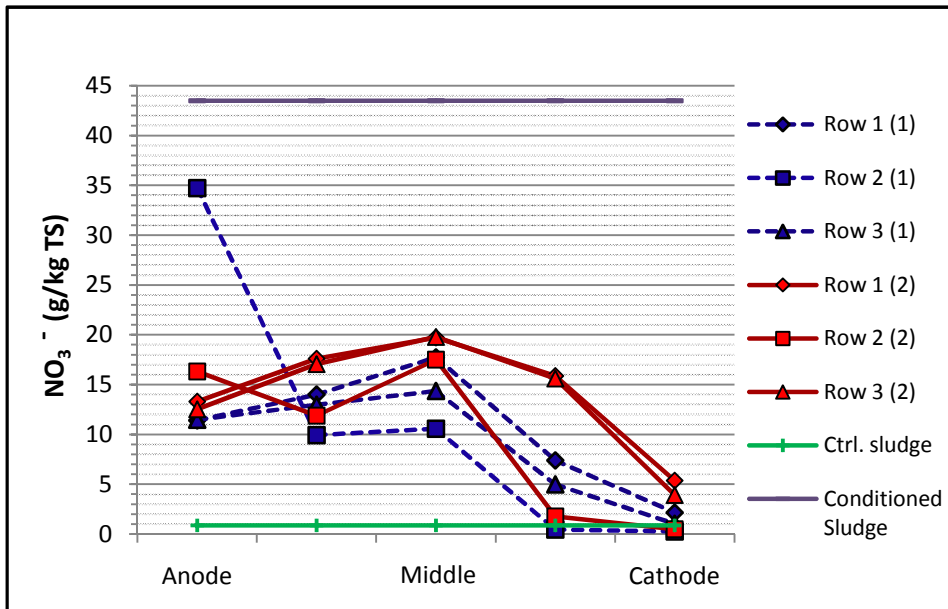


Figure 4.46 Nitrate distribution in pilot tests (1) and (2)

As shown in Figures 4.45 and 4.47, the greater part of the anolyte and catholyte fraction is represented by their respective anion (NO_3^-) and cation (NH_4^+); with a minor fraction comprising the inversely charged specie. The latter is due to a great extent by the fact that the electroosmosis and drainage are dominant over the ionic mobility in proximity of the electrodes; therefore, these ions are dragged along with the above mentioned flows. A consequence of this phenomenon is the transformation of these ions by electrochemical reactions at the electrode surface. At the anode, some of the NH_4^+ is oxidizes to NO_3^- , and thus added to the nitrate load. Conversely, at the cathode, some of the NO_3^- drawn in with electroosmosis is reduced to NH_4^+ , and thus added to the ammonium load (Figure 4.46).

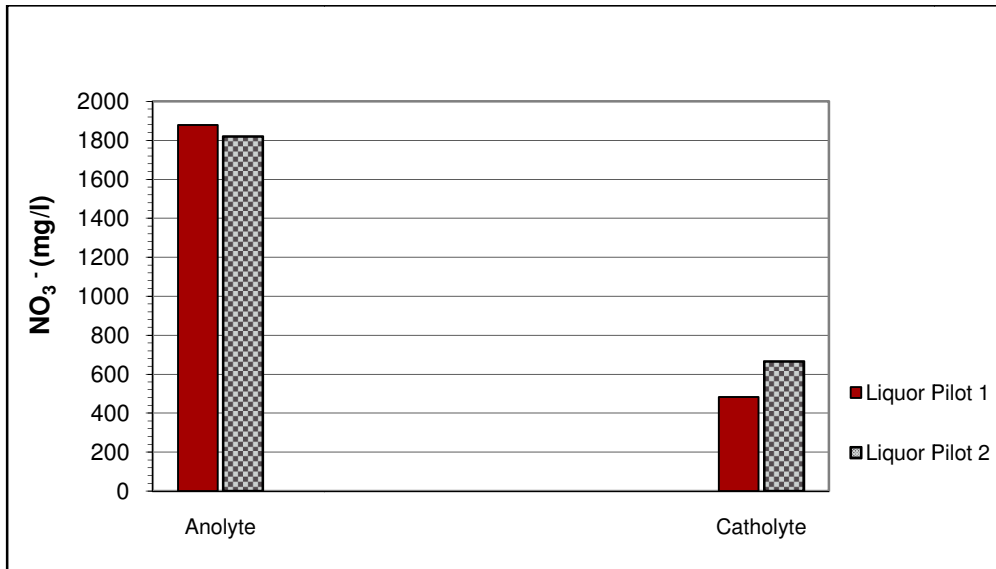


Figure 4.47 Nitrate concentration in the sludge liquor of pilot tests 1 and 2

The phosphate concentration in the initial sludge went from 340 mg/kg TS to 1540 mg/kg TS with the addition of the AN conditioner. Although the conditioner did not contain phosphate, it is assumed that the increase observe with the addition of the competing ions (NO_3^- and NH_4^+) results from the displacement of phosphate originally sorbed to the organic fraction of the sludge. Nevertheless, the final distribution of phosphate in both pilot tests, after 70 hours, showed a high removal level below the initial concentration.

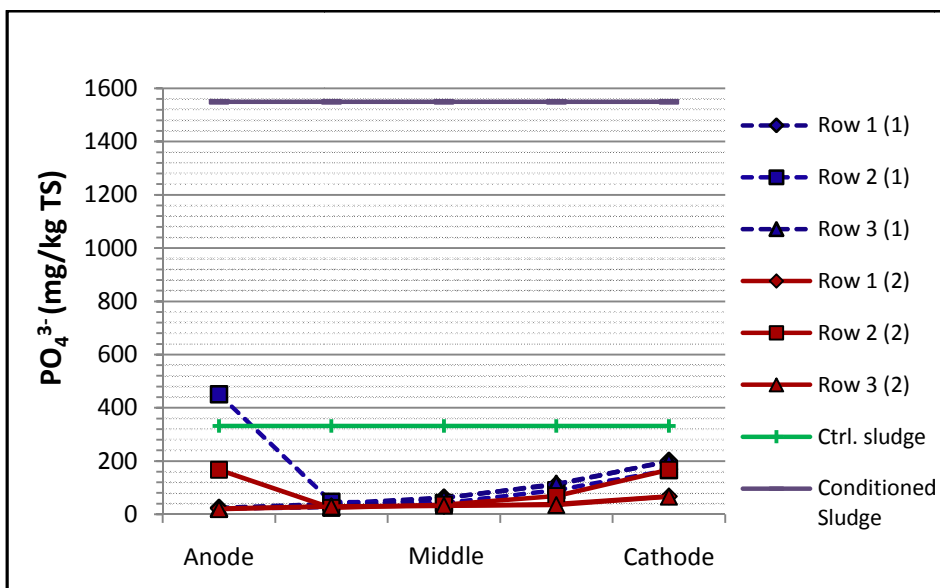


Figure 4.48 Phosphate distribution in pilot tests (1) and (2)

Electrophoresis can be seen to drive the extraction process in Figure 4.49, with a predominant migration towards the anode. The greater concentration of phosphate observed at the anode region, predominantly in test 1, can be explained by the larger accumulation of iron in this region (see Figure 4.58) and the resulting co-precipitation as iron phosphate.

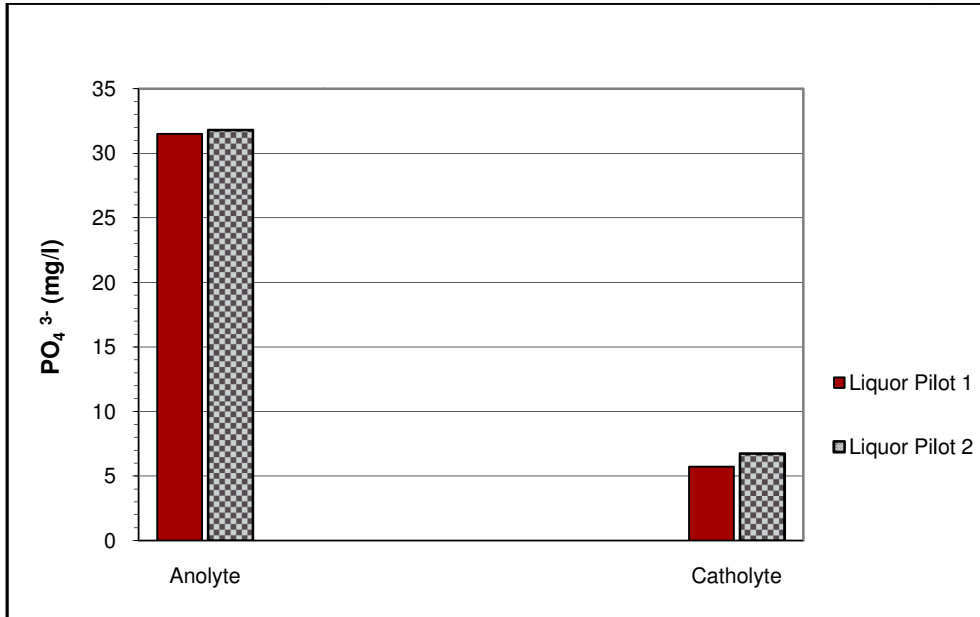


Figure 4.49 Phosphate concentration in the sludge liquor of pilot tests 1 and 2

4.2.3. Heavy Metal Distribution

The results of each heavy metal (Cd, Pb, Zn, Cr, Fe, and Cu) distribution in the pilot tests are given for the biosolids, the sludge liquors, and the ion exchange textiles in Figures 4.50 through to 4.61.

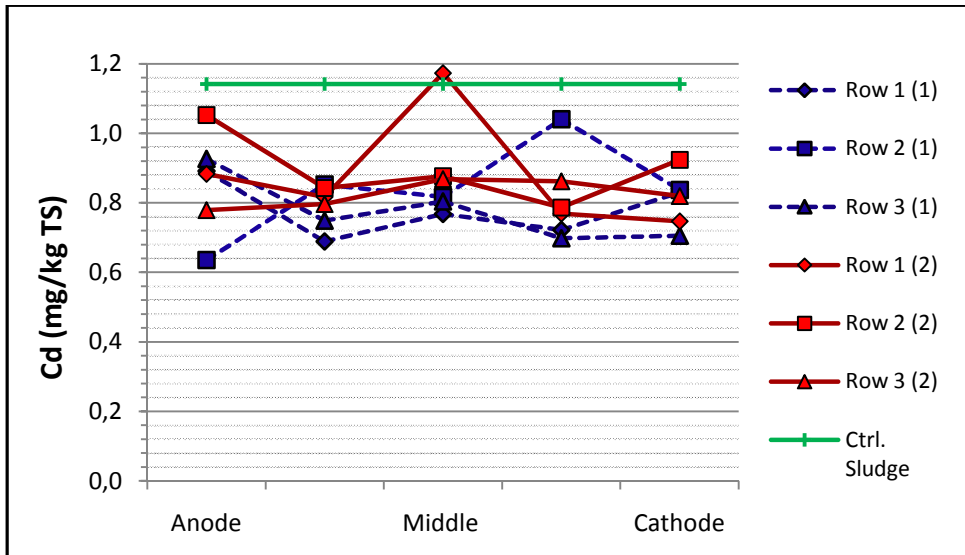


Figure 4.50 Cadmium distribution in pilot tests (1) and (2)

Although the initial concentration of cadmium in the wastewater sludge was very low, it was effectively removed from the system to below the initial level. A minor preferential migration towards the anode can be discerned, from Figures 4.50 and 4.51, for both trails. This trend can be explained in test 1 by the twofold accumulation of anolyte over catholyte seen in Table 4.4.

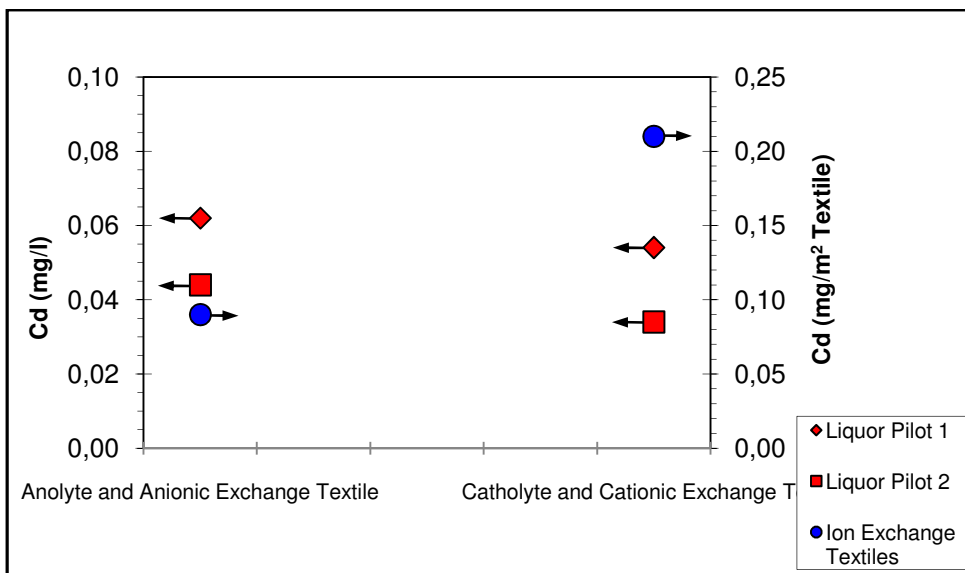


Figure 4.51 Collection of cadmium in sludge liquors of pilot tests (1) and (2) and onto the ionic exchange textiles of pilot test 2

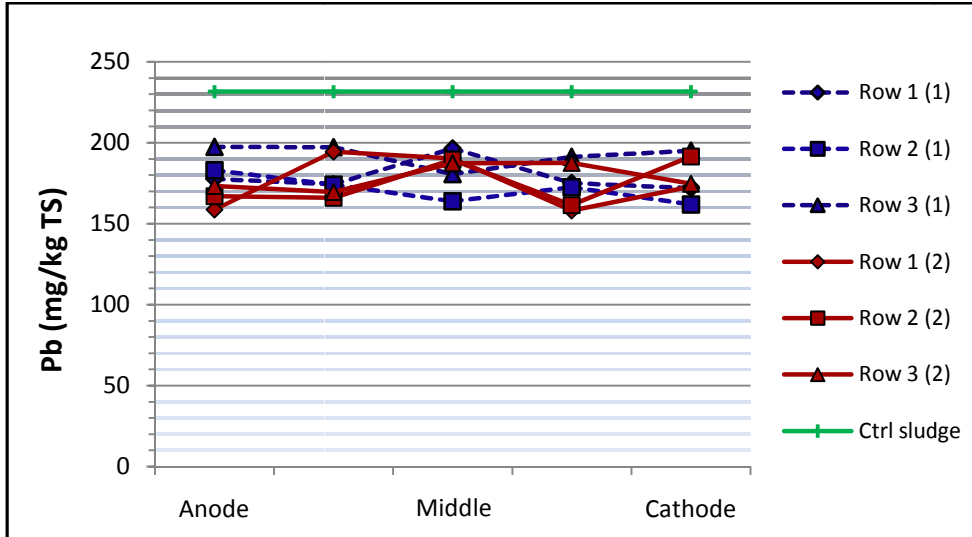


Figure 4.52 Lead distribution in pilot tests (1) and (2)

Figures 4.52 and 4.53 illustrate a uniform lead distribution in the systems. No clear migration pattern is discernable; although the cation exchange textile shows a higher concentration of lead, this could be due to its higher affinity over the anionic textile. An overall average removal efficiency of 24 % was appeared to be achieved during only 70 hours of treatment. The author suspects that an analytical error was introduced during the Flame AA analysis by the presence of a sample/matrix effect. As a result, there is a certain level of uncertainty associated with the values reported for this metal.

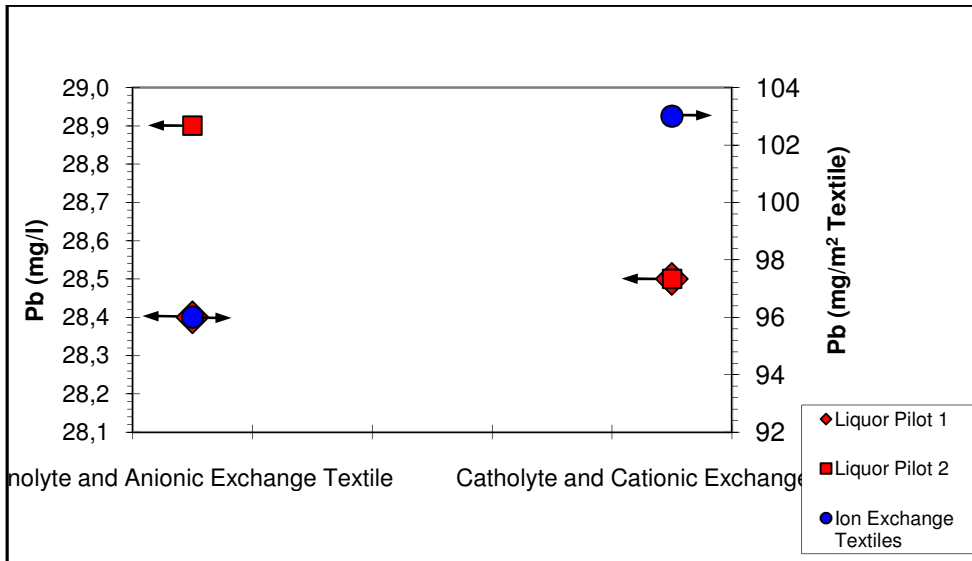


Figure 4.53 Collection of lead in sludge liquors of pilot tests (1) and (2) and onto the ionic exchange textiles of pilot test 2

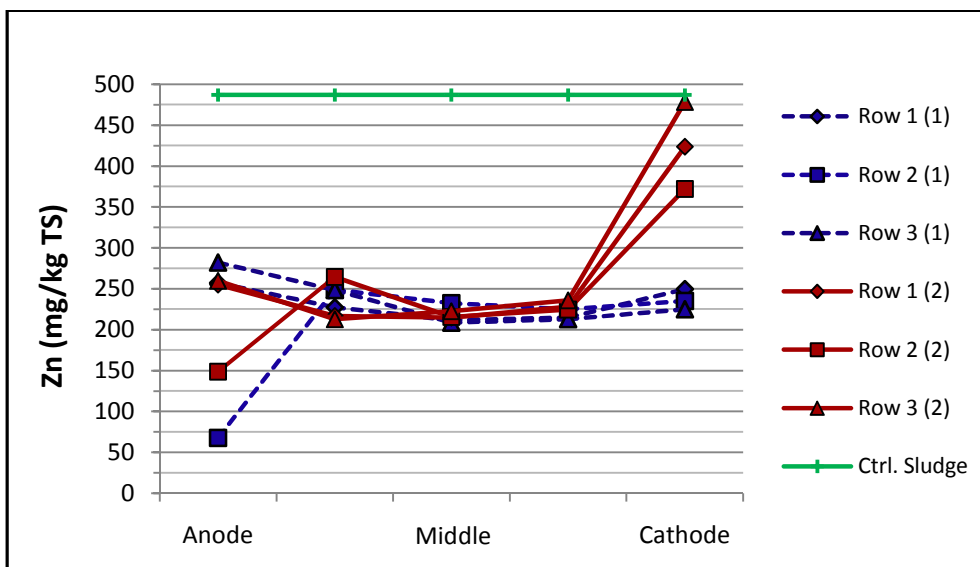


Figure 4.54 Zinc distribution in pilot tests (1) and (2)

The zinc distribution in figures 4.54 shows an overall reduction of 66 % compared to the initial concentration. The zinc appears to migrate towards the cathode as evident in pilot test 2. Figure 4.55 demonstrates a slightly greater accumulation of zinc in the extracted liquors for test 1, but this could be due to the unimpeded flow out of the unit as opposed to that observed in test 2.

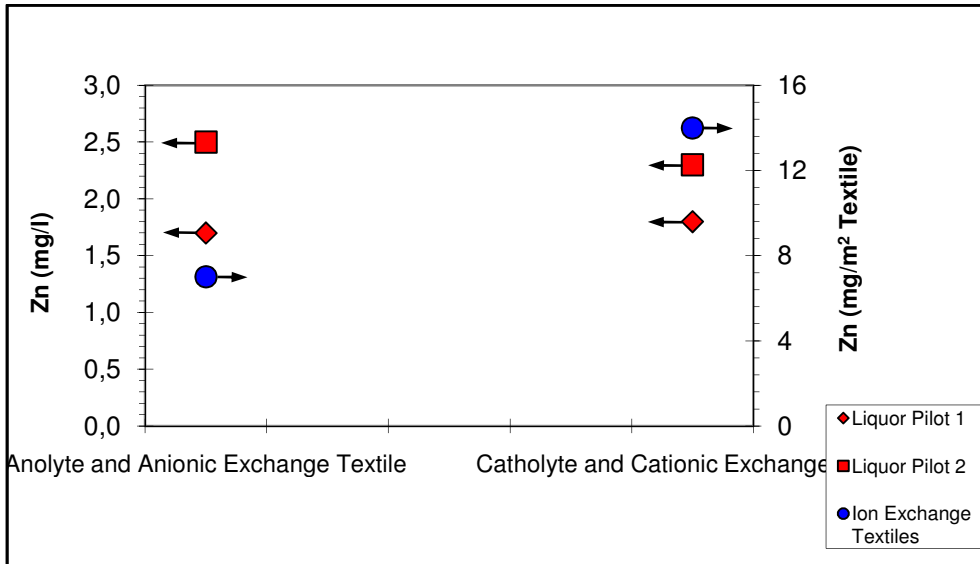


Figure 4.55 Collection of zinc in sludge liquors of pilot tests (1) and (2) and onto the ionic exchange textiles of pilot test 2

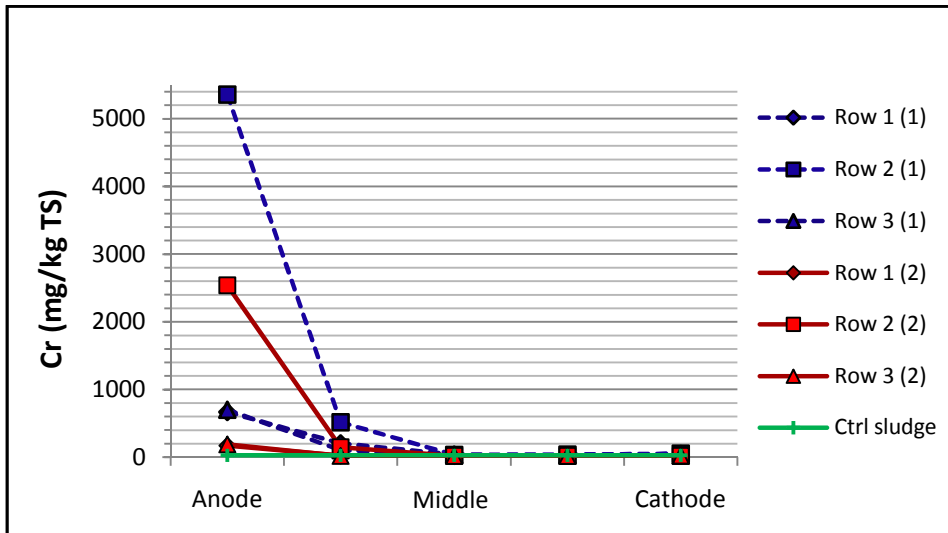


Figure 4.56 Chromium distribution in pilot tests (1) and (2)

From Figures 4.56 and 4.57, a certain amount of chromium is seen to be introduced into the biosolids at the anode region and to migrate towards the cathode. The type 302 stainless steel used as the anode is an alloy composed of 18% chromium, 8% nickel, and other trace elements; the inevitable oxidation of which releases some quantities of these elements. Elsewhere in the system the concentrations of chromium remain around the

initial concentration of the sludge. The presence of the ion exchange textile in test 2 controlled the migration and diffusion of chromium away from the electrode, by acting as a barrier.

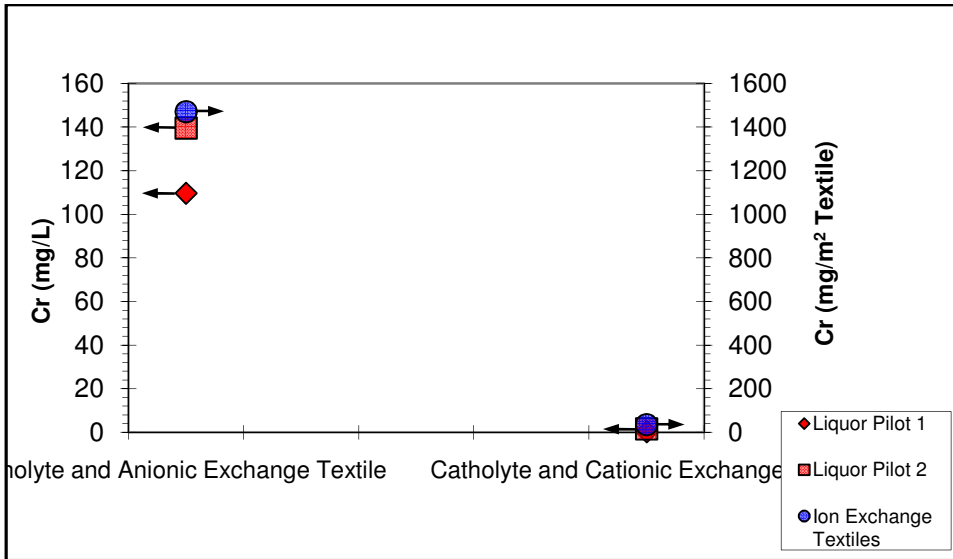


Figure 4.57 Collection of chromium in sludge liquors of pilot tests (1) and (2) and onto the ionic exchange textiles of pilot test 2

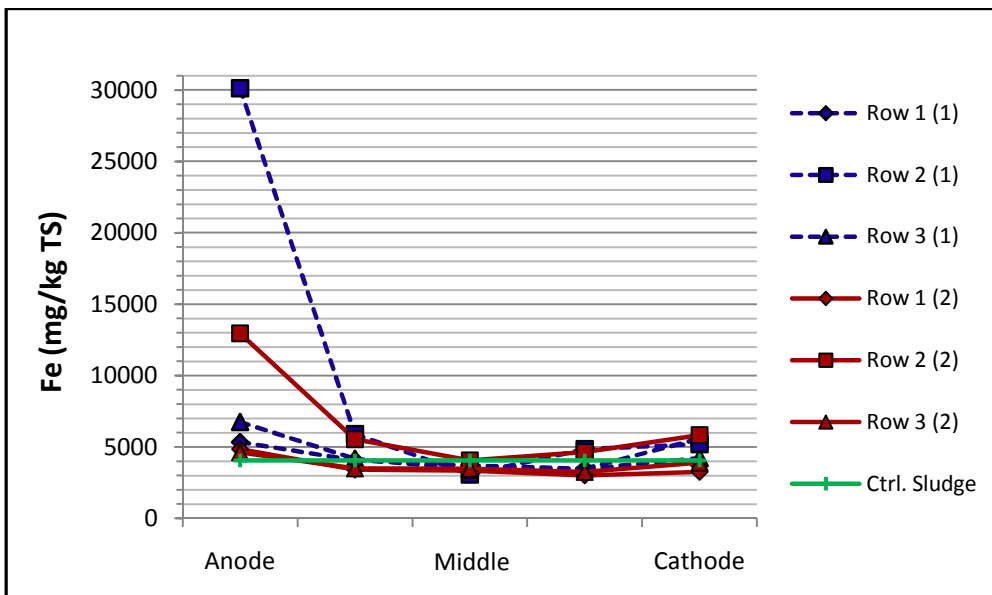


Figure 4.58 Iron distribution in pilot tests (1) and (2)

The iron distribution is represented in figures 4.58 and 4.59. The general profile of iron concentration is identical to that of chromium; with a difference of approximately 5 times the values. This result is expected considering the iron content is about 4 to 5 times that of chromium. Again, the presence of the anionic exchange textile at the anode reduced the introduction of this element into the biosolids by more than half.

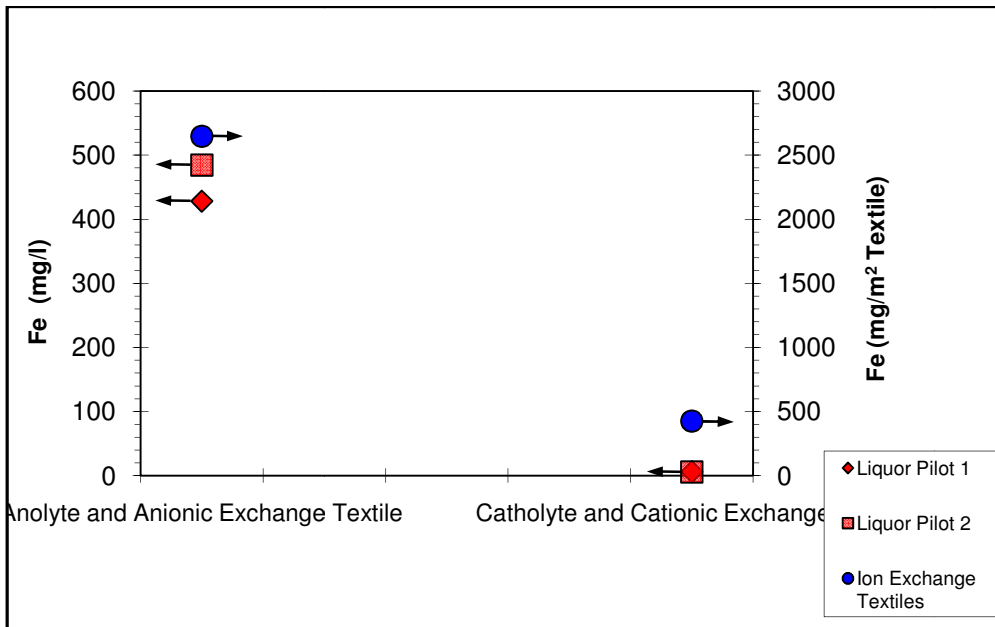


Figure 4.59 Collection of iron in sludge liquors of pilot tests (1) and (2) and onto the ionic exchange textiles of pilot test 2

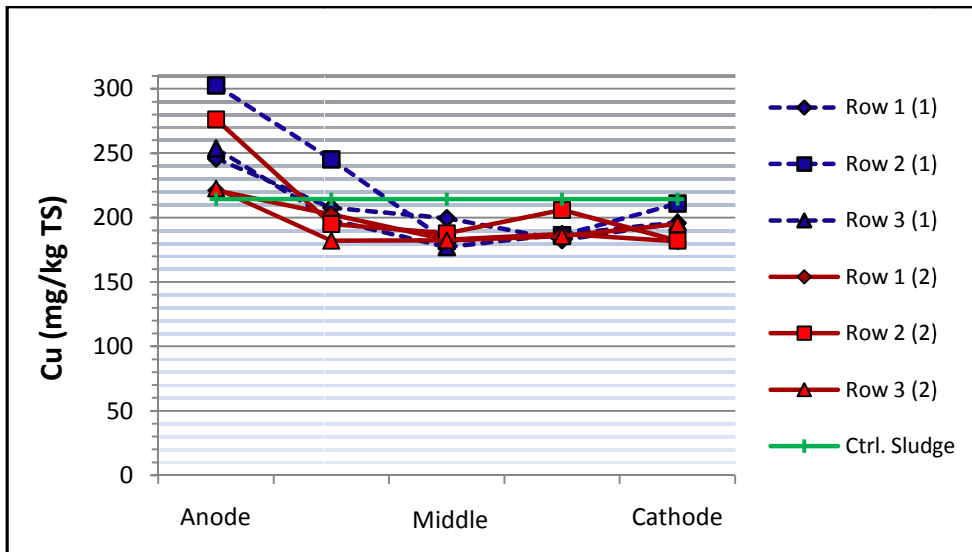


Figure 4.60 Copper distribution in pilot tests (1) and (2)

Copper appears, in Figures 4.60 and 4.61, to collect at the anode. This trend is also visible in the higher concentration of copper in the anolyte. The higher concentrations observed in pilot test 1 compared to the second test can be due to the presence of the textile around the electrode acting as a barrier to the diffusion of the copper likely originating from the stainless steel electrode during its oxidation. At the cathode end, no significant differences in the overall distribution of copper are seen between the two tests.

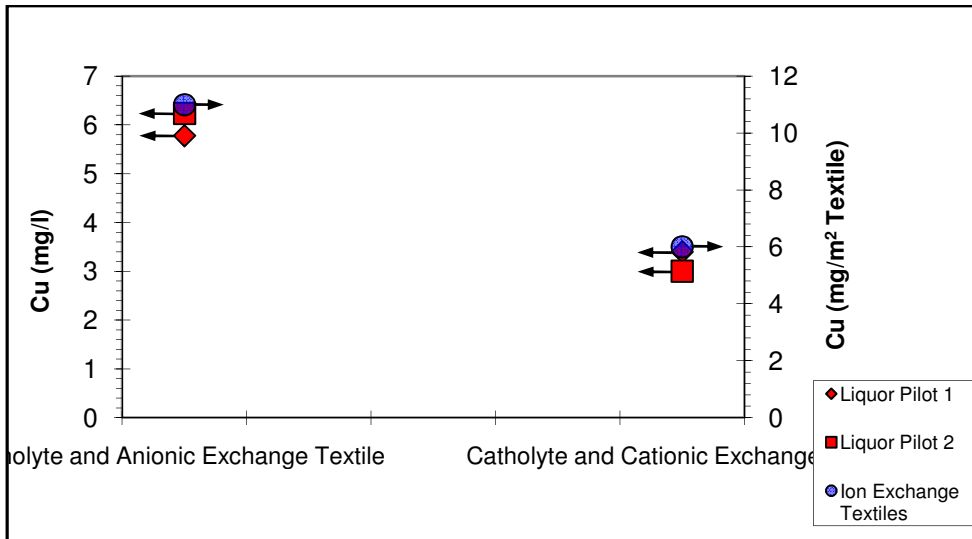


Figure 4.61 Collection of copper in sludge liquors of pilot tests (1) and (2) and onto the ionic exchange textiles of pilot test 2

5. Discussion and Conclusion

The objective of this study was to determine optimal conditions and strategies for wastewater sludge dewatering, heavy metal removal, and pathogen inactivation using a coupled process of ohmic heating and electrokinetic treatment within an EKDIM design system. Several screening tests were performed to determine these optimum conditions; while four bench-scale and two pilot-scale electrokinetic tests were implemented to verify their effects on these physical, chemical, and biological parameters. From these experiments, important conclusions were drawn and recommendations were presented for further studies.

In general, the results obtained from the *Ascaris* inactivation experiments demonstrated a rapid and successful electrokinetic process for the inactivation of helminth eggs from wastewater sludge thus upgrading the treated biosolids to exceptional quality standards while simultaneously dewatering and removing pollutants. This process offers several benefits over conventional methods that necessitate several unit operations to produce exceptional quality biosolids.

Although a combined heavy metal removal and pathogen inactivation is difficult to achieve, the experiments performed permitted the removal of certain metals. For instance, zinc had about 60 % removal efficiency in an experimental run of only 70 hours thus reaching a C1P1 quality standard for biosolids. This technology can eventually deliver a cost effective method to produce exceptional quality biosolids so a greater portion of this fertilizing residual material can be safely applied to agricultural use.

The main advantages of the electrokinetic treatment of biosolids are the greater dewatering capacity over mechanical pressure alone, as electroosmotic flow is normally independent of porosity, and the metal contaminants can usually be recovered in useful form, that is to say, as concentrated compounds by migrating towards the electrodes. A further advantage is the possibility of pathogen inactivation and sludge disinfection by manipulating the voltage gradient to initiate a period of ohmic heating. In general, ohmically heated systems are more advantageous over convective systems due to a greater efficiency in heating rates and energy consumption, and better controls over the system. Although experiments were not conducted to differentiate the influence of heat on the sludge dewaterability, it can be suggested that the generated heat may have promoted electroosmosis by decreasing the viscosity of the sludge thus increasing the flux of ions and fluids.

5.1. Assessment of *Ascaris suum* Ova Inactivation by Joule Heating

The treatment condition imposed during the bench and pilot-scale trials were sufficient to reduce the viability of *Ascaris* ova to less than 0.001 %, ascertained by the enumeration of over 1000 ova per sample point, effectively achieving 100 % inactivation when subjected to temperatures of 55°C and greater for a minimum of 10 minutes in conjunction with an AN conditioner concentration of 13 g/l. The inactivation of *Ascaris* eggs in wastewater sludge was largely dependent on temperature generated through the application of an electric field and to the enhanced electrokinetic phenomena, as illustrated in Figure 4.1. The class A pathogen criteria are based on those pathogens believed to be the most resistant to sludge treatment and helminth ova are considered to

be the most resistant to inactivation (US EPA, 1999). However, the EPA time-temperature regimes imposed on the thermal sewage sludge treatments are not compatible with the high rate of *Ascaris* egg inactivation observed in this present and previous study (Aitken, et al., 2005). The time-temperature regime selected for this study of 10 minutes at 55°C was extrapolated from Aitken et al. (2005) study on the partial inactivation kinetics of *Ascaris* ova in anaerobic biosolids subjected to temperatures between 49°C and 55°C. Although this time-temperature regime was shown to be adequate, it may not be the optimal treatment under the combined effect of an electric field and the conditioner. These added stressors may in fact reduce the treatment period of 10 minutes even further; as the inactivation results in Figure 4.1 suggested by a 2°C offset in the critical inactivation temperatures when comparing convective and ohmically heated sludge. Furthermore, the treatment conditions may have been sufficient to inactivate (i.e. destroy) the *Ascaris* embryo in the ova, but not necessarily required to eliminate their infectivity to their host. Whether the eggs subjected to EK treatment were infective or not was not determined in this study; it is possible that threshold treatment conditions required to irreversibly impair the infective larval stage may be less stringent, in terms of either heat or conditioner exposure, than that required to inactivate *Ascaris* ova.

Studies conducted by Mbela (1989) at Tulane University on the inactivation of *Ascaris suum* ova at various temperature regimes predicted detention times of 10 days in aerobic sludge and 9 days in anaerobic sludge for complete (100 %) inactivation at a temperature of 55°C. It is, therefore, suggested that other important factors in addition to temperature are most probably affecting *Ascaris* inactivation in the current sets of EK experiments.

This hypothesis is supported by the bench-scale EK trial results of the ohmically heated but unconditioned sludge whereby the *Ascaris* eggs located in the cathode region witnessed an 86.5 % reduction in viability despite reaching only 44°C.

Given the type of conditioner used in this present study, the inactivation results may be attributed to the range of the nitrogen content of the sludge, and specifically to ammonia nitrogen which exists in aqueous solutions either as ammonium ion (NH_4^+) or as free ammonia (NH_3) depending on the pH of the sludge. The NH_3 species which predominates at pH above 9, is more lipophilic compared to NH_4^+ and can more easily diffuse through the inner lipid membrane of biological organisms (Pecson and Nelson, 2005). Other probable factors which contributed to enhance the inactivation of *Ascaris* eggs include the electric field, hydroxide anions and protons, and other intermediate reactive species generated at the electrode surfaces under oxidative and reductive conditions.

A possible mechanism for the superior inactivation of the *Ascaris* ovum subjected to ohmic heating is the impairment of various protein structures controlling the exchange with the external environment and embedded in an otherwise impermeable inner lipid layer that protect the vital elements of the ovum. The crippled membrane is, consequently, incapable to mediate the movement of ions and the ovum's ultimate inactivation is hasten by the high free ammonia content of the AN conditioned sludge which is able to cross the lipid layer leading to ammonia toxicity by disrupting the pH balance within the cell (Pecson and Nelson, 2005).

5.2. Selection of Treatment Parameters

Analysis of the theoretical aspects of the EK processes and the preliminary bench-scale trials clearly demonstrated the importance of the medium's conductivity in all the practical aspects of the EK phenomena. Solubility and ionic strength are of the principal bases for selecting a sludge conditioner, as these two parameters together demonstrated the highest influence on the electroosmotic and electrophoretic capacity of the system. Furthermore, as demonstrated by Joule's law, the applied voltage gradient can be significantly reduced for the same attainable ohmic heat treatment outcome by increasing the conductivity of the sludge. An obvious and inexpensive means of increasing the inherent conductivity of the sludge, as depicted in Figure 4.8, is field storage. The sludge compounds naturally degrade and mineralize under biological and physical processes to release various organic acids. The longer organic materials are stored, the greater the potential for the nutrient content, total solids, and salt content or pH to change (USEPA, 2000). The sludge conductivity was elevated from an initial 1.49 mS/cm to 3.76 mS/cm over a two-month period, an increase of 250 %, and this under cold storage conditions.

Although the *Ascaris* inactivation trials were conducted with the selected AN conditioner based on its high conductivity and dewatering ability, the effect of DAP or urea, in conjunction with heat, on *Ascaris* inactivation rates may have revealed them to be as effective given they both have the potential to introduce free ammonia into the system.

When contrasting the bench-scale results between direct and alternative current, the use of AC for the ohmic heating phase did seem to have an optimal effect on heating rates and energy use, as demonstrated in Figures 4.16 and 4.17. When a current is applied to an

electrolyte solution, the fraction of that current involved in heat generation is the capacitive current. The other fraction, the Faradic current, is associated with the electrode-solution interface and generates electrochemical reactions (Tzedakis, et al., 1999). This latter current can be regarded as a wasted current and a loss of useful electrical energy when ohmic heat production is the desired aim. The Faradic electrolytic reactions that can occur at the electrode-solution interface depend on such factors as, the electrode composition, the electrolytic solution, and the current density. If the potential difference across the electrical double layer is maintained within its Faradic reaction-free potential, electrons from the electrode cannot be transferred to the electrolyte nor can ions from the electrolyte react at the electrode surface. The only phenomenon occurring at the electrode is a periodic change in charge density on both sides of the interface. Under such circumstances the current flowing through the interface becomes purely capacitive. These Faradic electrolytic processes can be minimized with an increase in current frequency or in electrode capacitance (Tzedakis, et al., 1999). It is presumed the higher efficiencies observed when using the 60 Hz AC power source was the result of a reduction in the Faradic electrolytic effect, an assumption supported by the absence of gas generation at the electrodes when AC power was applied. As Figure 4.17 also illustrates, the amount of energy require to heat the sludge to a temperature of 60°C was inversely correlated to the applied voltage gradient. The greater heating rates achieved at higher voltage gradients may have minimized the energy losses by means of heat transfer, generally dominated by convective heat dissipation.

A linear trend is revealed in Figure 5.1 between the average heating rates achieved and the initial AC power input for the same conductivity value regardless of the scale of the

unit or its electrode configuration. The field strength of 2.4 V/cm used during the pilot-scale trials is seen to roughly fall between the 2 and 2.5 VAC/cm voltage gradients of the bench-scale trials. The volumetric heat generation rate for the pilot unit can be seen to conform to the values expected from the bench-scale studies.

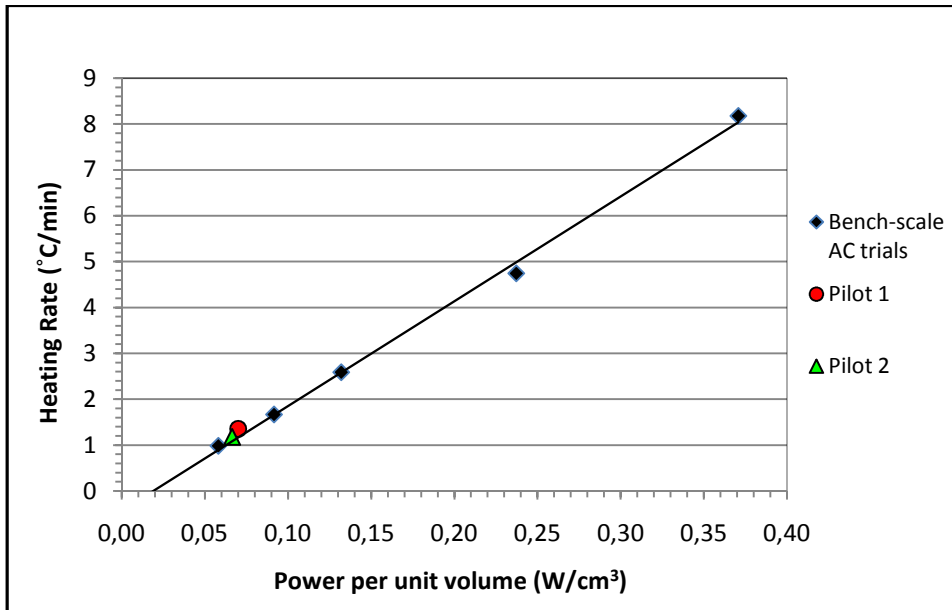


Figure 5.1 Heating rates in function of initial power input per unit volume (all AC ohmic heating trials)

The use of a high AC voltage gradient to heat the sludge, however, does not produce the intended electrokinetic advantages observed during the bench-scale inactivation trials where the dewatering and the removal of ions from the system was enhanced by the brief application of a high DC voltage potential as demonstrated in Figure 4.20. The latter figure clearly reveals the impact of the application of a high voltage gradient at the onset of the EK trials on the final values of total solid percentages, an increase in approximately 2 %.

The estimated energy costs, assuming a price of \$0.08/kWh, calculate from the bench and pilot scale experiments are presented in Table 5.1:

Table 5.1 Energy cost estimate for the enhanced EK experiments

Enhanced EK experiment	Cost on wet sludge basis (\$/t sludge)	Cost on total solid basis (\$/t TS)
Bench test: ohmic heat treatment	5.9	122
Bench test: no heat treatment	2.7	56
Pilot test 1	6.0	123
Pilot test 2	4.9	102

The brief application of a high voltage gradient for the purpose of ohmic heating more than doubled the energy expenditure at the bench-scale level; however, the added cost benefits of pathogen inactivation and increase TS content it is believed balances the extra costs.

The trends and relationships among the various electrical parameters elucidated from these EK experiments should assist subsequent experimenters to manipulate the key parameters and operate their EK apparatus to achieve specific desired results, and should support them in their design activities, including the design of new and improved EK reactors.

5.3. Contaminant Removal Efficiencies

In general, it can be said that the ion analysis demonstrated the most consistent and reliable results compared to the metals analysed for both bench and pilot-scale trials. The results usually conformed to the theoretical framework of eletrokinetics elaborated in the literature revue, with the majority of each charged ionic species migrating towards the

oppositely charged electrode. Nitrate (NO_3^-) and phosphate (PO_4^{3-}), both anions, were observed with highest concentrations in the anode region of the bench and pilot-scale EK units and a significant reduction or relative absence towards the cathode. In contrast, the ammonium (NH_4^+) cation concentration prevailed near the cathode.

With respect to metal removal, the results of both bench and pilot-scale EK trials demonstrated some removal efficiencies in spite of a relatively short test period. The oxidation and dissolution of the anode material introduced some quantities of iron, chromium, and copper during the pilot tests. Among the six metals analyzed, zinc demonstrated the best removal efficiency.

Although sludge pH is a major factor that affects heavy metal speciation, the bench and pilot-scale studies did not show that metals can be predictably transported, although their mobility across the biosolids were evidently visible. Clearly, the EK treatment would benefit from longer test runs to achieve metal concentration, compartmentalization, and recovery.

With regard to the pilot tests, although the same sets of experimental parameters were used, the presence of the ion exchange textile did have a significant impact on the treatment objectives. At best, the use of textile mitigated the migration and diffusion of the heavy metals generated by the oxidation of the anode material. However, it was observed that the presence of the textiles created a barrier between the electrode and the biosolids thus altering the common EK processes.

In the first pilot test, fouling of the cathode by the deposition of carbonate (CaCO_3) deposit on the surface of fine stainless steel mesh was seen to have created an obstacle to

efficient dewatering. A solution to prevent this fouling phenomenon could be to temporarily invert the polarity of the electrodes when required, thereby ensuring anodic dissolution of the carbonate deposit. The anodically polarized electrode produces H⁺ ions that will react with the insoluble CaCO₃ to give a more soluble Ca(HCO₃)₂ (Drogui, et al., 2001).

6. Recommendations for Further Studies

The results obtained in these experiments show the complex nature of the electrokinetic treatment of sludge. More studies are required to optimize power consumption by manipulating the conductivity and voltage parameters. An optimum balance is achievable between the conditioner dosage with its effect on conductivity and the applied voltage gradient to produce a reasonable heating rate.

Although the present treatment method provided satisfactory *Ascaris suum* inactivation, further research would be required to optimize the time-temperature regime in order to ascertain the lower time and temperature limits where effective sludge sanitation can still be obtained.

As pointed to in the discussion, a higher voltage gradients correlates to a greater electroosmotic flow; however, the direct consequence of ohmic heating on the electroosmotic performance of the system was not fully disentangle and further experiments are required to isolate its effect.

An improved EK reactor design is needed to prevent the electrochemically induced clogging of the cathode and allow for a better drainage of liquor out of the system. Also various conductive electrode material can be explored that would reduce the dissolution of their elements into the sludge.

Heavy metal partition between the sludge solids and the pore water before and after EK treatment would be necessary to understand the impact of the enhanced EK process on the speciation and solubilization of the metals.

Lastly, further thermodynamic modeling of the complex sludge system is suggested.

7. References

- Abdoli, H. (2009). *A Pilot scale study for Dewatering, Metal Removal and Organic Matter Reduction in Biosolids Using Electrokinetic Phenomena*. Master's Thesis, Montreal, Quebec: Concordia University.
- Acar, Y. B., & Alshawabkeh, A. N. (1993). Principles of Electrokinetic Remediation. *Environmental Science and Technology* , 27 (3), 2638-2647.
- Acar, Y., & Alshawabkeh, A. (1996). Electrokinetic Remediation. I: Pilot-Scale Tests with Lead-Spiked Kaolinite. *Journal of Geotechnical Engineering* , 173-185.
- Acar, Y., Gale, R., Alshawabkeh, A., Marks, R., Puppala, S., Bricka, M., et al. (1995). Electrokinetic remediation: Basics and technology status. *Journal of Hazardous Material*, 40, 117-137.
- Acquisto, B. A., Reimers, R. S., Smith, J. E., & Pillai, S. D. (2006). Factors Affecting Disinfection and Stabilization of Sewage Sludge . *Proceedings of the Water Environment Federation, WEFTEC 2006: Session 61 through Session 70* (pp. 5345-5361). Water Environment Federation.
- Aitken, M., Sobsey, M., Blauth, K., Shehee, M., Crunk, P., & Walters, G. (2005). Inactivation of *Ascaris suum* and Poliovirus in Biosolids under Thermophilic Anaerobic Digestion Conditions. *Environ. Sci. Technol.* , 39 (15), 5804–5809.
- Alshawabkeh, A., & Acar, Y. (1996). Electrokinetic remediation. II: Theoretical model. *Journal of Geotechnical Engineering* , 122 (3), 186-196.
- Alshawabkeh, A., Sheahan, T. C., & Wu, X. (2004). Coupling of electrochemical and mechanical processes in soil under DC field. *Mechanics of Materials* , 36, 453–465.
- Alshawabkeh, A., Yeung, A., & Bricka, M. (1999). Practical Aspects of In-situ Electrokinetic Extraction. *Journal of Environmental Engineering* , 125 (1), 27-35.
- Amatore, A., Berthou, M., & Hébert, S. (1998). Fundamental principles of electrochemical ohmic heating of solutions. *Journal of Electroanalytical Chemistry* , 457, 191-203.
- Anderson, T., & Jaenike, J. (1997). Host specificity, evolutionary relationships and macrogeographic differentiation among *Ascaris* population from humans and pigs. *Parasitology* , 115, 325-342.
- Andrews, A. T. (1983). *Electrophoresis : Theory, Techniques, and Biochemical and Clinical Applications*. Oxford University Press.

Apedaile, E. (2001). A perspective on biosolids management. *Can J Infect Dis.* , 12 (4), 202-204.

Aquarius Technologies PTY ltd. (2000, August). *Electrolytic Conductivity Measurement Theory and Application (Aquarius Technical Bulletin- NO. 08)*. Retrieved 01 07, 2009, from instrumentationguide:
<http://www.instrumentationguide.com/utilities/Conductivity/conductivity.pdf>

Atkins, P., & de Paula, J. (2002). *Atkins' Physical Chemistry* (7th ed.). New York: Oxford University Press.

Babel, S., del Mundo Dacera, D. (2006). Heavy metal removal from contaminated sludge for land application: A review. *Waste Management*, 26, 988–1004.

Barron, J.J., Ashton, C. (2005). The effect of temperature on conductivity measurement. TSP-07, Issue 3, available at <http://www.reagecon.com/supportarticles.shtml>

Barrett, J. (1976). Studies on the induction of permeability in *Ascaris lumbricoides* eggs. *Parasitology* , 73, 109-121.

Bowman, D. D. (2003). Precision and accuracy of an assay for detecting *Ascaris suum* eggs in various biosolid matrices. *Water Research* , 37, 2063-2072.

Brallier S., Harrison, R.B., Henry, C.L., Dongsen, X., (1996), Liming effects on availability of Cd, Cu, Ni and Zn in a soil amended with sewage sludge 16 years previously, *Water, Air and Soil Pollution*, 86, 195-206.

Brewster, J., Oleszkiewicz, J., Bujoczek, G., Reimers, R., Abu-Orf, M., Bowman, D., et al. (2003). Inactivation of *Ascaris suum* eggs in digested and dewatered biosolids with lime and fly ash at bench scale and full scale. *J. Environ. Eng. Sci.* , 2, 395-400.

Brooks, C.S., (1991). *Metal Recovery from Industrial Waste*. Lewis Publishers, Chelsea, MI, USA.

Capizzi-Banas, S., Deloge, M., Remy, M., & Schwartzbrod, J. (2004). Liming as an advanced treatment for sludge sanitation: helminth eggs elimination-*Ascaris* eggs as model. *Water research* , 38, 3251-3258.

Capizzi-Banas, S., Deloge, M., Remy, M., & Schwartzbrod, J. (2004). Liming as an advanced treatment for sludge sanitisation: helminth eggs elimination — *Ascaris* eggs as model. *Water Research* , 38, 3251–3258.

Choudhury, A. (1998). *Removal of nickel and lead from natural clay soil through the introduction of EDTA and coupling Ion exchange processes with electrokinetic methodolog*. Master's Thesis, Montreal, Quebec: Concordia University.

- de Alwis, A. (1990). *Ohmic heating of foods*. PhD Thesis. Cambridge: University of Cambridge.
- De Alwis, A., & Fryer, P. (1992). Operability of ohmic heating process: electrical conductivity effect. *J. Food Eng.* , 15, 21-48.
- Dobbs, D. (1978). *Electrochemical Data: A Handbook for Electrochemists in Industry and Universities*. Elsevier Scientific Publishing Company, Oxford, New York.
- De Souza, J. A., Bocchi, B., & Rocha-Filho, R. C. (1995). Weight loss investigation of alternating voltage corrosion of 301, 304, and 316 stainless steels in boiling NaCl solution. *British Corrosion Journal* , 30 (3), 243-244.
- Dewil, R., Baeyens, J., & Neyens, E. (2005). Fenton proxidation improves the drying performance of waste activated sludge. *Journal of Hazardous Materials* , 161-170.
- Drogui, P., Elmahe, S., Rumeau, M., Bernard C. and Ramaud. A. (2001) Oxidising and Disinfecting by Hydrogen Peroxide Produced in a Two-Electrode Cell. *Wat. Res.*, 35 (13), 3235–3241.
- Eaton, A., Clesceri, L., & Ilsoe, P. (1995). *Standard Methods for the examination of Water and Wastewater*. Washington, DC.: American Public Health Association, American water Works Association.
- Ebbing, D., & Gammon, S. (2008). *General Chemistry* (8 ed.). Boston. MA: Houghton Mifflin Company.
- Elektorowicz, M. (1995). Technical Requirement Related to the Electrokinetic Removal of Contaminants from Soils. *ASCE/CSCE Joint Conference on Environmental Engineering*. Pittsburg, USA.
- Elektorowicz M, , Abdoli H., Oleszkiewicz J, A., (2007), Assessment of electrokinetic metal removal from biosolids, EREM 2007 6th Symposium on Electrokinetic Remediation, Vigo, Spain, 12-15 June, 2007
- Elektorowicz, M., & Boeva, V. (1996). Electrokinetic supply of nutrients in soil bioremediation. *Environmental Technology* , 17, 1339-1349.
- Elektorowicz, M., Chifrina, R., Kozak, M., & Hatim, J. (1996a). The behaviour of ion exchange membranes in the process of heavy metal removal from contaminated soils. '96 *CSCE-4th Environmental Engineering Specialty Conference*. Edmonton, Canada.
- Elektorowicz M, Oleszkiewicz J, A, 2009, Method of treating sludge material using electrokinetics, EKDIM, US Patent 12/571,482.

Elektorowicz, M., Oleszkiewicz, J., Huang, J., Safaei, E., Abdoli, H., & Habel, A. (2008). EKDIM - An electrokinetic process treats municipal wastewater sludge for safe land application. *XX-th Jubilee- National, VIII-th International Scientific and Technical Conference "Water Supply and Water Quality", 15-18 June, 2008*. Gniezno, Poland.

Eriksen, L., Andreasen, P., & Ilsoe, B. (1995). Inactivation of *Ascaris suum* eggs during storage in lime treated sewage sludge. *Water Research*, 30 (4), 1026-1029.

Esmaeily, A. (2002). *Dewatering, Metal Removal, Pathogen Elimination, and Organic Matter Reduction in Biosolids using Electrokinetic Phenomena*. Master's Thesis. Montreal, QC: Concordia University.

Esmaeily, A., Elektorowicz, M., Habibi, S., & Oleszkiewicz, J. (2006). Dewatering and coliform inactivation in biosolids using electrokinetic phenomena. *J. Environ. Eng. Sci.*, 5, 197-202.

Eykholt, G., & Daniel, D. (1994). Impact of System Chemistry on Electroosmosis in Contaminated Soil. *Journal of Geotechnical Engineering*, 120 (5), 797-815.

Feachem, R., Bradley, D., Garelick, H., & Mara, D. (1983). *Sanitation and Disease. Health Aspects of Excreta and Wastewater Management; World Bank Report 11616*. New York: John Wiley and Sons.

Friedl, W., Reijenga, J., & Kenndler, E. (1995). Ionic strength and charge number correction for mobilities of multivalent organic anions in capillary electrophoresis. *Journal of Chromatography A*, 709, 163-170.

Halvin, J., Beaton, J., Tisdale, S., & Nelson, W. (1999). *Soil Fertility and fertilizers, 6th Edition*. Upper Saddle River, NJ.: Prentice-Hall, inc.

Hébert, M. (2005). Pathogènes dans les biosolides municipaux et autres MRF : normes et critères de bonnes pratiques. *Agrosol*, 16 (2), 105-122.

Hiemenz, P. C., & Rajagopalan, R. (1997). *Principles of Colloid and Surface Chemistry (3rd edition)*. New York: CRC.

Huang, J., Elektorowicz, M., & Oleszkiewicz, J. A. (2008). Dewatering and disinfection of aerobic and anaerobic sludge using an electrokinetic (EK) system. *Water Science & Technology*, 57 (2), 231-236.

Incropera, F. P., & DeWitt, D. P. (2002). *Fundamentals of Heat and Mass Transfer, 5th Edition*. NJ: John Wiley and sons inc.

Jenkins, R.L., Scheybeler, B.J., (1981). Metals removal and recovery from municipal sludge. *J. Water Pollut. Control Fed.* 5, 25-31.

- Kato, S., Fogarty, E., & Bowman, D. (2003). Effect of aerobic and anaerobic digestion on the viability of *Cryptosporidium parvum* oocysts and *Ascaris suum* eggs. *International Journal of Environmental Health Research* , 13, 169-179.
- Kiely, P. (1997). *Environmental Engineering*. New York: McGraw-Hill .
- Knox, J. H., & McCormack, K. (1994). Temperature effects in capillary electrophoresis. I: Internal capillary temperature and effect upon performance. *Chromatographia* , 38, 207-214.
- Kok, W. (2000). Capillary Electrophoresis: Instrumentation and Operation. *Chromatographia Supplement* , 51, S1-S89.
- Larsen, M. N., & Roestoff, A. (1999). Seasonal variation in development and survival of *Ascaris suum* and *Trichuris suis* eggs on pastures. *Parasitology* , 119, 209-220.
- Li, X. Y. (2004). Electrochemical Wastewater Disinfection: Identification of its Principal Germicidal Actions. *Journal of Environmental Engineering* , 130 (10), 1217-1221.
- Li, X. Y., Diao, H., Fan, F., Gu, J., Ding, F., & Tong, A. (2004). Electrochemical Wastewater Disinfection: Identification of its Principal Germicidal Actions. *Journal of Environmental Engineering* , 130 (10), 1217-1221.
- Lui, W., Brown, M., & Elliott, T. (1997). Mechanisms of the bacteriacidal activity of low amperage electric current (DC). *Journal of Antimicrobial Chemotherapy* , 39, 687-695.
- Malcolm Pirnie Inc. (1995). *Wastewater Treatment and Sludge Management: Energy Reference Guide*. Buffalo, NY: The New York State Department of Environmental Conservation.
- Mbela, K.K., (1989). Evaluation of Temperature Effects on Inactivation of *Ascaris* eggs in both Aerobic and Anaerobic Digestion Processes, Master's Thesis, Tulane University, New Orleans, Louisiana
- MDDEP. (2008). *Guidelines for the Beneficial Use of Fertilizing Residuals: Reference Criteria and Regulatory Standards*. Bibliothèque National du Québec, 2008 edition (with addenda 1, 2, and 3).
- Metcalf and Eddy, inc. (2003). *Wastewater Engineering, Treatment and Reuse* (4th ed.). NY: McGraw-Hill .
- Mitchell, J. (1991). Conduction phenomena: From theory to geotechnical practice. *Geotechnique* , 41 (3), 299-340.
- Nelson, K. L. & Darby, J. L., (2001). Inactivation of Viable Eggs by Reagents during Enumeration, *Appl. Environ. Microbiol.*, 67(12), 5453-5459.

- Neter, J., Kutner, M. H., Nachtsheim, C. J., Wasserman, W., (1996). Applied Linear Statistical models, 4th ed. WCB/McGraw-Hill, Boston, Mass.
- Ohshima, H. (2006). *Theory of colloid and interfacial electric phenomena*. Academic Press.
- Oleszkiewicz, J., & Mavinic, D. (2002). Wastewater biosolids: an overview of processing, treatment, and management. *J. Environ. Eng. Sci.* , 1, 75–88.
- Patermarakis, G., & Fountoukidid, E. (1990). Disinfection of water by electrochemical treatment. *Water Research* , 24 (12), 1491-1496.
- Peavy, H., Rowe, D., & Tchobanoglous, G. (1985). *Environmental Engineering*. New York: McGraw-Hill.
- Pecson, B., & Nelson, K. (2005). Inactivation of *Ascaris suum* eggs by ammonia. *Environ. Sci. Technol.* , 39, 7909-7914.
- Pecson, B., Barrios, J., Jiménez, B., & Nelson, K. (2007). The effects of temperature, pH, and ammonia concentration on the inactivation of *Ascaris* eggs in sewage sludge. *Water Research* , 41, 2893-2902.
- Petersen, N., Nikolajsen, R., Morgensen, K., & Kutter, J. (2004). Effect of Joule heating on efficiency and performance for microchip-based and capillary-based electrophoretic separation systems: A closer look. *Electrophoresis* , 25, 253-269.
- Pomes, V., Fernandez, A., & Houi, D. (2002). Effect of Applied Electrical Field and the Initial Soil Concentration on Species Recovery During Application of the Electroremediation Process. *Trans IChemE* , 80 (B), 256-264.
- Raj, C., & Hunter, J. (1991). Analysis of joule heating in electrophoretic processes. *Int. Comm. Heat Mass Transfer* , 18, 843-852.
- Rajeshwar, K., & Ibanez, J.G. (1997). *Environmental Electrochemistry: Fundamentals and Applications in Pollution Abatement*. San Diego: Academic Press inc.
- Reimers, R.S., McDonell, D.B., Little, M.D., Bowman, D.D., Englande, A.J., Henriques, W.D. (1986b). Effectiveness of wastewater sludge treatment processes to inactivate parasites. *Water Sci. Technol.* 18 (7-8), 397-404.
- Reimers, R. S., Pilla, S. D., Bowman, D. D., Fitzmorris, K. B., & Pratt, L. S. (2005). Stressors Influencing Disinfection in Residuals. *Proceedings of the Water Environment Federation, Disinfection 2005* (pp. 658-672). Water Environment Federation.

- Reimers, R.S., Sharma, V.K., Pillai, S.D., Reinhart, D.R., Boyd, G.R., Fitzmorris, K.B. (2005). The Future Is Ferrate. *Biosolids Technical Bulletin: Water Environmental Federation*, 10(6), 1-4.
- Safaei, E. (2007). *Enhanced Electrokinetic (EK) Technology: A comparative study for the inactivation of Clostridium perfringens and Reovirus in anaerobically digested biosolids*. Master's Thesis. Montreal, QC: Concordia University.
- Samaranayake, C. P. (2003). *Electrochemical reactions during ohmic heating*. PhD Thesis. Columbus: Ohio State University.
- Samaranayake, C., & Sastry, S. (2005). Electrode and pH effect on the electrochemical reactions during ohmic heating. *Journal of Electrochemical Engineering*, 577, 125-135.
- Sastry, S., & Palaniappan, S. (1992). Mathematical modeling and experimental studies on ohmic heating of liquid-particle mixtures in a static heater. *Journal of Food Process Engineering*, 15, 241-261.
- Smoluchowski, M. (1914). *Handbuch der Elektrizität und des Magnetismus*. Leipzig, Germany.
- Spinosa, L. (2007). *Wastewater sludge: a global overview of the current status and future prospects*. IWA Publishing.
- Station d'Épuration Auteuil. (n.d.). Retrieved 11 14, 2008, from <http://www.info.ville.laval.qc.ca/wlav2/docs/folders/documents/environnement/auteuil.pdf>
- Sun, D.-W. (2005). *Emerging technologies for Food Processing*. Academic Press.
- Tchobanoglous, G. B. (2003). *Wastewater Engineering: Treatment and Reuse, Metcalf and Eddy, 4th Edition*. New York: McGraw-Hill.
- Tzedakis T., Basseguy R., & Comtat M. (1999). Voltammetric and coulometric techniques to estimate the electrochemical reaction rate during ohmic sterilization. *Journal of Applied Electrochemistry*, 29(7), 821- 828.
- US EPA. (2000). *Guide to Field Storage of Biosolids*. EPA/832-B-00-007. Washington, DC: US EPA.
- US EPA. (1999). *Control of pathogens and vector attraction in sewage sludge. Report EPA/625/R-92/013*. Revised edition. Washington, DC: US EPA.

USEPA. (1999). *Environmental regulations and technology control of pathogens and vector attraction in sewage sludge*. Washington, D.C.: Office of Research and development, US Environmental Protection Agency.

Wang, W., & Sastry, S. K. (1997). Starch gelatinization in ohmic heating. *Journal of Food Engineering* , 34 (3), 225-242.

Warren, K.S. (1962). Ammonia toxicity and pH. *Nature*, 195, 47-49.

Wharton, D. (1983). The production and functional morphology of helminth egg-shells. *Parasitology* , 86, 85-97.

Wong, J.W.C. (1999). Effects of lime amendment on availability of heavy metals and maturation in sewage sludge composting, *Environmental Pollution*, 106 (1), 83-89

Yuan, C., & Weng, C.-H. (2006). Electrokinetic enhancement removal of heavy metals from industrial wastewater sludge. *Chemosphere* , 65, 88-96.